



FE200615

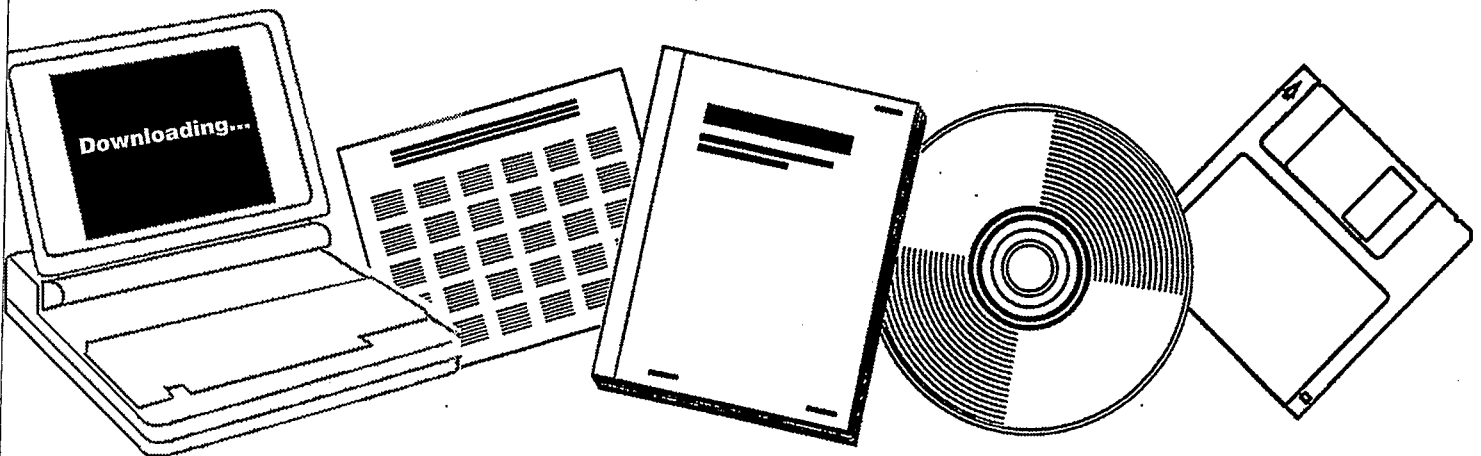
**NTIS**

One Source. One Search. One Solution.

**APPLIED RESEARCH AND EVALUATION OF PROCESS  
CONCEPTS FOR LIQUEFACTION AND GASIFICATION  
OF WESTERN COALS. QUARTERLY PROGRESS  
REPORT, JANUARY-MARCH 1979**

UTAH UNIV., SALT LAKE CITY. DEPT. OF  
MINING AND FUELS ENGINEERING

JUL 1979



U.S. Department of Commerce  
**National Technical Information Service**

**One Source. One Search. One Solution.**

# NTIS



## **Providing Permanent, Easy Access to U.S. Government Information**

National Technical Information Service is the nation's largest repository and disseminator of government-initiated scientific, technical, engineering, and related business information. The NTIS collection includes almost 3,000,000 information products in a variety of formats: electronic download, online access, CD-ROM, magnetic tape, diskette, multimedia, microfiche and paper.



### **Search the NTIS Database from 1990 forward**

NTIS has upgraded its bibliographic database system and has made all entries since 1990 searchable on [www.ntis.gov](http://www.ntis.gov). You now have access to information on more than 600,000 government research information products from this web site.

### **Link to Full Text Documents at Government Web Sites**

Because many Government agencies have their most recent reports available on their own web site, we have added links directly to these reports. When available, you will see a link on the right side of the bibliographic screen.

### **Download Publications (1997 - Present)**

NTIS can now provide the full text of reports as downloadable PDF files. This means that when an agency stops maintaining a report on the web, NTIS will offer a downloadable version. There is a nominal fee for each download for most publications.

For more information visit our website:

**[www.ntis.gov](http://www.ntis.gov)**



U.S. DEPARTMENT OF COMMERCE  
Technology Administration  
National Technical Information Service  
Springfield, VA 22161

FE200615



Applied Research and Evaluation of  
Process Concepts for Liquefaction  
and Gasification of Western Coals

Quarterly Progress Report  
for the Period Jan - Mar 1979

Dr. Wendell H. Wiser

University of Utah - Department  
of Mining and Fuels Engineering  
Salt Lake City, Utah 84112

Date Published - July 1979

Prepared for the United States  
Department of Energy  
Under Contract No. E(49-18) - 2006

## CONTENTS

I	Cover Sheet	1
II	Objective and Scope of Work	3
III	Summary of Progress to Date	5
IV A-1	Catalytic Gasification of Coal to High BTU Gas	7
A-2	Dissolution of Coal in Hydrogen Donor Solvents with Application of Catalysts and Energized Conditions to Produce Clean Fuels	10
A-4	Steam Reforming of Aromatic Compounds	Inactive
A-6	Production of Hydrogen from Char Produced in Coal Hydrogenation Under High Pressure	Inactive
A-7	Study of Thermal and Vapor Phase Catalytic Upgrading of Coal Liquids	22
A-8	Synthesis of Light Hydrocarbons from CO and H <sub>2</sub>	41
A-9	Development of an Inexpensive Recycle Pump	Inactive
B-1	Development of Optimum Catalysts and Supports	64
B-2	(alternate) The Effects of Poisoning on the Desulfurization Activity of Cobalt-Molybdate Catalysts	67
B-3	Fundamental Studies on Hydrogen Transfer Over Coal Conversion Catalysts	Completed
B-4	Mechanism of Catalytic Hydrogenation by Metal Halide Catalysts	73
C-1	The Mechanism of Pyrolysis of Bituminous Coal	80
C-2	Heat Transfer to Gas-Solids Suspension in Vertical Cocurrent Downflow	82
D-1	Coal Particle and Catalyst Characteristics for Hydrogenation Evaluation and Testing	92
D-2	The Effect of Structure on Coal Reactivity	Completed
D-4	Pyrolytic Studies and Separation and Characterization of Coal-Derived Liquids	102
	Supplemental Work	105
V	Conclusion	109

## II. OBJECTIVE AND SCOPE OF WORK

The research reported herein is all of fundamental importance in support of either a process for development of liquefaction of coal, catalysis or some related research. The information which will be gained by research on this contract should materially assist the application of coal in the solution of the energy problems now facing the United States and the world. In particular, the projects reported herein are intended to apply the expertise developed by the coal research team at the University of Utah to problems in four general areas:

- a) Evaluation of process concepts in relation to liquefaction and gasification of coal,
- b) Catalysis studies of fundamental importance in liquefaction and gasification of coal,
- c) Studies of fundamental principles involved in processes for liquefaction and gasification of coal,
- d) Properties of coal and coal conversion products of significance in liquefaction and gasification of coal.

A-1 Coal will be gasified by direct catalytic hydrogenation to produce a high-BTU gas. A liquid will be produced in a first stage reaction at 400-450°C. This product will be further hydrogenated to produce a high-BTU gas. Catalysts and reaction conditions for each stage will be studied.

A-2 Kinetics, yields and optimum reaction conditions for extraction of coal will be determined. Hydrogen donor solvents, ultrasonic energy, hydrogen pressures and catalysts will be employed. Extraction products will be analyzed and characterized.

A-4 Aromatic liquids derived from coal hydrogenation or extraction will be considered as feedstocks for steam reforming to make a high BTU gas. Optimum conditions for the production of hydrogen or high-BTU gas, optimum catalysts, the effects of poisons and the degree of coke formation will be determined.

A-6 The gasification of coal char will be studied at 2000-3000 psi to produce hydrogen for coal hydrogenation. Steam and oxygen will be used for gasification. The thermal efficiency of producing hydrogen at the pressure at which it will be used will be studied.

A-7 Thermal hydrogenolysis of coal slurried with recycle solvent will be studied as such or in the presence of a vapor-phase catalyst to determine the extent of upgrading.

- A-8 Fischer-Tropsch synthesis of C<sub>2</sub>-C<sub>4</sub> hydrocarbons will be studied. New catalysts will be developed and a continuous test unit for long-term catalyst testing will be constructed.
- A-9 The capacity and durability of a previously developed high-pressure gas recycle pump will be increased. A goal of 3000 psi operating pressure at 500°C is desirable.
- B-1 Adsorption properties and penetration of aromatic molecules on typical cracking catalysts will be determined. These properties will be used to evaluate the ability of such catalysts to crack the large molecules present in coal-derived liquids.
- B-2 (alternate) The mechanism of deactivation of molybdena hydrodesulfurization catalysts by coal-derived liquids will be studied. Kinetic studies involving the model compound benzothiophene will be employed.
- B-3 Hydrogen transfer by metal halide catalysts during coal hydrogenation will be studied. Deuterium labeled hydrocarbons will be used to elucidate reaction mechanisms.
- B-4 The mechanism of catalytic hydrogenation of coal by metal halide catalysts will be investigated. The nature of active catalyst sites will be studied. Changes in properties of the reacting coal will be determined and the nature of reaction products will be determined. Catalyst regeneration will also be studied.
- C-1 The mechanism of pyrolysis of coal will be studied by the use of isotopically labeled model compounds. Products of pyrolysis will be examined to determine their precursors in coal.
- C-2 Fluid mechanics and heat transfer studies involving gas-solid suspensions in vertical downward cocurrent flow systems will be conducted to obtain information on the effect of these variables in the University of Utah coal hydrogenation reactor.
- D-1 The effect of coal and catalyst properties and pretreatment on the hydrogenation of western coals will be studied in the University of Utah short-residence-time, entrained-flow reactor.
- D-2 The effect of coal structure on reactivity to hydrogenation, pyrolysis and dissolution will be studied. Pretreatment of the coal by specific reactions will be used to obtain samples with special structural features.
- D-4 Liquid products from coal hydrogenation in the University of Utah reactor will be separated and characterized. Coal pyrolysis and hydrogenation mechanisms and model compound reactions will be studied.

Research Highlights

Hydrotreated SRC liquids undergo smooth catalytic cracking at 325-425°C to yield light liquid products with little gas and coke formation. The cracking reaction can be controlled to yield gasoline-range products.

Increasing the temperature of the carbon monoxide hydrogenation reaction over iron-manganese catalyst increased the olefin selectivity and reduced methane production. At constant conversion the olefin selectivity increased with increasing space velocity and decreased with increasing H<sub>2</sub>/CO ratio. The C<sub>2</sub>-C<sub>4</sub> hydrocarbon yield is insensitive to process changes at constant temperature and conversion. At constant temperature the olefin selectivity increased with increasing space velocity and decreased with increasing H<sub>2</sub>/CO ratio.

Publications, Presentations and Activities

D.M. Bodily and H. Itoh, "A Comparison of the Chemical Structure of Coal-Derived Liquids," International Symposium on Coal Science and Technology for the Eighties, Dhanbad, India, Feb. 1-3, 1979.

J.R. Kim, B.S. Brewster and J.D. Seader, "Heat Transfer and Pressure Drop in Downward Cocurrent Flow of Coal-Gas Suspensions," Rocky Mountain Fuel Society, Salt Lake City, Utah, Feb. 9-10, 1979.

R. Yoshida, Y. Yoshida and D.M. Bodily, "Chemical Structure Changes in Coal Asphaltenes During Hydrogenolysis," Rocky Mountain Fuel Society, Salt Lake City, Utah, Feb. 9-10, 1979.

J.M. Lytle and R.E. Wood, "Kinetics of Coal Liquefaction: Effect of Coal Particle Size and Temperature," Rocky Mountain Fuel Society, Salt Lake City, Utah, Feb. 9-10, 1979.

F.E. Massoth, C. Kim and M.W. Moora, "Diffusion of Polyaromatics in Catalyst Supports," Rocky Mountain Fuel Society, Salt Lake City, Utah, Feb. 9-10, 1979.

R.R. Beishline, B. Gould, G. Davis, S. Speak and K. Calvert, "The Role of Hydrogen Donor Solvent in Coal Hydroliquefaction: Hydrogen Transfer Within the Solvent System," Rocky Mountain Fuel Society, Salt Lake City, Utah, Feb. 9-10, 1979.

G.T. Garr, J.M. Lytle and R.E. Wood, "The Effect of Coal Characteristics on the Catalytic Liquefaction of Utah Coals," Rocky Mountain Fuel Society, Salt Lake City, Utah, Feb. 9-10, 1979.

S. Yokiyama, D.M. Bodily and W.H. Wiser, "Structural Characterization of Coal Hydrogenation Products by Proton and Carbon-13 Nuclear Magnetic Resonance," Fuel, 58, 162 (1979).

K.W. Zilm, R.J. Pugmire, D.M. Grant, R.E. Wood and W.H. Wiser, "A Comparison of the Carbon-13 NMR Spectra of Solid Coals and Their Liquids Obtained by Catalytic Hydrogenation," Fuel, 58, 11 (1979).



Catalytic Gasification of Coal to High BTU Gas

Single Stage Coal Gasification

Faculty Advisor: Wendell H. Wiser  
Graduate Student: Ted J. Ajax

Introduction

Single stage catalytic coal gasification has attracted a great deal of interest as a direct method of producing high BTU synthetic gas from coal. This process involves the introduction of a coal-solvent slurry and hydrogen into a single fixed bed catalytic reactor to produce a combustible gas containing high yields of methane. Thermodynamic calculations show this process to be essentially autothermal, which offers significant energy savings over a similar multi-stage approach.

The primary objective of this research is to optimize the process variables for the reactions involved and to develop suitable catalysts for the process. These catalysts must have both hydrogenation and cracking activity to produce high yields of methane from the feed coal slurry. The -200 mesh coal is slurried in a hydrogen donor solvent, tetralin, and a ratio of 2 parts solvent to one part coal is employed. Previous work utilized a solvent to coal ratio of 4 to 1.

The process conditions have been tentatively set as

temperature            400 - 550°C

pressure                ~ 1500 psi

residence time        10 - 30 min

Initially, Ni-Mo/SiO<sub>2</sub>-Al<sub>2</sub>O<sub>3</sub> and Pd/SiO<sub>2</sub>-Al<sub>2</sub>O<sub>3</sub> catalysts will be used.

Project Status

Presently a new reactor and tubing system is being designed and the existing equipment is being modified. Several catalysts are being examined and those chosen will be ordered. A special slurry metering pump suitable for the coal slurry feed has been ordered. A schematic of the single stage catalytic coal gasification apparatus is shown in Figure 1.

### Future Work

The system will be assembled as the required equipment arrives. Catalysts will be sulfided and the system will be operated for several shakedown runs before the experimental runs are made.

1. Hydrogen Supply
2. Nitrogen Supply
3. Cylinder Valves
4. Regulating Valves
5. Pressure Gauges
6. Preheater
7. Thermocouple
8. Burette
9. Slurry Container
10. Slurry Pump
11. Relief Valve
12. Fixed-Bed Reactor
13. Condensor
14. Gas-Liquids Separator
15. Wet Test Meter

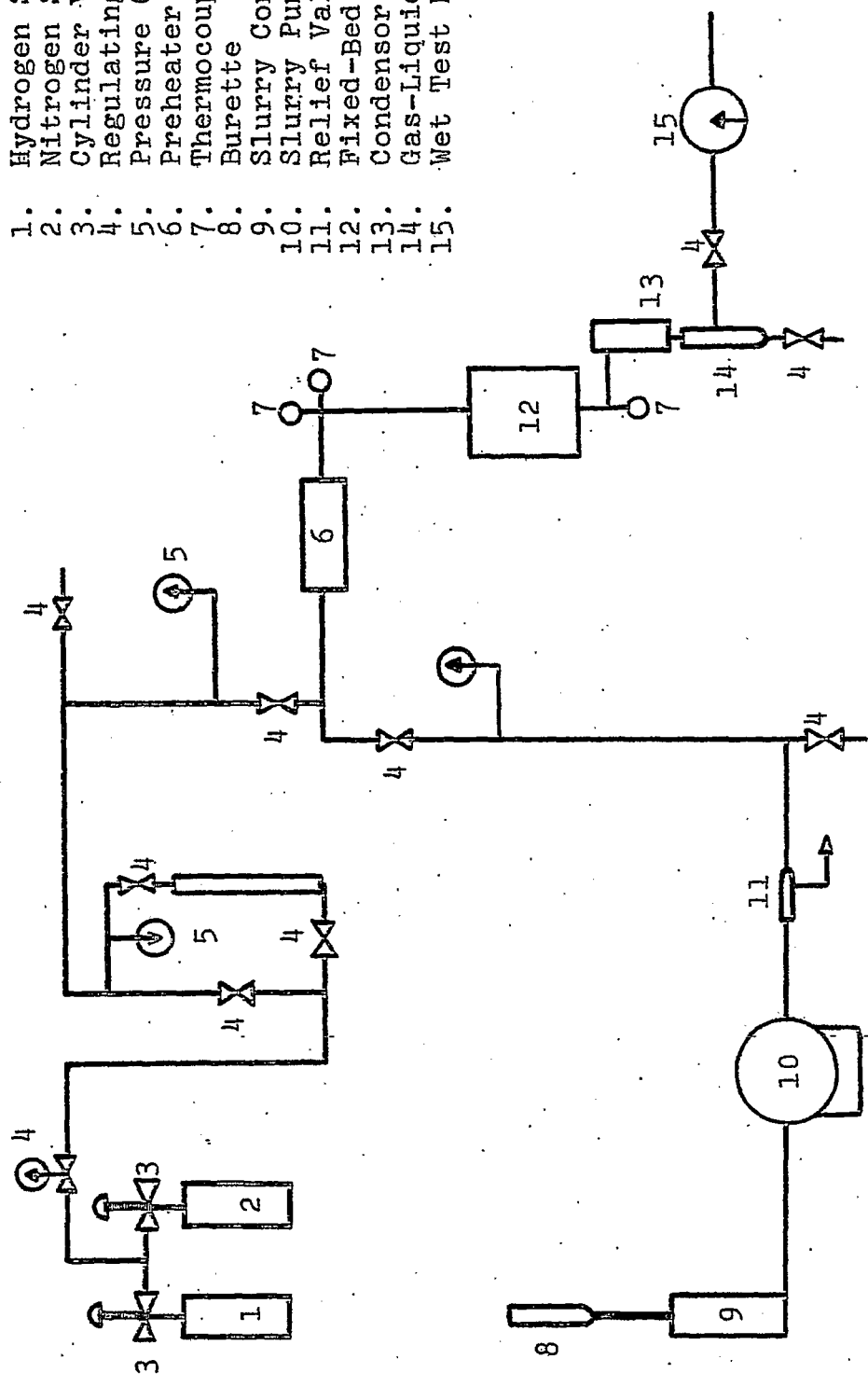


Figure 1. A schematic of the single stage catalytic coal gasification apparatus.

Solvent Treatment of Coal-Derived Liquids (CDL)

Faculty Advisor: L.L. Anderson  
Graduate Student: Kwang Eun Chung

Introduction

The objective of this investigation is to separate CDL into chemically different fractions of potential commercial value. Major developments have included (1) the isolation of paraffinic material, (2) the separation of CDL into highly H-bonded and less H-bonded fractions, (3) the observation of free -OH bonds in the infrared spectra of CDL fractions in dilute solutions, (4) a new activity expression in liquid solutions, (5) a new procedure for molecular weight determination by vapor phase osmometry and (6) a characterization scheme for CDL. The data from the characterization work are being further examined to relate these to the structure of coal and its liquefaction behavior.

Project Status

The experimental work in progress includes (1) testing of an acetylation method for hydroxyl group determination and (2) reproducing results on the solubilization of coal. Liquefaction data have been evaluated to ascertain the chemical structure of the CDL-P fractions and to determine the significance of reduction of molecular size during the liquefaction process (Table 2 of previous report).

Possible structures of the CDL-P fractions are shown in Figure 1. These structures contain the appropriate number of aromatic rings, aromatic clusters and naphthenic rings. The presence of functional groups or side chains on the structures are qualitative. The four fractions were regrouped into three, A, B and C, instead of two as in an earlier report.<sup>1</sup> These groups are significantly different from each other in molecular weight and in the number of aromatic and naphthenic rings.

These groups probably have originated from different structural units in coal as discussed earlier.<sup>1</sup> Another supporting interpretation has been made: little change, if any, occurred in the number of aromatic rings per cluster,  $R_A/C_1$ , in producing CDL and Sol-Prod. The number,  $R_A/C_1$ , can be found by dividing the number of rings,  $R_A$ , by the number of clusters,  $\#C_1$ , in Table 2. The average cluster in Sol-Prod has 2.5 aromatic rings and that in CDL-P has 2.2 rings.

Considering 15% of char yield in producing CDL, the two values are close to each other and indicate that aromatic clusters were changed little, if any, in the solubilization and liquefaction processes. Thus it appears that the structural units or aromatic clusters of coal were conserved during the liquefaction process and appeared as Groups A, B and C in the product.

Examination of the conversion of Sol-Prod to CDL-P fractions (discussed in previous report) reveals that apparently the conversion was accompanied by removal of peripheral attachments to the clusters which resulted in reduction of the molecular size. The structural parameters in Table 2 are related to the molecular size reduction.

The reduction of molecular size during liquefaction may occur in two ways: (1) the removal of aliphatic carbons as gaseous and paraffinic products and (2) the cleavage of linkages connecting aromatic clusters. The evolution of gaseous products results in a relatively small decrease in molecular weight and an increase in aromaticity ( $f_a$ ) of CDL. Production of paraffinic material also affects the molecular weight and aromaticity of CDL. The cleavage of linkages involves a significant reduction of molecular size, but has no effect on the aromaticity as long as the products from the cleavage remain in the CDL. Thus the change in  $f_a$  reflects reduction of molecular size due to the removal of aliphatic carbons from the coal or CDL.

The change in  $f_a$  was considered in estimating the structural parameters of Pred in the last report. The comparison of the  $f_a$ 's of CDL-P and Pred (or Sol-Prod) indicates that 17% of the molecular weight of the Sol-Prod need to be removed as gaseous and/or paraffinic products. About one-third of this 17% resulted from the removal of oxygen as revealed by the number of O's of the Pred and Sol-Prod.

The total reduction in molecular size is 45% from the molecular weight of 485 to 268. Since 17% is due to the production of gases and paraffinic material, the rest (28%) is attributable to the cleavage of linkages between aromatic clusters. The estimated number of clusters (1.5) of Pred according to this breakdown is close to 1.3 of Sol-Prod. The breakdown reveals that (1) the cleavage of the linkages produces small molecules like light and middle fractions in CDL-P, (2) the oxygen removal itself is not significant in reducing the molecular size and (3) the production of gases and paraffinic material plays a significant role in changing the molecular size and aromaticity of CDL. Statement (1) agrees with the conclusion drawn in the last report which considered the  $R_A$  and #Cl of CDL-P and Sol-Prod fractions.

Information on the cleavable linkages in Sol-Prod is not available. However, one important aspect is that cleavage has not taken place at temperatures below 320°C in reaction with NaOH and ethanol. Linkages in Sol-Prod compounds are apparently strong and their cleavage requires higher temperatures. Thus

an investigation on the linkages in the Sol-Prod will be helpful in lowering the reaction temperature for coal liquefaction processing.

Using the information obtained, units comprising the total structure of the coal can be constructed (Figure 2) and their distribution can be quantified: (1) the structural units comprising the coal are similar to the component-groups of the CDL-P; (2) structural units, X, are connected to each other, but the nature of the linkages is unknown and (3) the distribution of the units were estimated from the data on Sol-Prod.

Considering the heterogeneity of coal and its inaccessibility by conventional analytical means, this approach appears to be a practical, useful way to characterize the chemical structure of CDL and relate this information to the structure of coal. Although only one coal has been examined, the same approach could be effective with other coals which can be liquefied. The proposed structural units could related to product potential in liquefaction, solvent refining and pyrolysis of coal. The structure also will be useful in the study of the gasification and carbonization of coal.

#### Future Work

Additional experiments are being conducted to complete the studies and to define the liquefaction products more precisely. Findings will be combined with data from others involved in coal liquefaction and coal structure to further define the significance of these results.

#### Reference

1. W.H. Wiser et al., DOE Contract No. (49-18) - 2006, Quarterly Progress Report, Salt Lake City, Utah, July-Sept 1978.

Table 2. Structural Parameters for the Solubilization Product and CDL-P.

	Yield <sup>a</sup>	Mol. Wt.	R <sub>A</sub>	R <sub>N</sub>	#Cl <sup>b</sup>	f <sub>a</sub>	#O <sup>b</sup>
Solub. Product <sup>c</sup>	76.5	485	3.2	2.4	1.3	0.50	2.32
Fraction A	26.6	478	3.2	2.5	1.4	0.54	2.31
B	23.8	444	2.4	2.3	1.3	0.47	2.36
C	26.1	538	4.0	2.3	1.1	0.50	2.27
CDL-P <sup>c</sup>	46.2	268	2.4	0.9	1.1	0.60	0.77
Light	9.6	183	1.2	0.6	1.0	0.55	0.63
Middle	7.8	210	1.6	0.7	1.1	0.58	0.67
Heavy	8.8	272	2.4	1.3	1.1	0.59	0.75
Resid	20.0	396	4.4	1.2	1.3	0.68	1.01
Pred. <sup>d</sup>		485	3.6	1.4	~1.5	0.50	1.2

<sup>a</sup>Weight % of coal (MAF).

<sup>b</sup>Number of aromatic clusters, and number of oxygen/molecule, resp.

<sup>c</sup>The parameters are calculated from those of respective fractions.

<sup>d</sup>Pseudo-predecessor of CDL-P (See text).

Light Middle  
 └──────────┘  
 A

Heavy  
 B

Resid  
 C

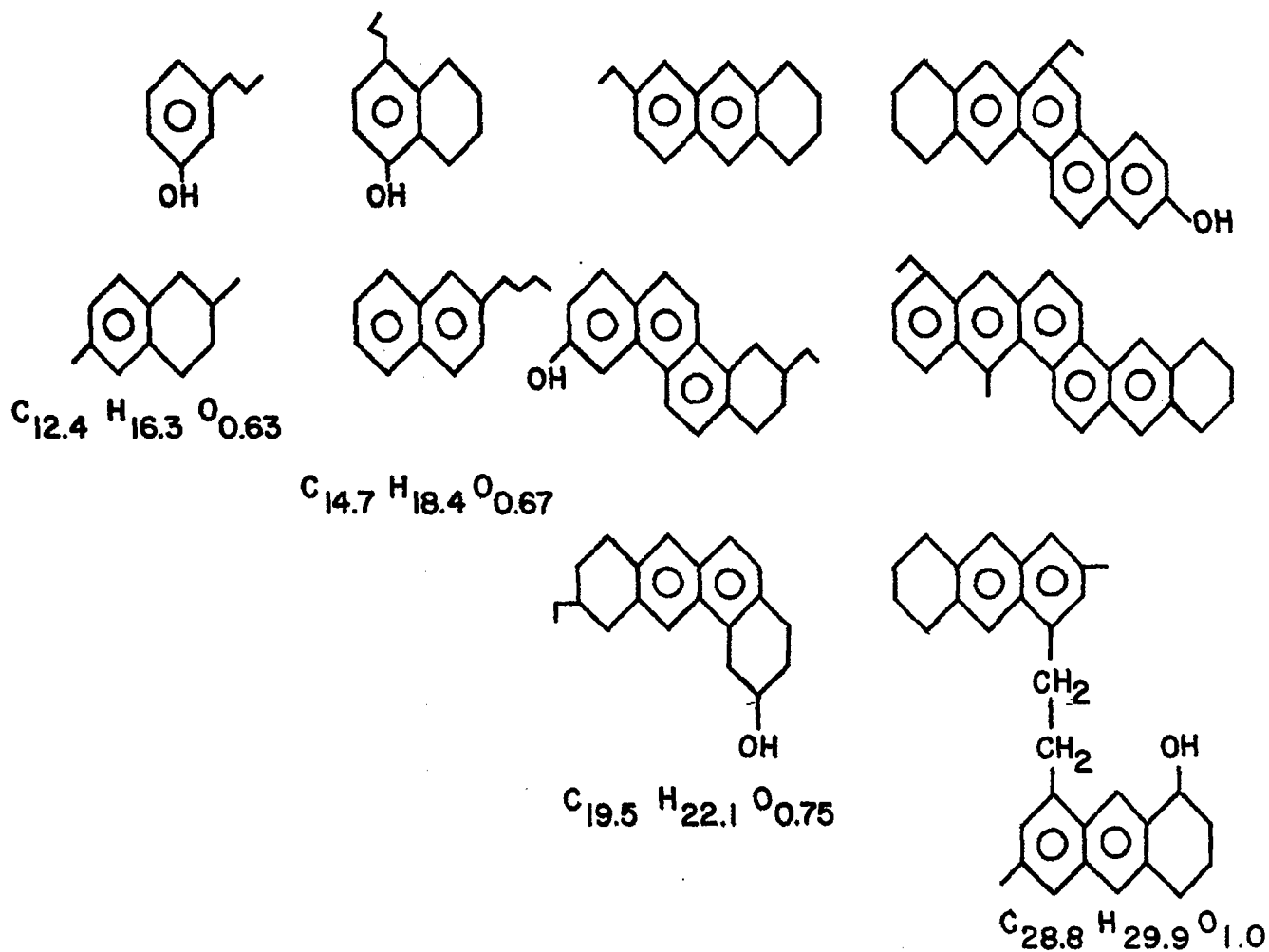
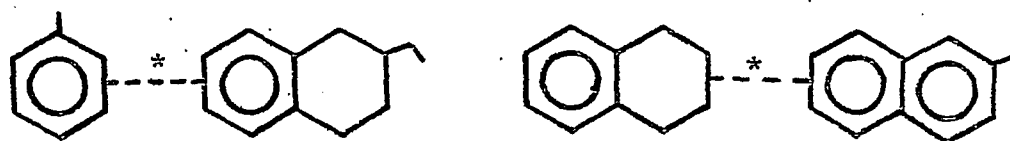


Figure 1. Sketches of Possible Structures of CDL-P Fractions



Structural Units X ( 39 mole % )



Structural Units Y ( 36 mole % )



Structural Units Z ( 25 mole % )

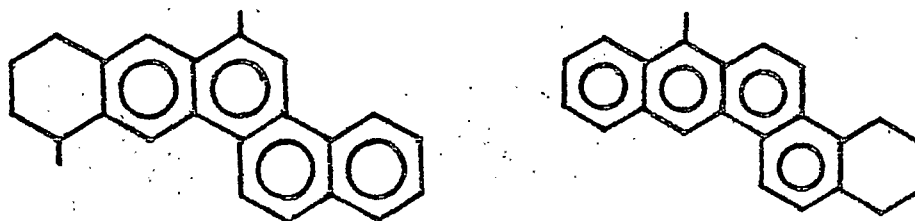


FIG. 2. Structural Units Comprising  
A hvb Coal

\* Linkages exist but are not identified.

A Systematic Study of Coal Structure  
by Extractive Liquefaction Under  
Mild Reaction Conditions

Faculty Advisor: J. Shabtai  
Graduate Student: H.B. Oblad

Introduction

This study is concerned with extractive coal liquefaction under mild experimental conditions, using a variety of solvents and homogeneous catalysts. Coal slurries will be processed in a small integral flow reactor which will be operated at temperatures of 100-300°C, hydrogen pressures of 100-1000 psig and very short residence times. The mild conditions will be adjusted to obtain very low coal conversions, e.g., 2-5 percent to avoid secondary reactions. The slurry will be quenched, the liquids will be removed and analyzed, and the washed solids will be reloaded into the reactor with fresh solvent and catalyst. Repetition of this procedure coupled with the application of selective catalysts should yield relatively simple primary products. The information gathered should reveal the types of original structural components and inter-connecting functional groups present in coal.

Project Status

Hiawatha coal from Utah was extracted with cyclohexane by the following procedure. In four large test tubes was placed a total of 35.88 grams of fine powdered coal. To each tube, 75 ml of cyclohexane was added. The tubes were then placed in an ultrasonic bath and kept for 1 hour. During this time the bath temperature rose from approximately 20°C to 43°C. The tubes were then transferred to a large centrifuge and spun at 2300 rpm for 1 hour. The liquid was decanted and the cyclohexane was evaporated, leaving a resin which was weighed and stored. The same process was repeated with the residual coal six more times. The total solvent-free extract obtained comprised about 3.6% by weight of the coal sample.

The first and seventh extracts were dissolved in 3-5 ml of dichloromethane and the solution was dropped onto KBr crystals using a capillary pipette. The dichloromethane was evaporated, and the films deposited were analyzed by infrared

TABLE 1

Tentative Assignments of Infrared Absorption Maxima<sup>a</sup> Shown by Hiawatha Coal Extracts

<u>Absorption Maxima, cm<sup>-1</sup></u>	<u>Benzene Extracts</u>	<u>Assignment</u>
715 (w)	705 (w)	CH out-of-plane deformation (monosubstituted benzene rings)
760 (w)	740 (w)	CH out-of-plane deformation (mono- and ortho-disubstituted benzene rings)
800 (s)	810 (m)	CH out-of-plane deformation (1,2,3-trisubstituted and 1,2,3,4-tetrasubstituted benzene rings)
835 (w)	830 (m)	Same as above
1030 (m)	1035 (s)	C-O stretching (ester and/or ether groups)
1090 (m)	--	C-O stretching (ester and/or ether groups)
1260 (w)	1265 (w)	C-O stretching (benzoates)
1375 (s)	1380 (s)	CH symmetric bending in CH <sub>3</sub>
1450 (s)	1455 (s)	CH asymmetric bending in CH <sub>3</sub>
1600 (w)	1600 (m)	Aromatic ring breathing
1710 (m)	1710 (s)	C=O stretching (aryl conjugated ester or aliphatic keto groups)
1735 (m)	1735 (w)	C=O stretching (saturated ester groups)
2840-2960 (s)	2840-2960 (s)	C-H stretching frequencies
	3360 (m)	O-H stretching (bonded OH groups)

a (s) - strong; (m) - medium; (w) - weak.

spectroscopy. The spectra obtained are given in Figure 1.

The coal samples left from the repeated cyclohexane extraction were then sequentially extracted by an identical procedure six times with benzene. The benzene extractions produced a total solvent-free extract, comprising 1.6% of the coal. Infrared spectral analyses were performed on the first and last benzene extracts and compared with those of the cyclohexane extracts. The spectra of extracts No. 8 and No. 13 are given in Figure 2. The observed infrared absorption maxima, and corresponding tentative assignments of these maxima, are summarized in Table 1. Although the cyclohexane and benzene extracts show generally similar IR absorption patterns, there are some significant differences in the relative intensities of certain bands. For example, whereas the two C=O stretching bands at  $1710\text{ cm}^{-1}$  (aryl-conjugated ester group) and  $1735\text{ cm}^{-1}$  (aliphatic ester group) are of comparable intensity in the cyclohexane extract, the former band ( $1710\text{ cm}^{-1}$ ) is strongly predominant in the benzene extract. This observation is in line with a corresponding increase in the intensity of the aromatic ring breathing mode (at  $1600\text{ cm}^{-1}$ ) of the benzene extract. Differences in relative band intensities are also observed in the  $700\text{--}840\text{ cm}^{-1}$  region (aromatic C-H out-of-plane deformations), indicating differences in the degree and type of ring substitution in the two extracts. For example, while with the cyclohexane extract the strongest band in this region is at  $800\text{ cm}^{-1}$ , the strongest band with the benzene extract is at  $835\text{ cm}^{-1}$  (accompanied by a band of decreased intensity at  $800\text{ cm}^{-1}$ ).

The indicated higher aromaticity of the benzene extracts, as compared to the cyclohexane extracts, was corroborated by  $\text{C}^{13}\text{NMR}$  analysis of these extracts (Table 2). The aromatic carbon content of the benzene extracts is markedly higher than that of the cyclohexane extract 1 and increases with an increase in the depth (time) of extraction.

Table 2  
 $\text{C}^{13}\text{NMR}$  Analysis of Hiawatha Coal Extracts

<u>Extract No.</u>	<u>Solvent<sup>a</sup></u>	<u>Aromatic C, %</u>	<u>Aliphatic C, %</u>
1	Cyclohexane	15.2	84.8
8	Benzene	28.5	71.5
13	Benzene	37.3	62.7

<sup>a</sup>Employed in the extraction and then completely removed prior to the analysis.

### Future Work

The systematic extractions of Hiawatha and other coals with nonreacting solvents of gradually increasing polarity will be continued. Solvents to be employed include oxygen-containing compounds, e.g., ketones, esters, ethers, etc., and halogenated derivatives. Extracts will be subjected to detailed infrared and  $C^{13}$ NMR analysis. The effect of extraction time and temperature upon the depth of solubilization and upon extract composition will be investigated.

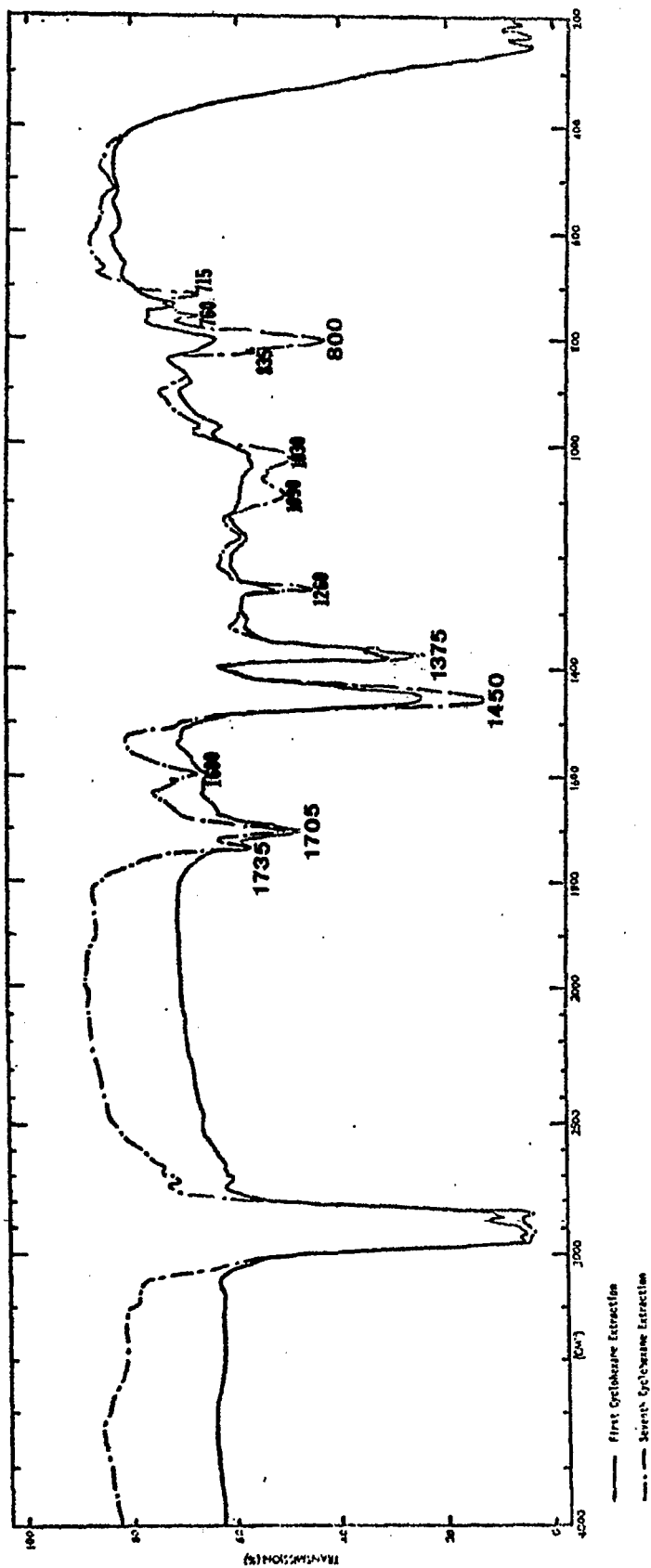


Figure 1. Infrared absorption maxima (in cm<sup>-1</sup>) shown by cyclohexane extracts of Hiawatha coal.

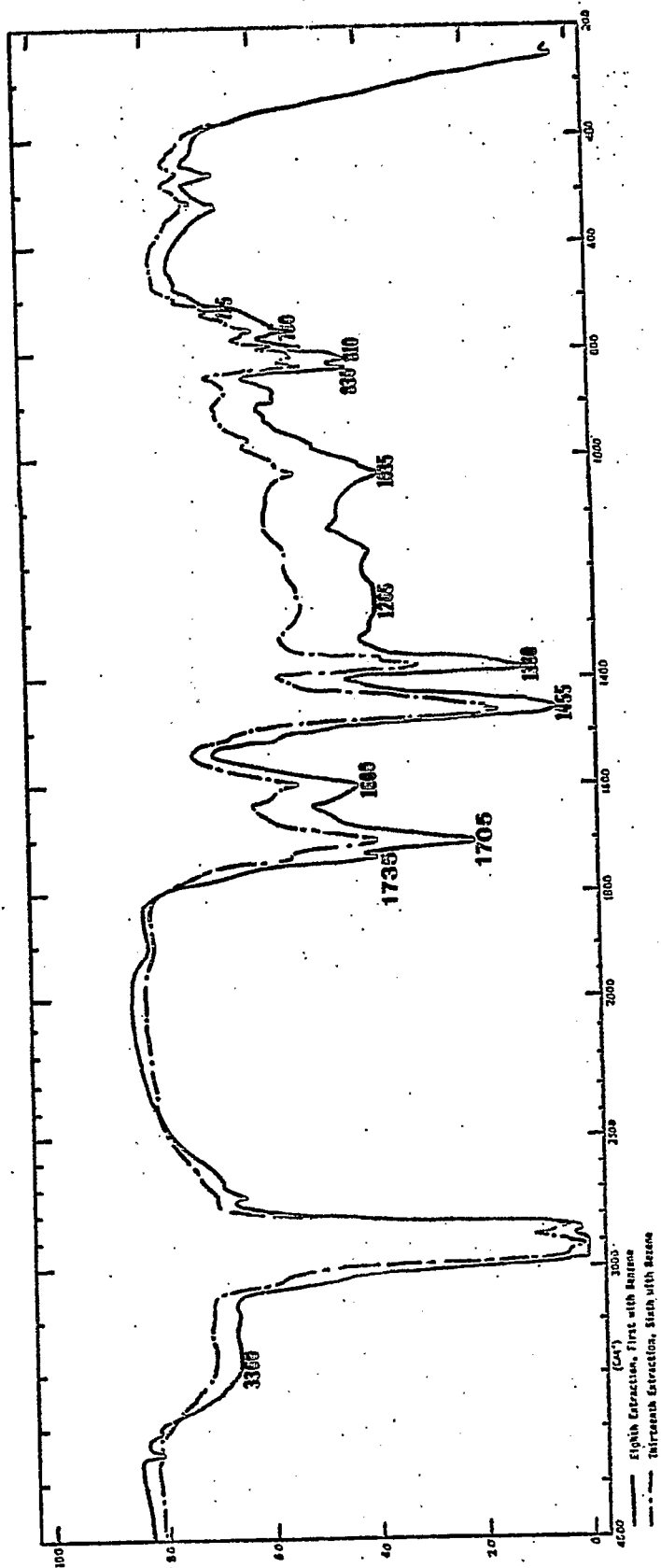


Figure 2. Infrared absorption maxima (in  $\text{cm}^{-1}$ ) shown by benzene extracts of Hiawatha coal.

Catalytic Cracking of Hydrogenated Coal  
Liquids and Related Polycyclic Naphthenes

Faculty Advisors: A.G. Oblad and  
J. Shabtai  
Graduate Student: S. Sunder

Introduction

Hydrogenation followed by catalytic cracking provides a feasible process sequence for conversion of coal liquids into conventional fuels. Such a sequence has certain advantages in comparison with a hydrocracking-catalytic reforming scheme.<sup>1</sup>

The present project is concerned with the following interrelated subjects:

- (1) Systematic catalytic cracking studies of model polycyclic naphthenes found in hydrogenated coal liquids, e.g., decalin, perhydrophenanthrene and perhydroanthracene, as a function of catalyst type and operating conditions.
- (2) Systematic catalytic cracking studies of hydrogenated coal-derived liquids (hydro-CDL) as a function of the same variables.

Catalysts applied in the study include both conventional zeolite-containing systems, e.g., Mobil Durabead, as well as newly developed large pore molecular sieves. The latter are prepared by cross-linking of layer silicates and are designated as CLS catalysts.<sup>2,3</sup> Strongly acidic forms of CLS are being tested as cracking catalysts.<sup>4</sup> Such CLS systems have an important advantage over conventional zeolites in possessing sufficiently large pore sizes, e.g., 10-20 Å, for admission of polycyclic naphthenes in the catalyst intracrystalline channel system.

The equipment used and the methods of identification of products have been previously reported.

Project Status

Systematic catalytic cracking studies of (a) model polycyclic naphthenes, e.g., decalin and perhydrophenanthrene; and (b) hydrotreated coal liquids, e.g., a hydrogenated SRC middle-heavy distillate, were carried out. Results from



cracking of one of the model compounds, i.e., decalin (1), using a zeolite-containing catalyst (Mobil Durabead) are summarized in Figures 1-6. As seen from Figure 1, in the mild temperature range of 300-450°C and LHSV 0.65 hr<sup>-1</sup>, the conversion of 1 increases with temperature from 44 to 94%. The selectivity for formation of liquid products is very high (90%), while formation of gases and coke is very low. Figure 2 shows the change in the distribution of C<sub>1</sub>-C<sub>4</sub> gaseous products as a function of reaction temperature. The products, consisting mostly of isobutane, n-butane and propane, are formed in significant yields only above 400°C. Figure 3 summarizes the change in liquid product composition as a function of reaction temperature. C<sub>10</sub> alkylcyclohexenes, which are indicated as primary cracking products, represent the major fraction (55 moles/100 moles of decalin cracked) at 300°C. These compounds steadily decrease in concentration with increase in temperature, while the concentration of C<sub>10</sub> alkylbenzenes, which are derived from the C<sub>10</sub> alkylcyclohexenes by hydrogen transfer, passes through a maximum at about 325°C and then decreases, due to dealkylation reactions, at higher temperature. C<sub>6</sub>-C<sub>9</sub> benzenes, formed by complete or partial dealkylation of the C<sub>10</sub> alkylbenzenes and by aromatization of dealkylated C<sub>10</sub> alkylcyclohexenes, increase steadily in concentration with temperature. C<sub>6</sub>-C<sub>8</sub> cyclanes, which consist mainly of methylcyclopentane, dimethylcyclopentane and methylcyclohexane, are also formed. Such products pass through a maximum around 425°C and then decrease due to secondary cracking. In addition to the above mentioned C<sub>6</sub>-C<sub>9</sub> alkylbenzenes, the most important cracking products at temperatures above 400°C are C<sub>5</sub>-C<sub>8</sub> paraffins and olefins. Figures 4-6 summarize the change in product composition from 1 as a function of space velocity at a constant temperature of 375°C. The changes in product distribution follow the same patterns as in the study of the temperature effect (Figures 1-3).

Results from cracking of perhydrophenanthrene (2) with a Mobil Durabead catalyst are summarized in Figures 7-9. Figure 7 shows that in the mild temperature range of 325-425°C and LHSV 0.76 hr<sup>-1</sup>, the conversion of compound 2 increases from 43 to 96% with preservation of high selectivity for production of liquid products. Figure 8 shows that the gaseous products consist mainly of C<sub>3</sub> and C<sub>4</sub> hydrocarbons. Again they are paraffinic, with isobutane and propane being the major components. Figure 9 shows the change in liquid product composition as a function of reaction temperature. As seen, C<sub>14</sub> octahydronaphthalenes, which are indicated as the primary cracking products, decrease steadily with increasing temperature. On the other hand, lower cyclenes and cyclanes derived from these primary products, e.g., C<sub>11</sub> octahydronaphthalenes and monocyclic C<sub>6</sub>-C<sub>10</sub> cyclenes and cyclanes, pass through a maximum and then decrease with further increase in temperature.

Some analytical data on a SRC middle-heavy distillate (230-455°C) and on the product obtained by catalytic hydrogenation of this fraction with a sulfided Ni-W catalyst, are shown in Table 1. The heteroatom contents are drastically reduced in the hydrogenated product. Likewise carbon aromaticity is decreased from 64 to 12% upon hydrogenation. Table 2 shows the product distribution from cracking of the hydrogenated SRC II fraction as a function of reaction temperature. As in the case of the polycyclic naphthenes 1 and 2, the selectivity for liquid product formation is very high (83-94%). Conversions shown relate to the total product boiling below the starting boiling point of the feed. Figures 10 and 11 show GC chromatograms of the liquid product from cracking of the hydrogenated SRC II distillate. Figure 11 indicates a gradual conversion to lower boiling liquids, occurring upon catalytic cracking, while Figure 12 illustrates the similarity in the bp range of the liquid products with those obtained from perhydrophenanthrene (2).

The following conclusions can be reached on the basis of results obtained:

(1) Hydrotreated SRC II liquids and structurally related polycyclic naphthenes and naphthenoaromatics undergo smooth catalytic cracking under mild temperature conditions (325-425°C) to yield predominantly light liquid products, with little concurrent gasification and very low coke formation.

(2) The composition of liquid products from catalytic cracking of hydro-SRC II and related polycyclic naphthenes is easily controllable, and by appropriate coordination of operating variables gasoline-range products containing high concentrations of isoparaffins, C<sub>5</sub>-C<sub>12</sub> naphthenes and C<sub>6</sub>-C<sub>12</sub> benzenes can be obtained.

#### Future Work

The effect of the depth of hydrogenation of SRC II liquids upon the rate of catalytic cracking and upon the type distribution of product components will be investigated. The catalytic cracking studies will be enlarged in scope to include partially hydrogenated polycyclic arenes, as well as additional types of coal liquids, e.g., partially hydrogenated fractions from the EDS and other processes.

#### References

1. L.R. Veluswamy, Ph.D. Thesis, University of Utah, Salt Lake City, Utah, 1977.
2. J. Shabtai and N. Lahav, Israel Patent 50548; U.S. Patent pending.

3. N. Lahav, V. Shani and J. Shabtai, Clays and Clay Minerals, 26 (2), 106-115 (1978).
4. J. Shabtai and R. Lazar, Amer. Chem. Soc. Preprints, Div. Petrol. Chem., 24, 622 (1979).

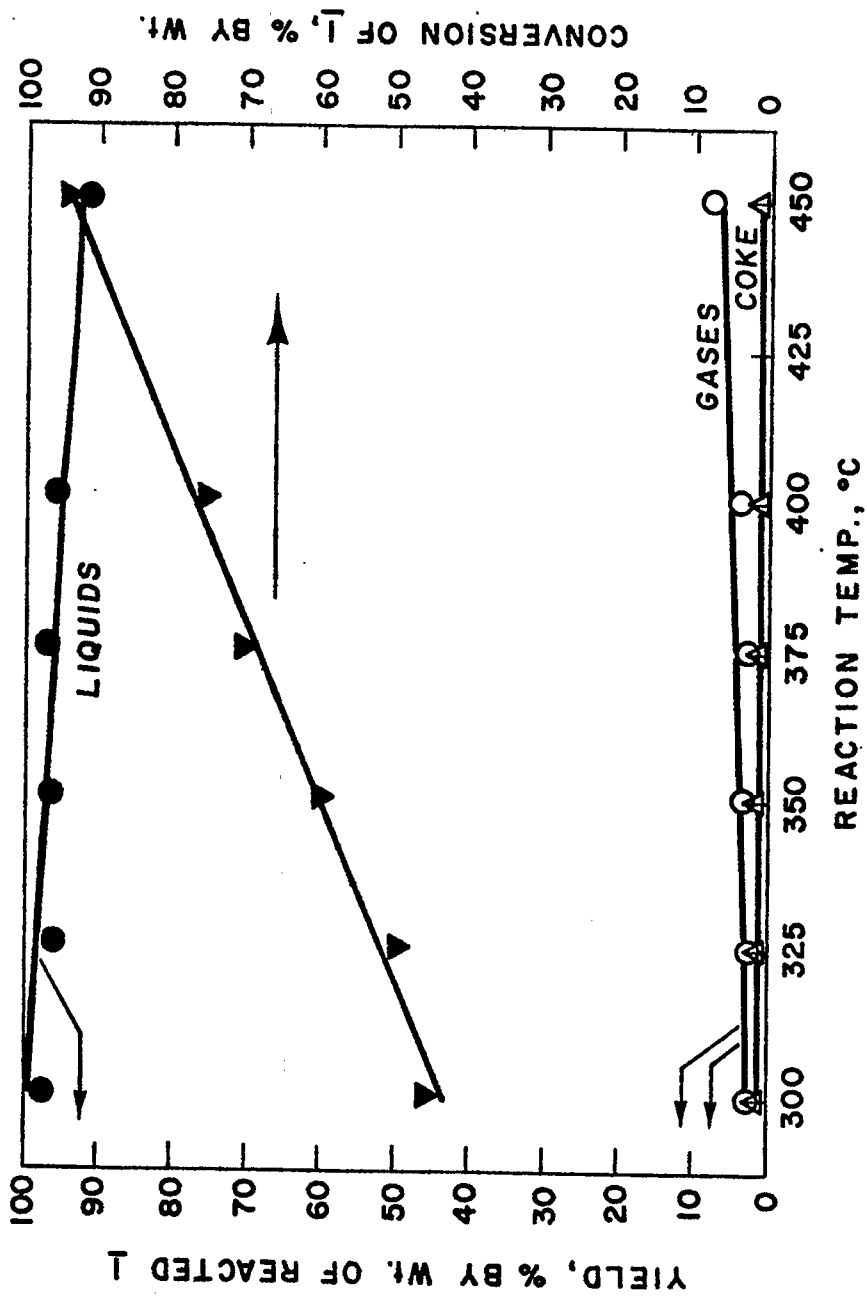


Figure 1. Distribution of liquid and gaseous products from cracking of decalin (I), as a function of reaction temperature, (Catalyst, Mobil-Durabead-8, LHSV = 0.65 hr<sup>-1</sup>).

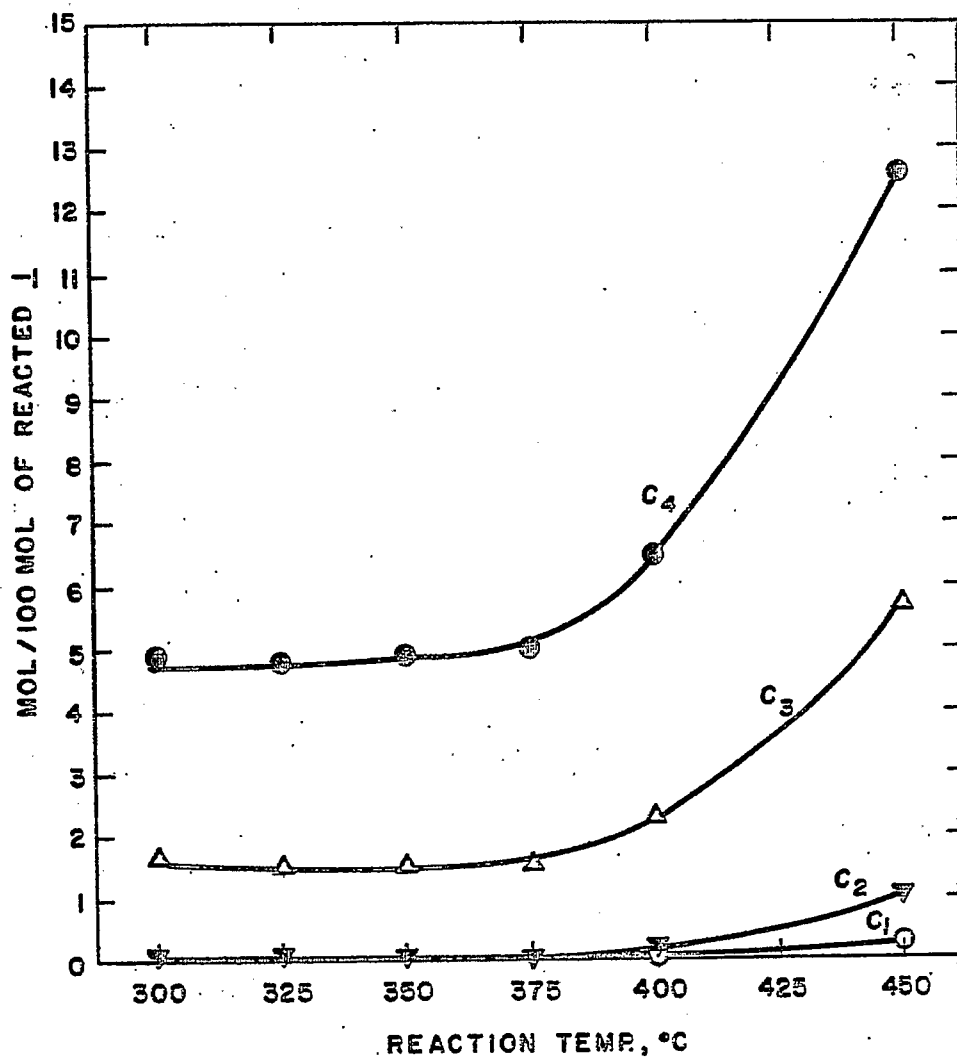


Figure 2. Change in gaseous product composition from cracking of decalin (1), as a function of reaction temperature, (Catalyst, Mobil-Durabead-8, LHSV = 0.65 hr<sup>-1</sup>).

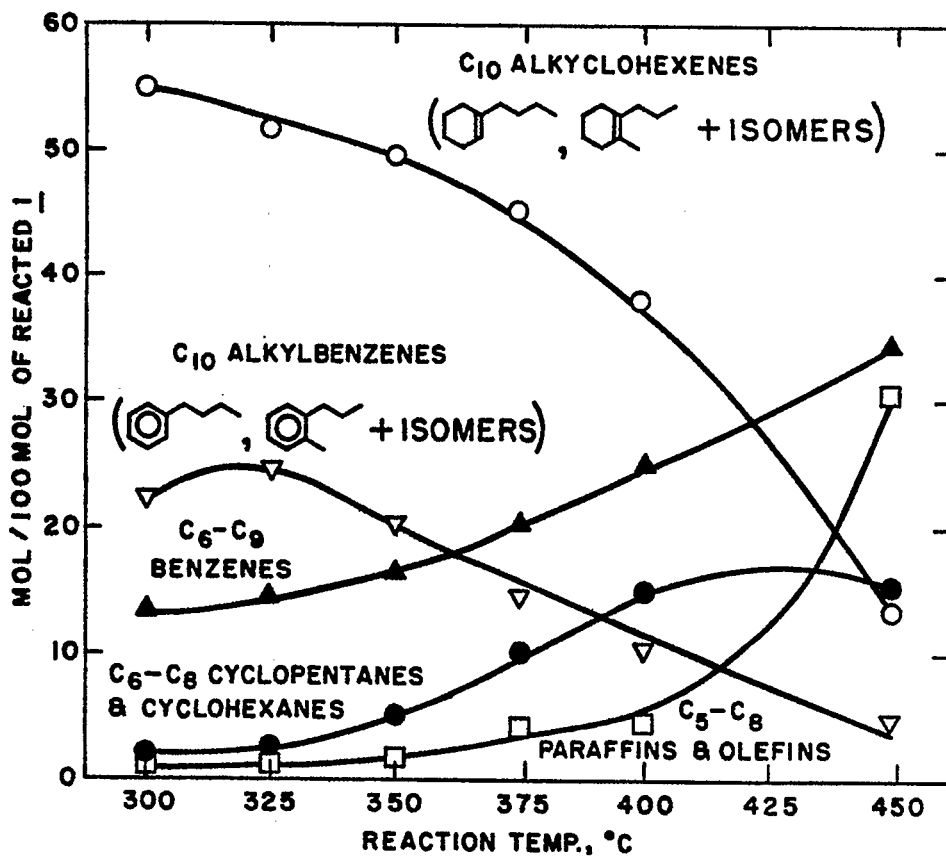


Figure 3. Change in product composition from cracking of decalin (1), as a function of reaction temperature (Catalyst, Mobil-Durabead-8, LHSV = 0.65 hr<sup>-1</sup>).

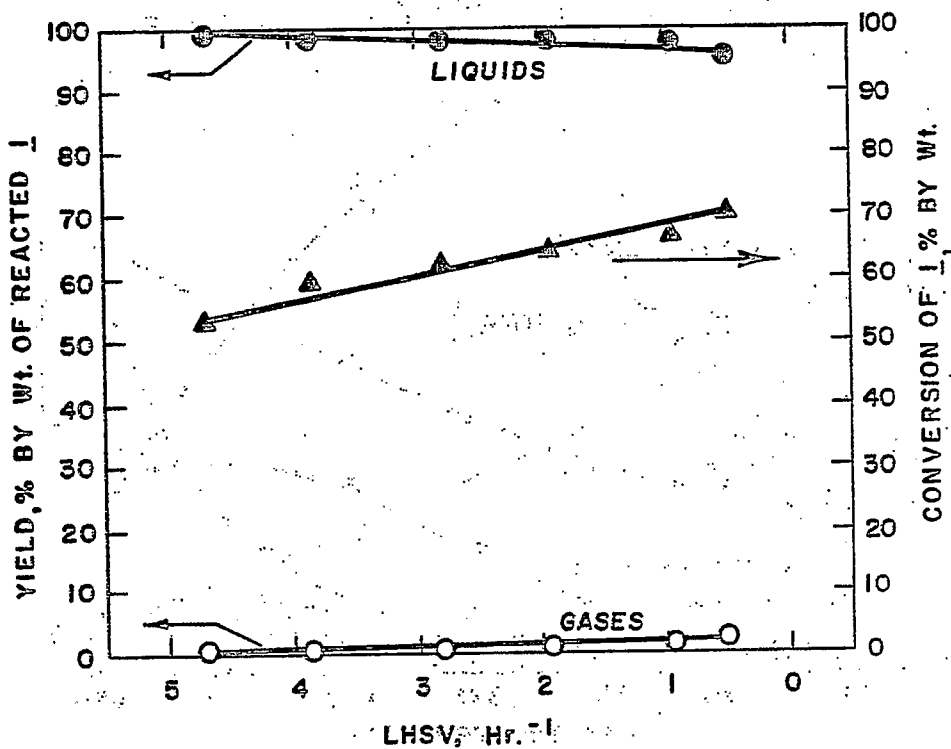


Figure 4. Distribution of liquid and gaseous products from cracking of decalin (1), as a function of LHSV (Catalyst, Mobil-Durabead-8, temperature, 375°C).

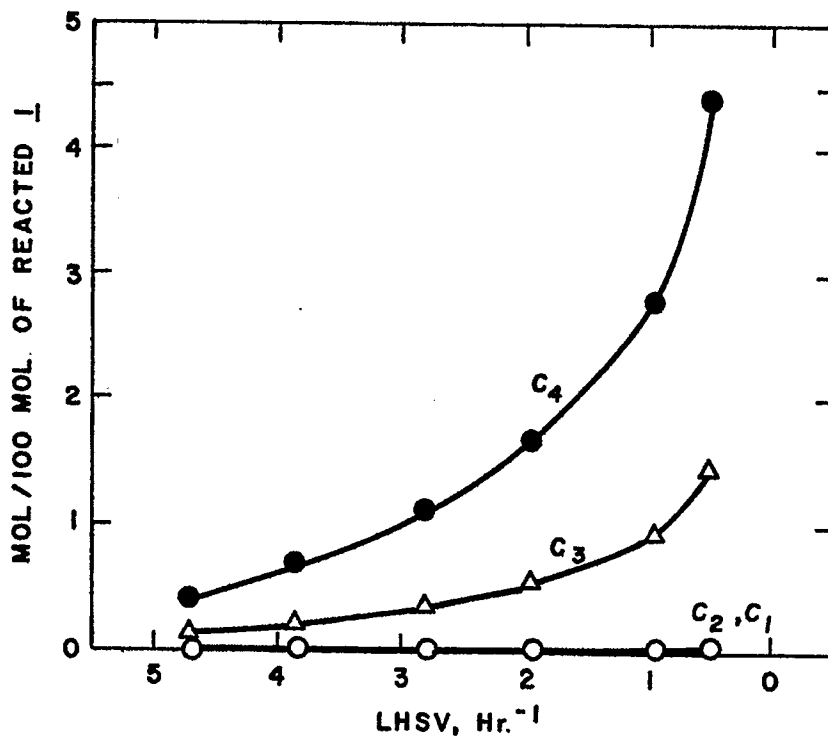


Figure 5. Change in gaseous product composition from cracking of decalin (1), as a function of LHSV, (Catalyst, Mobil-Durabead-8, reaction temperature, 375°C).



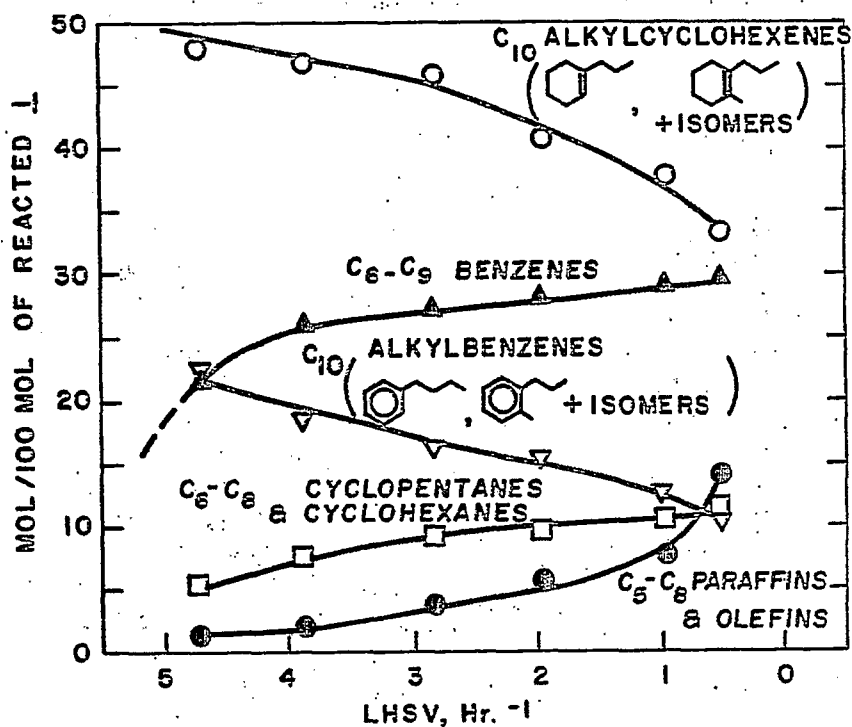


Figure 6. Change in product composition from cracking of decalin (I), as a function of LHSV (Catalyst, Mobil-Durabead-8, temperature, 375°C).

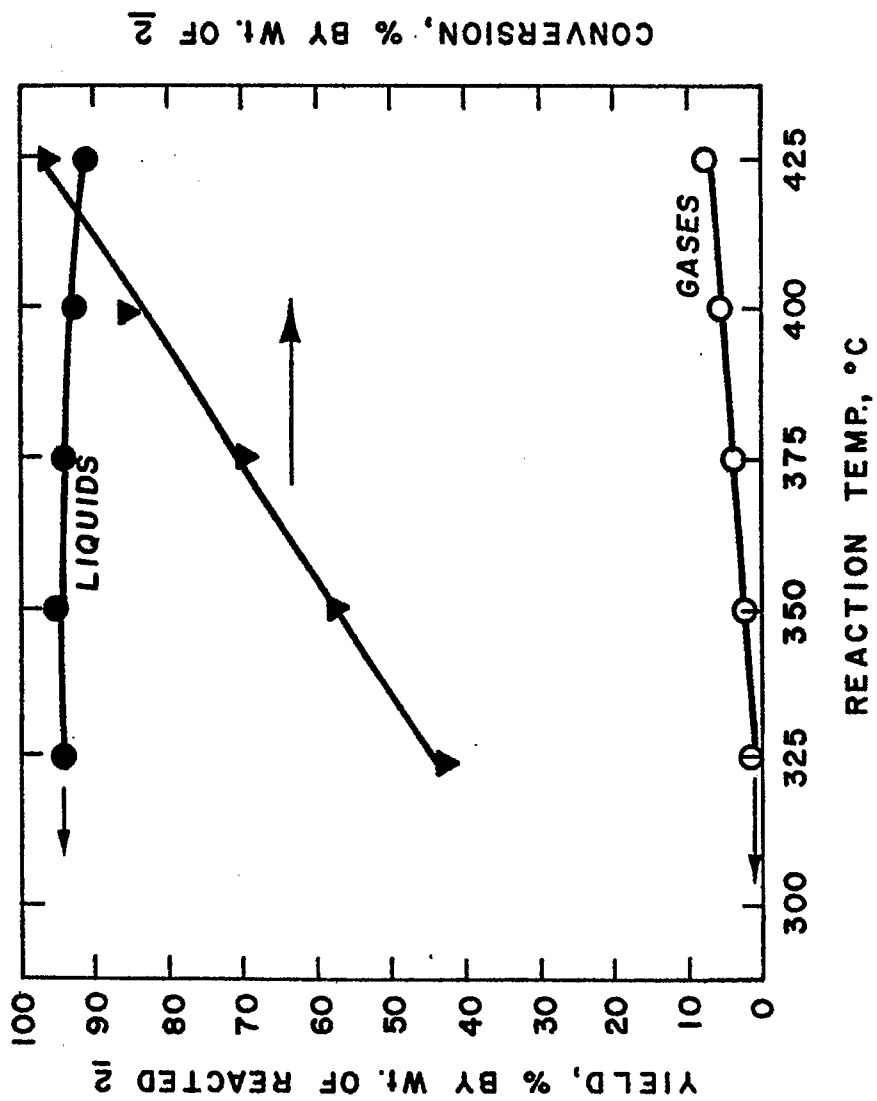


Figure 7. Distribution of products from cracking of perhydrophenanthrene (2), as a function of reaction temperature (Catalyst, Mobil-Durabead-8, LHSV = 0.76 hr<sup>-1</sup>).

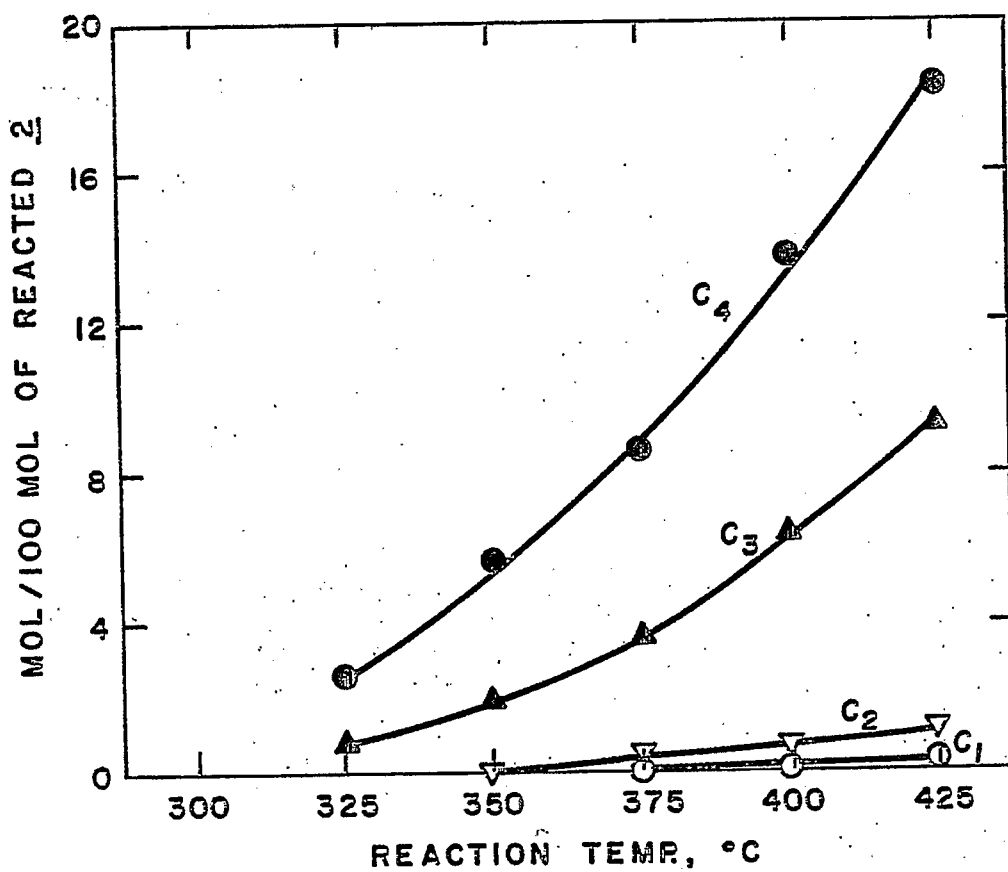
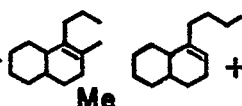
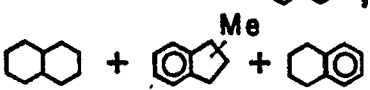


Figure 8. Change in gaseous product composition from cracking of perhydrophenanthrene (2), as a function of reaction temperature, (Catalyst, Mobil-Durabead-8, LHSV = 0.76 hr<sup>-1</sup>).

N = NAPHTHALENE

C<sub>14</sub>: ALKYL OCTAHYDRONS —  + ISOMERS

C<sub>11</sub>: TETRAHYDRONS 

C<sub>10</sub>:  + ALKYL CYCLOHEXENES

C<sub>6</sub>-C<sub>9</sub> BENZENES:  (R = C<sub>1</sub>-C<sub>3</sub>, or H)

C<sub>6</sub>-C<sub>7</sub> CYCLANES: 

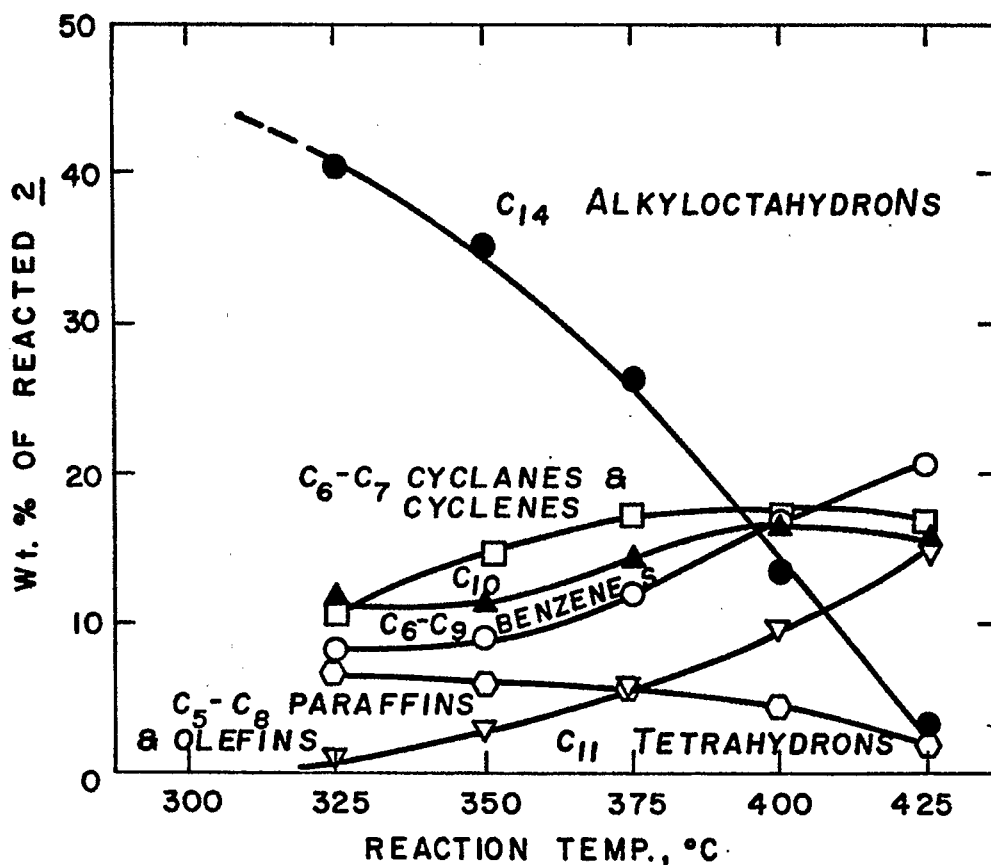
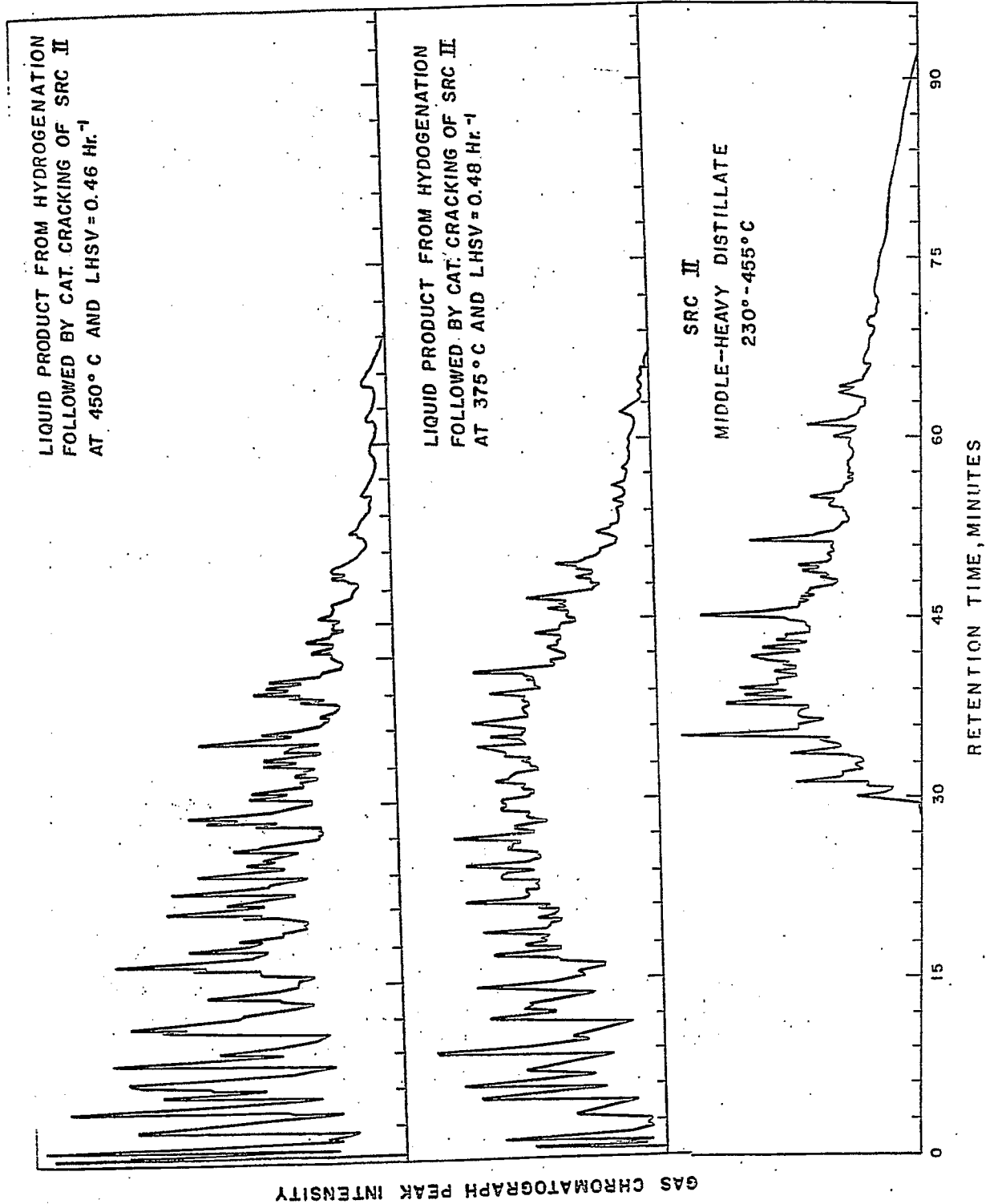


Figure 9. Change in liquid product composition from cracking of perhydrophenanthrene (2), as a function of reaction temperature (Catalyst, Mobil-Durabead-8, LHSV = 0.76 hr<sup>-1</sup>).

Figure 10. Chromatograms of SRC middle-heavy distillate and the liquid product from catalytic cracking (Catalyst, Mobil-Durabead-8).



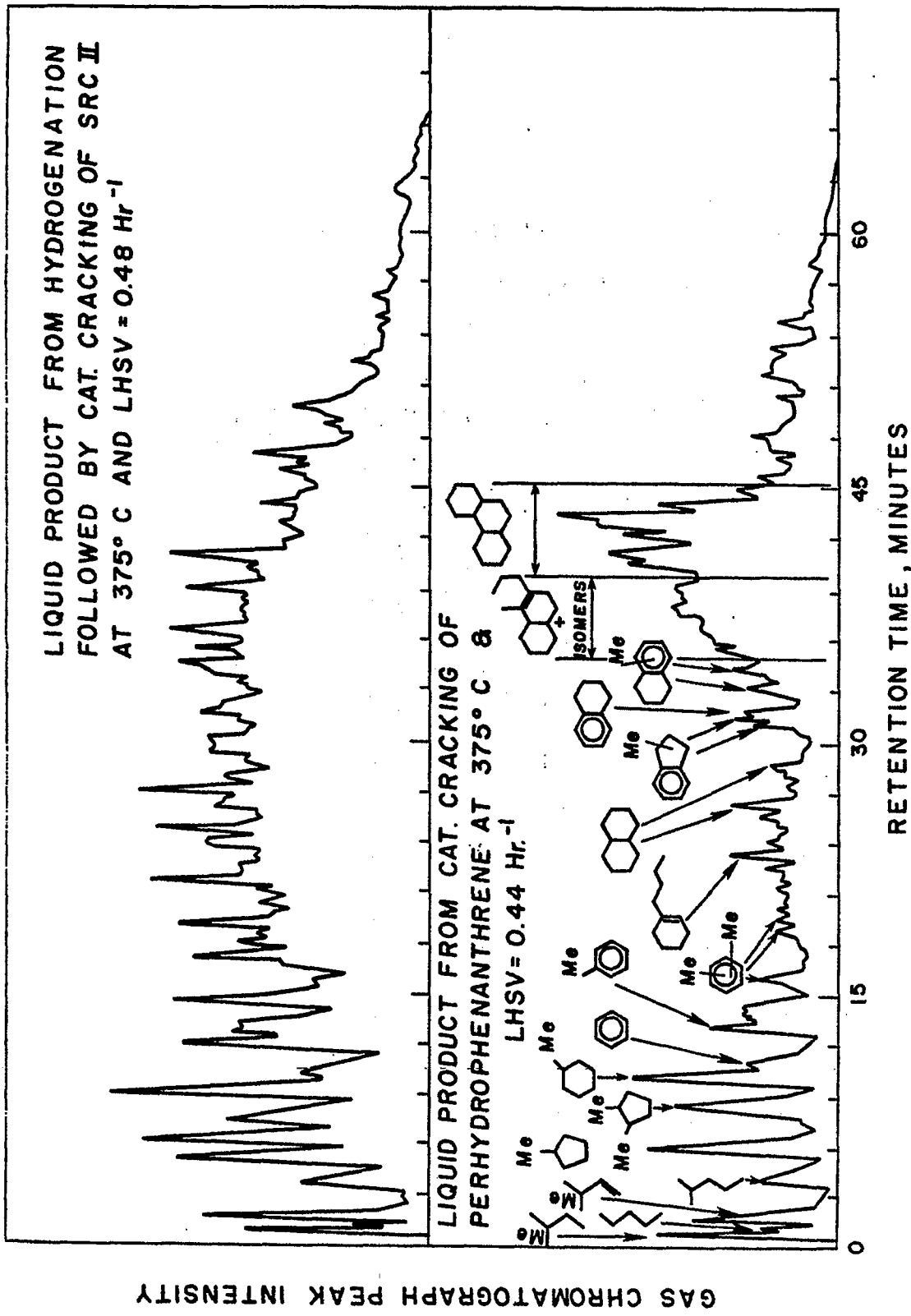


Figure 11. Chromatograms of liquid product from catalytic cracking of perhydrophenanthrene and hydrogenated SRC II (Catalyst, Mobil-Durabead-8).

TABLE 1  
SOME ANALYTICAL DATA ON SRC  
MIDDLE-HEAVY DISTILLATE

	SRC IIA <sup>a</sup>	HYDROGENATED SRC IIB <sup>b</sup>
S	0.36	< 0.01
N	1.25	< 0.1
C	88.65	89.0
H	8.28	10.8
O	1.46	< 0.1
H-AROMATICITY <sup>c</sup> , %	33.8	4.2
C-AROMATICITY, %	64.0	12.0

a - MIDDLE - HEAVY DISTILLATE (230 - 455°C)

b - CATALYST - SULFIDED Ni-W/Al<sub>2</sub>O<sub>3</sub>:

- TEMPERATURE - 370°C;

- PRESSURE - 2900 psig;

- REACTION TIME - 5 HR.

c - AROMATIC HYDROGENS, % OF TOTAL HYDROGENS.

TABLE 2  
 CATALYTIC CRACKING OF A HYDROGENATED  
 SRC II MIDDLE-HEAVY DISTILLATE (230-455°C)<sup>a</sup>

EXPT. NO.	SRC 102	SRC 105	SRC 103	SRC 104
REACTION TEMP., °C	375	400	425	450
DISTRIBUTION OF PRODUCTS, % BY WT.				
GASES	3.1	5.7	9.9	12.9
LIQUIDS	93.8	89.9	85.2	83.0
COKE & HEAVY ENDS	3.1	4.3	4.9	4.1
CONVERSION OF SRC <sup>b</sup> , % BY WT.	56.0	67.3	75.1	90.4

a - CATALYST - MOBIL DURABEAD - 8

- LHSV - 0.45 HR<sup>-1</sup>

- PRESSURE - ATMOSPHERIC

b - CONVERSION = GASEOUS + LIQUID PRODUCTS LIGHTER THAN THE SRC FEEDSTOCKS (b. p < 230°C)



## Catalytic Cracking of Coal-Derived Liquids

Faculty Advisor: F.V. Hanson  
Graduate Student: Jay Dorius

### Introduction

The catalytic cracking of coal-derived liquids may provide a viable means of upgrading these liquids to a marketable product. Previous studies have demonstrated that short residence time, high temperature fluid catalytic cracking of petroleum derived heavy gas oils to fuel oil and/or gasoline is feasible. The objective of the present investigation is to extend this work to coal-derived liquids.

### Project Status

Seventeen experimental runs have been made using a zeolite cracking catalyst (Mobil Durabead 9) and a gas oil from Altamont Crude Oil to shake down the equipment and to obtain base data for future work with coal-derived liquids. During these runs, several problems in the equipment have been discovered, causing some delay in the experimental work.

Material balance calculations were made for some of the latter runs. The best material balance obtained for any of the runs was 82%. The desired balance for this equipment would be in the range of 97-102%. Because of this problem, the feed system has been redesigned to ensure more accurate metering of the feed rate. The new design involves a special burette, which is presently being fabricated.

The catalyst hopper-regenerator has also been a source of difficulty. The heating system for the hopper failed, requiring a shutdown for repairs. When the insulation had been removed, it was discovered that the hopper material itself had failed. This required the fabrication of a new regenerator-hopper.

The original hopper was made of mild steel, which was not sufficiently strong for the high temperatures and long time required for catalyst regeneration. Therefore, 316 stainless steel was chosen as the material for the new hopper. An order has been placed for the necessary materials. After the materials have been obtained, the fabrication will probably take two to three weeks to complete.

## Future Work

When fabrication has been completed, the catalyst hopper will be installed and the catalyst flow rates will be recalibrated. After this work is completed, experiments will be conducted using a typical petroleum cracking feedstock to provide a basis for the catalytic cracking of coal-derived liquids.

Synthesis of Light Hydrocarbons From  
CO and H<sub>2</sub>

Faculty Advisor: F.V. Hanson  
Graduate Student: Y. S. Tsai

Introduction

The hydrogenation of carbon monoxide for the production of low molecular weight olefins (C<sub>2</sub>-C<sub>4</sub>) has been investigated over a variety of metallic catalysts. In particular, iron-manganese catalysts have exhibited significant selectivity for low molecular weight olefins. The initial catalyst screening data indicated that an iron-manganese catalyst composed of 2.2 parts of manganese per 100 parts of iron (atomic basis) would be the preferred composition with which to conduct a process variable investigation. The standard operating conditions for the iron-manganese catalyst screening studies were 500 psig, 1.06 g g<sup>-1</sup> s<sup>-1</sup> WHSV, H<sub>2</sub>/CO ratio of 2/1 and 7-9% conversion (single pass).

Project Status

The process variable investigation is virtually completed, that is, selected experiments are being repeated to assure that all trends that were observed can be reproduced. The primary variables investigated were temperature, space velocity, H<sub>2</sub>/CO ratio and pressure. The influence of the space velocity, H<sub>2</sub>/CO ratio and the pressure on the yield of C<sub>2</sub>-C<sub>4</sub> hydrocarbons and on the selectivity for the production of olefins was determined at 220°C. The influence of these variables was also explored at constant conversion. The C<sub>2</sub>-C<sub>4</sub> yield and the olefin selectivity for the 2.2/100 :: Mn/Fe catalyst as a function of temperature at the standard conditions are presented in Figure 1. The C<sub>2</sub>-C<sub>4</sub> yield and the olefin selectivity at constant conversion as a function of space velocity, H<sub>2</sub>/CO ratio and pressure are presented in Figures 2-4. The yield and selectivity at 220°C as a function of space velocity, H<sub>2</sub>/CO ratio and pressure are presented in Figures 5-7. The following preliminary conclusions were drawn from these experiments:

- 1) The C<sub>2</sub>-C<sub>4</sub> hydrocarbon yield was insensitive to process variable changes at constant conversion and at constant temperature.
- 2) Increasing temperature brought about greater olefin selectivity and reduced methane production.
- 3) At constant conversion the olefin selectivity improved with increasing space velocity and decreased with

increasing H<sub>2</sub>/CO ratio. The effect of pressure is being rechecked due to the inconsistent data at 750 psig.

4) At constant temperature the olefin selectivity increased with increasing space velocity and decreased with increasing H<sub>2</sub>/CO ratio. Again the pressure data was inconsistent.

#### Future Work

The response of three additional catalysts of different Mn/Fe composition will be investigated to process variable changes. Catalyst preparation and in-situ activation procedures will also be investigated.

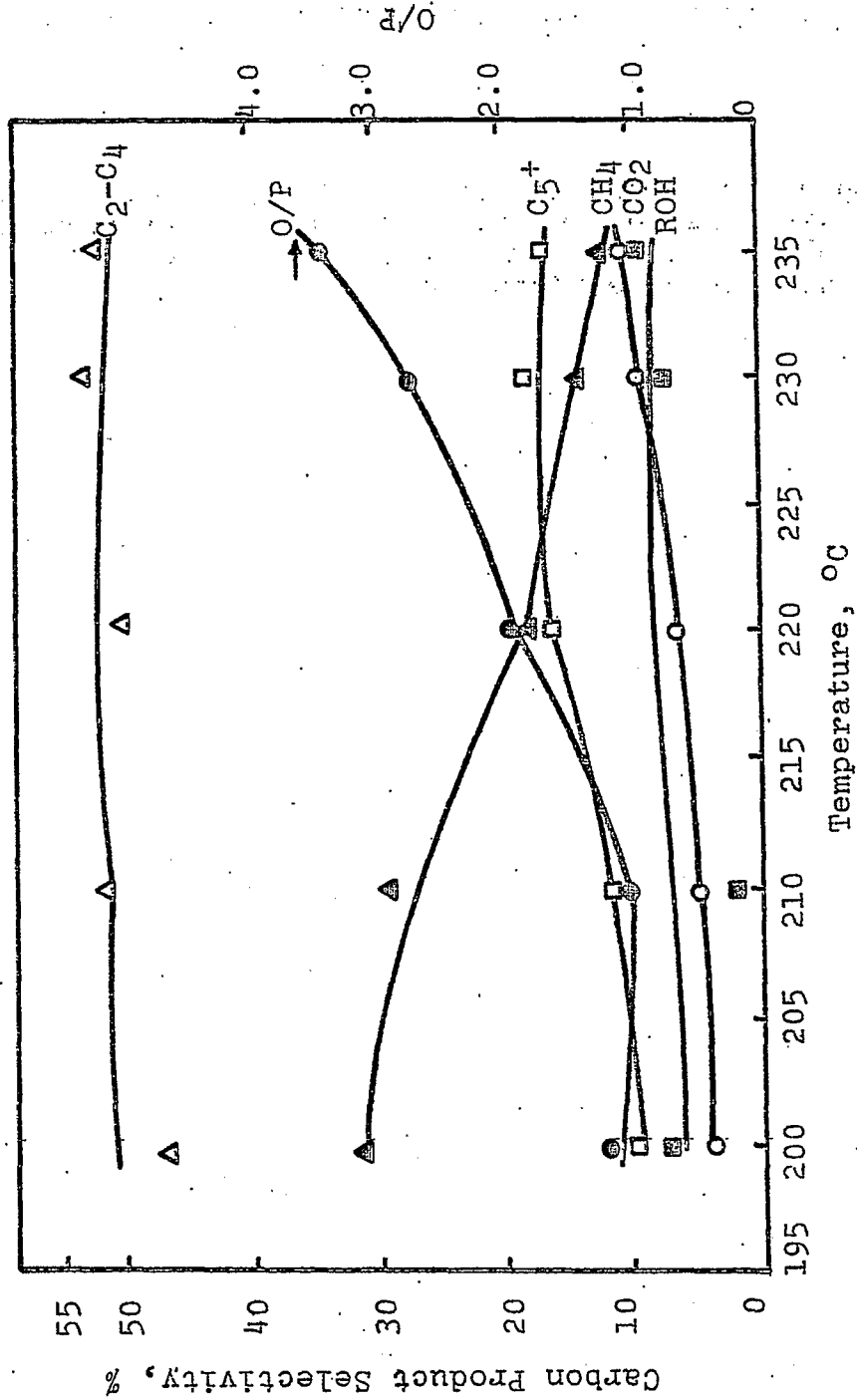


Figure 1. Effect of temperature.  
 FM #3, Atomic 2.2 Mn/100 Fe, 500 psig, 1.06 cc/g/sec, H<sub>2</sub>/CO=2/1

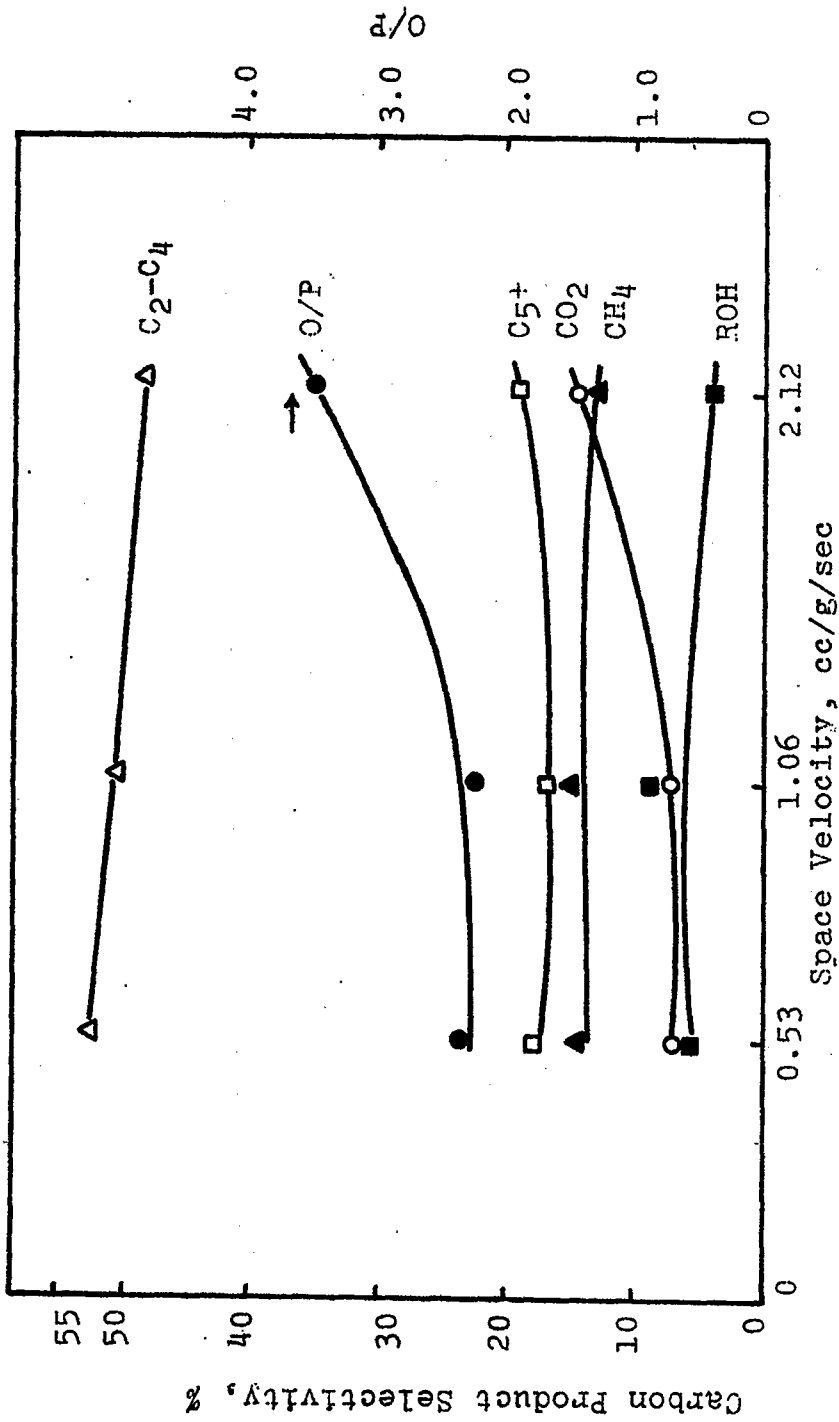


Figure 2. Effect of space velocity (based on constant CO conversion).  
 7.0% CO conversion, Atomic 2.2 Mn/100 Fe, 500 psig, H<sub>2</sub>/CO=2/1

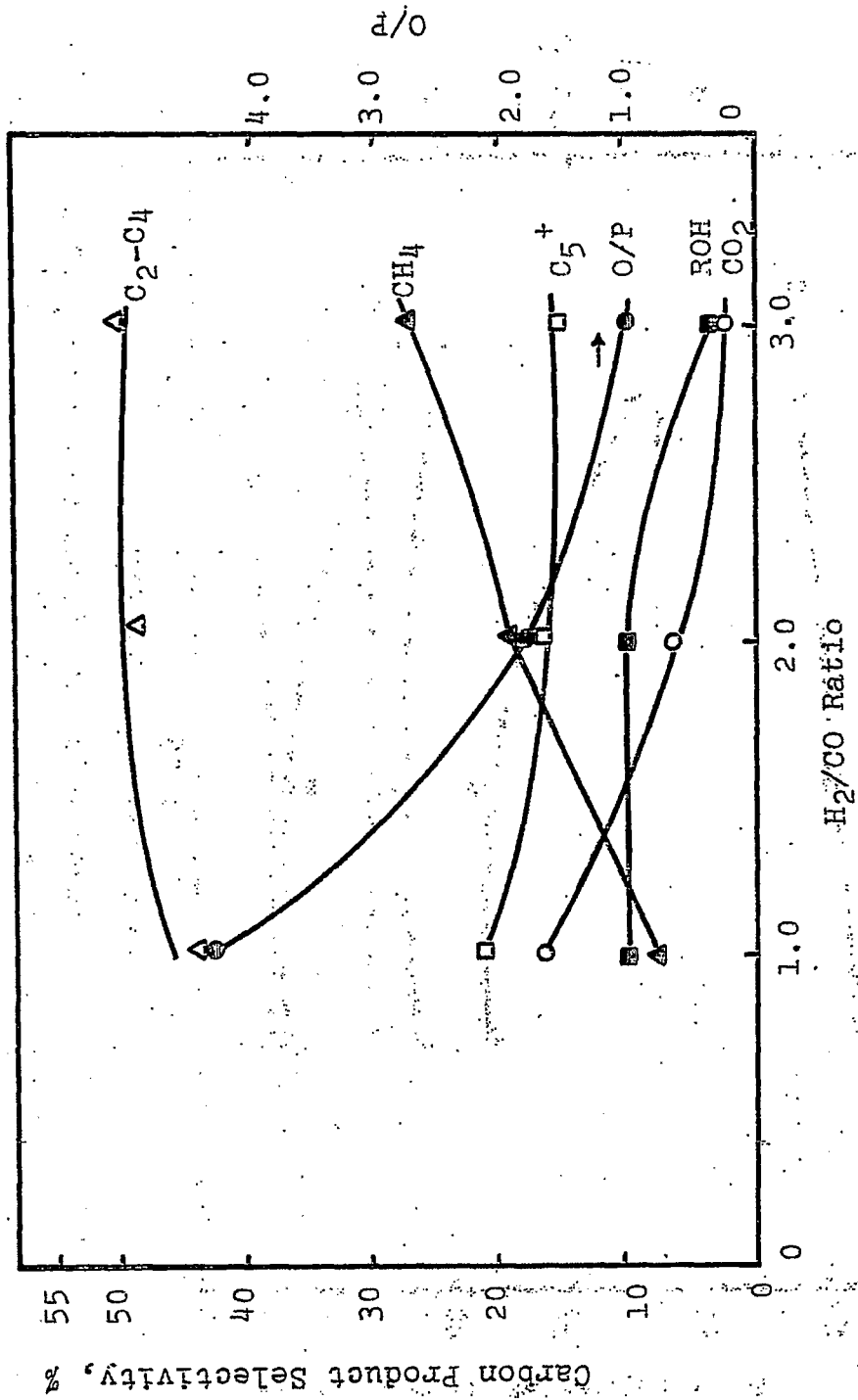


Figure 3. Effect of H<sub>2</sub>/CO ratios (based on constant CO conversion).  
 5.5% CO conversion, Atomic 2.2 Mn/100 Fe, 1.06 cc/g/sec, 500 psig

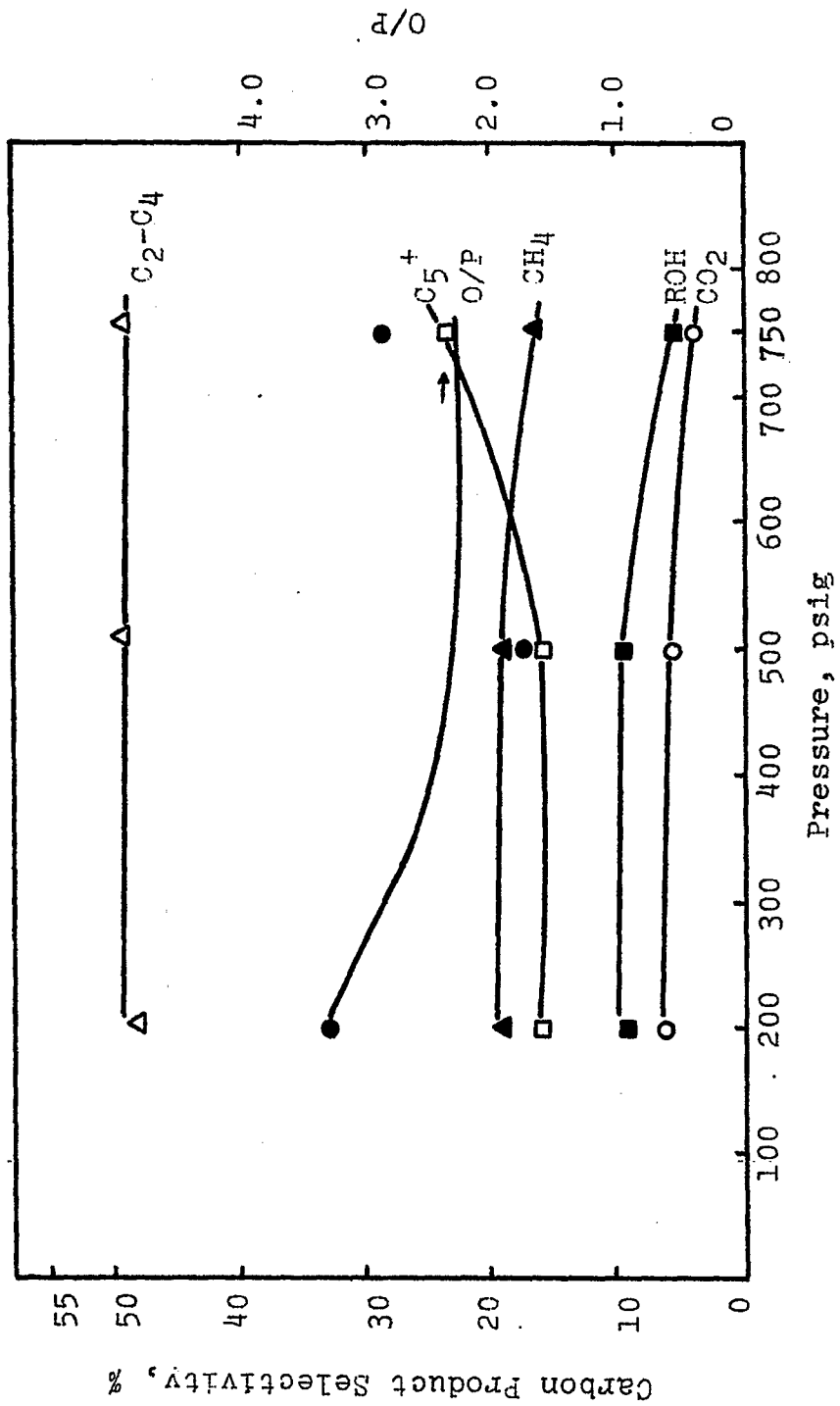


Figure 4. Effect of pressures (based on constant CO conversion).

5.0~6.0% CO conversion, Atomic 2.2 Mn/100Fe, 1.06 cc/g/sec, H<sub>2</sub>/CO=2/1



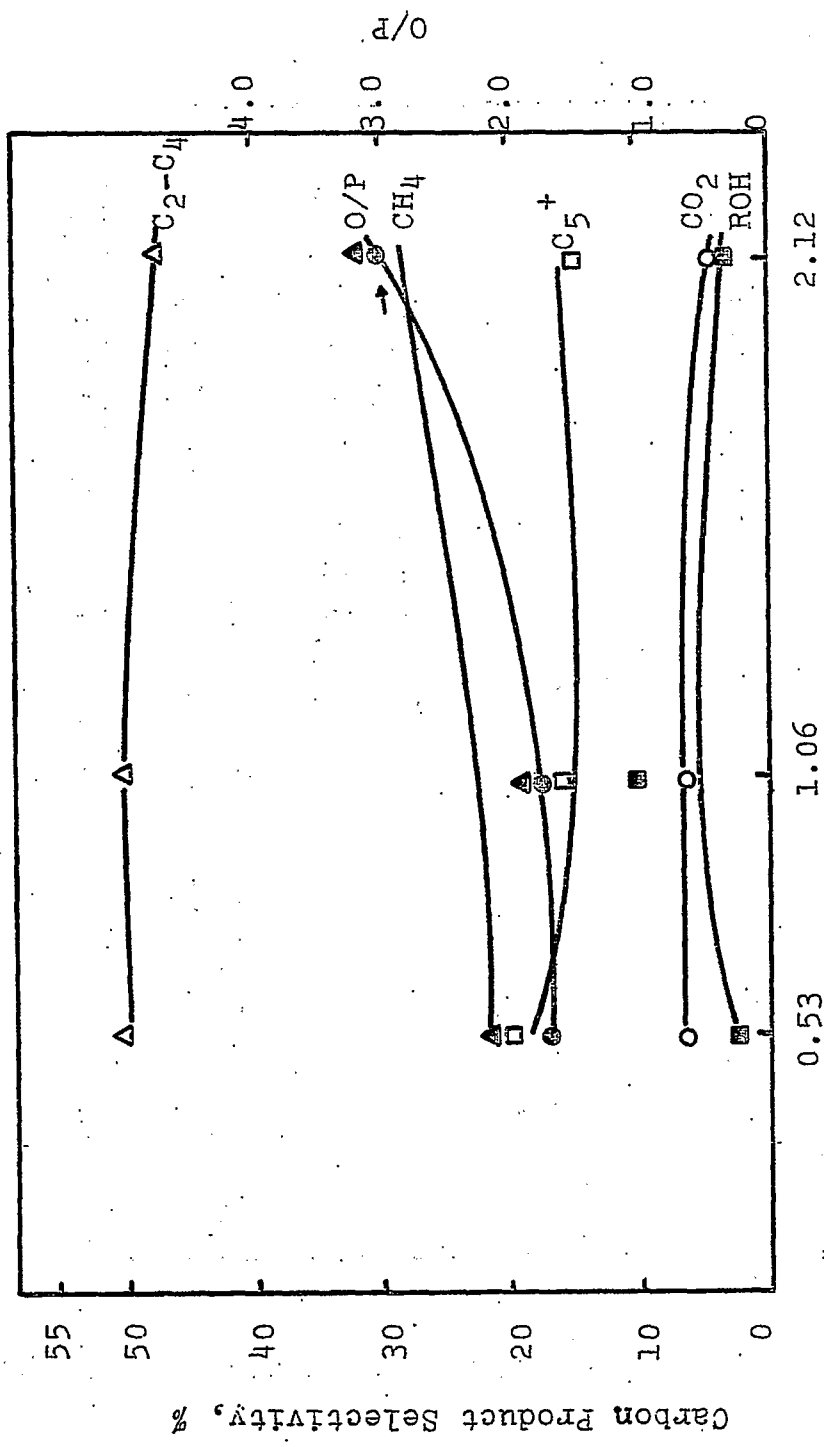


Figure 5. Effect of space velocity (based on constant temperature) 220°C, Atomic 2.2 Mn/100 Fe, 500 psig, H<sub>2</sub>/CO=2/1

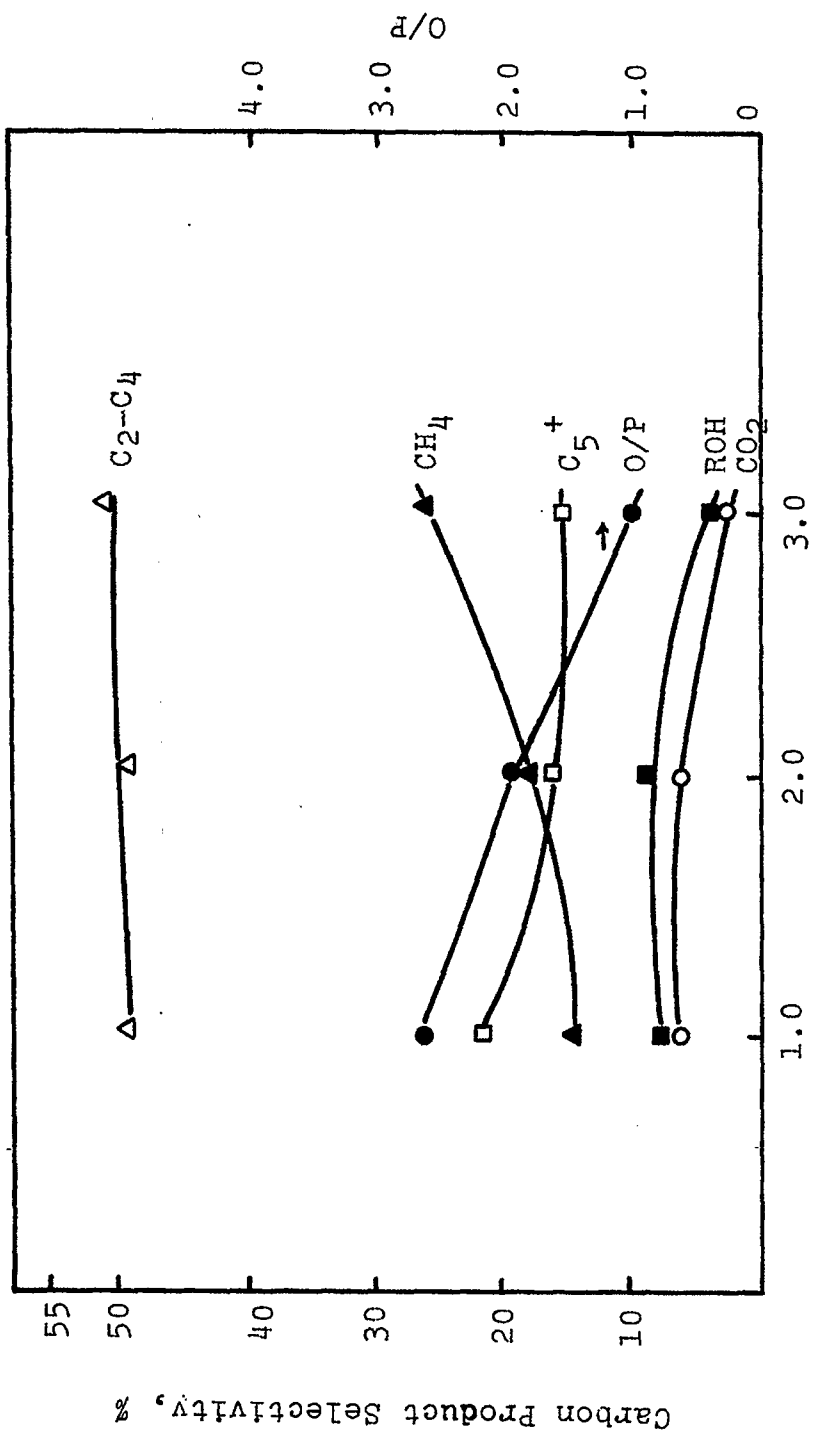


Figure 6. Effect of H<sub>2</sub>/CO ratios (based on constant temperature).  
 220°C, Atomic 2.2 Mn/100 Fe, 1.06 cc/g/sec, 500 psig

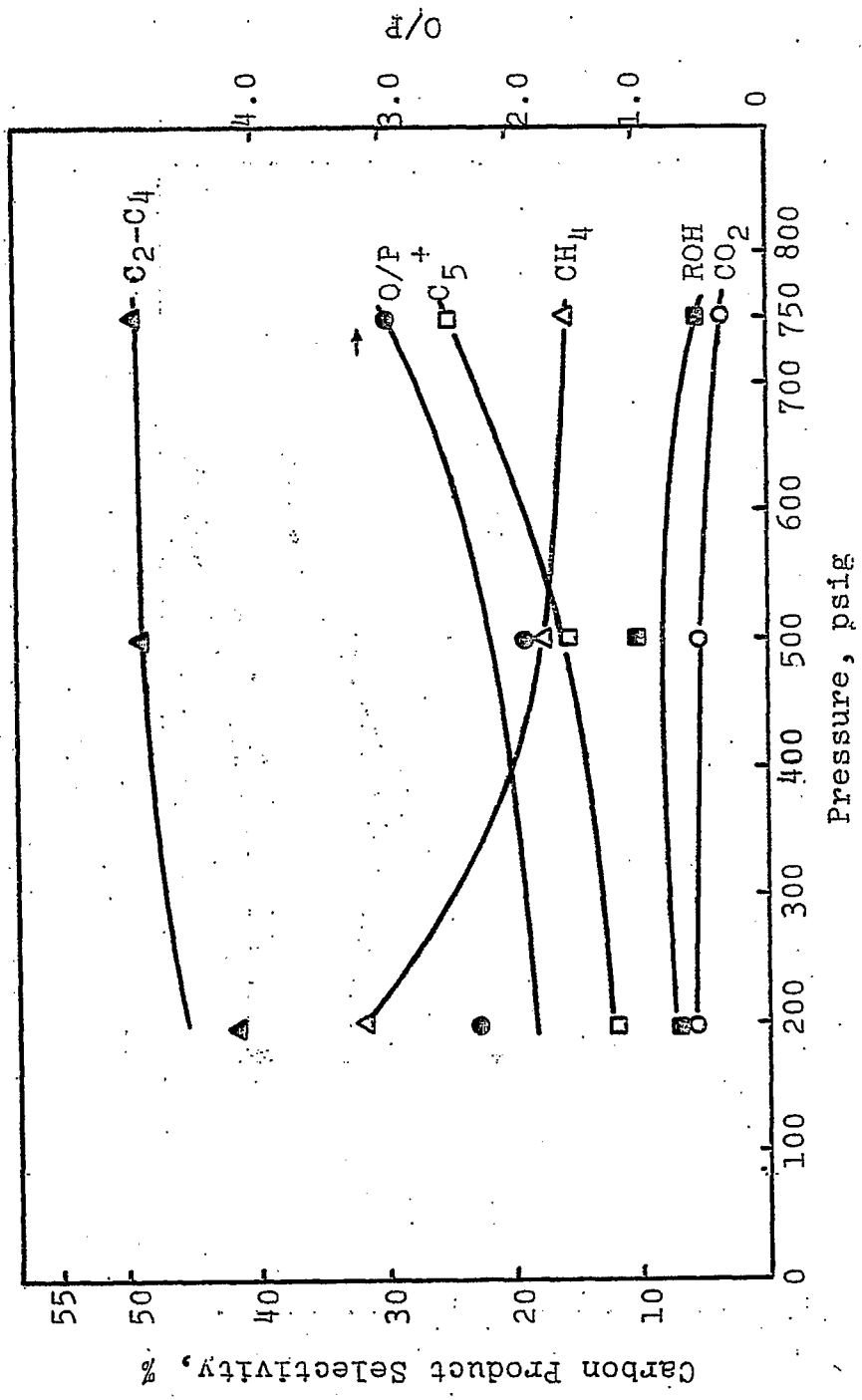


Figure 7. Effect of pressures (based on constant temperature) 220°C, Atomic 2.2 Mn/100 Fe, 1.06 cc/g/sec, H<sub>2</sub>/CO=2/1

Synthesis of Light Hydrocarbons from  
CO and H<sub>2</sub> (Continued)

Carbon Monoxide Hydrogenation in a Slurry Reactor

Faculty Advisor: F.V. Hanson  
Graduate Student: W.P. Tai

Introduction

The exothermic nature of the carbon monoxide hydrogenation reaction severely limits the conversion level that can be attained in a fixed-bed reactor. The "hot spot" observed in fixed-bed operation accelerates the Boudouard reaction (disproportionation of CO to CO<sub>2</sub> and carbon) with the concomitant fouling of the catalyst and shifts the selectivity in the direction of methane. Thus, the global heat release must be dissipated to suppress these undesirable side reactions. The objective of this investigation is to explore the potential of the slurry reactor for the dissipation of the heat generated during reactions, thereby maintaining the catalyst activity and selectivity.

Project Status

The fixed-bed slurry reactor unit design has been completed and is under construction. The reactor section has been completed and is undergoing preliminary testing. The preliminary testing consists of a hydrostatic and a dynamic pressure test, an assessment of the gas-liquid mixing at the reactor inlet and gas-liquid separation downstream of the reactor. All preliminary tests are being conducted with a stainless steel tube in place of the reactor.

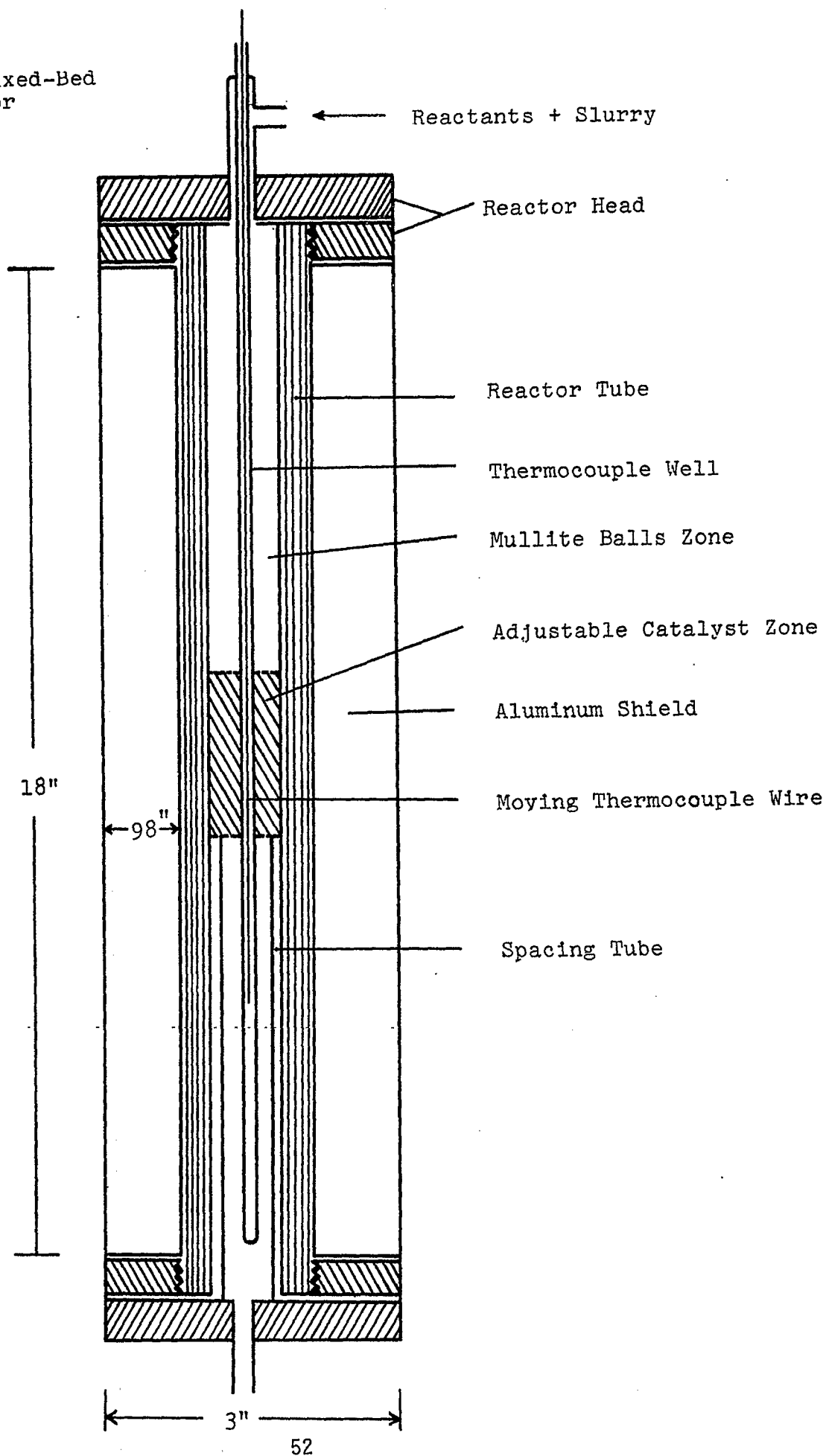
The fixed-bed reactor has been designed and fabricated on site. The reactor is shown in Figure 1. The core of the reactor is a stainless steel tube with an inside diameter of 0.8 of an inch. This tube is surrounded by an aluminum shield 0.8 of an inch thick which serves as a heat reservoir for the reactor. The catalyst bed is confined to the center zone of the reactor by spacers, and a bed of mullite balls in the upper zone of the reactor serves as a preheater to bring the liquid-gas mixture to the reaction temperature. The reactor is fitted with a thermowell to permit the axial temperature profile to be continuously monitored.

The product recovery zone has not yet been completely designed and is only partially constructed.

### Future Work

The fabrication and preliminary testing of the system will be completed. The initial catalytic test will involve the hydrogenation of carbon monoxide over a commercially available ammonia synthesis catalyst in the fixed-bed gas phase mode of operation. The data from this experiment will then be compared to data obtained in the slurry-bed mode of operation at identical processing conditions. Once the operating procedure has been developed and refined, a series of Fe-Mn catalysts will be tested in the slurry-bed mode of operation.

Figure 1. Fixed-Bed Slurry Reactor



Synthesis of Light Hydrocarbons From CO and H<sub>2</sub>  
(Continued)

Catalyst Characterization Studies

Faculty Advisor: F.E. Massoth  
Graduate Student: K.B. Jensen

Introduction

This phase of the project is intended to supplement the high pressure reactor studies by detailed examination of the catalyst properties which enhance catalyst activity and selectivity. This is accomplished by characterization studies performed on the same catalysts which have been run in the reactor. Of particular interest are metal areas, evidence of alloy formation, phase structures and catalyst stability. Also, variables in catalyst preparation and pretreatment are examined to establish effects on catalyst properties. Finally, in-situ adsorption and activity are studied under modified reaction conditions with a number of well-characterized catalysts to obtain correlating relationships.

Previous characterization work was devoted to the copper-cobalt-alumina catalyst system. This study has been completed. Current work involves characterizing iron-based catalysts. The latter catalysts have shown significant improvements in production of light olefins over that achieved by the Co-Cu-Al<sub>2</sub>O<sub>3</sub> catalyst. Characterization techniques similar to those developed for the Co-Cu-Al<sub>2</sub>O<sub>3</sub> catalyst are being applied to the iron-based catalysts.

Project Status

Studies this period were directed to a more detailed examination of one of the manganese-promoted iron catalysts, viz., catalyst #76, having a Mn/Fe = 0.43. Previous results had shown the major components of the reduced catalyst (H<sub>2</sub>, 500°C) to consist of iron metal and manganese (II) oxide.<sup>1</sup> A physical mixture of powdered iron and manganese (II) oxide was prepared of about the same composition for comparison with the reduced catalyst #76. The X-ray diffraction spectra of the catalyst matched that of the prepared mixture with respect to the number of peaks and approximate peak position, confirming the existence of two phases in the catalyst, a metal iron phase and an oxide phase. A slow

scan across the region of the major MnO peak showed a slight shift in position from that of the physical mixture and of MnO alone; the peak was also broader than that of bulk MnO. Figure 1 shows this shift relative to peak positions for bulk MnO and FeO. The peak shift can be attributed to the presence of FeO in the oxide phase. Generally, FeO and MnO can form a solid solution and the X-ray lattice constant of this solution is directly proportional to the fraction of FeO present.<sup>2</sup> The accepted lattice constant of FeO is 4.306 Å (Fe-Fe distance) and that of MnO is 4.446 Å; the experimental values resulting from the present work are 4.30 Å and 4.44 Å, respectively. The experimental lattice constant of the oxide phase of reduced catalyst #76 is 4.414 Å. The lattice constant indicates about 0.2 mole fraction FeO in the oxide phase of the reduced catalyst.

Thermodynamically the amount of FeO can be predicted and depends upon the water partial pressure during reduction. The particular sample of catalyst #76 was reduced in the micro-balance for 20 hours at 500°C; the hydrogen flow rate and perhaps mass transfer conditions were not sufficient for complete reduction resulting in the presence of some FeO in the Mn oxide phase.

The X-ray diffraction peaks of the oxide phase showed definite broadening. How much of this results from the FeO and MnO combination effects is not presently known. However, a calculation of the particle size of the oxide phase can be made based on the pure MnO peak width. The calculated value is about 200 Å.

A BET surface area measurement was made on reduced catalyst #76 and the commercial MnO used in the physical mixture. The surface area of the catalyst was 5.4 m<sup>2</sup>/g while that of the MnO was very low, about 0.5 m<sup>2</sup>/g. Based on the composition of catalyst #76, an average particle density of 6.8 g/cm<sup>3</sup> can be calculated. This particle density gives an average spherical particle diameter of about 1600 Å for the catalyst. This information along with that from the X-ray line broadening begin to establish the micro-structure of the catalyst; the data is preliminary, however.

The X-ray data indicate an oxide particle size of about 200 Å. This corresponds to a BET surface area of 55 m<sup>2</sup>/g MnO. In catalyst #76, which is 36% oxide by weight, this would give a BET surface area of 20 m<sup>2</sup>/g catalyst from the oxide phase alone. However, the BET value of 5.4 m<sup>2</sup>/g indicates that not all the oxide phase is available as BET surface or that the oxide phase is not as dispersed as calculated. The iron particle size may be larger than that calculated for the iron and oxide mixture, to accommodate the larger surface area associated with the oxide particles. However, the iron would not normally encapsulate the oxide phase. Additional information is needed



before a model of the iron-manganese oxide micro-structure can be established.

A chemisorption run was made in the microbalance on a commercial MnO sample. The sample was first heated in hydrogen to 500°C to remove any easily available oxygen. The sample was then cooled to room temperature in hydrogen or helium, and depending upon the desired adsorbate, oxygen or carbon monoxide was introduced to the system. This cycle was repeated several times. The adsorbate loss and addition was monitored by observing weight changes of the sample. To help compensate for gas buoyancy effects, the weight values were noted with the sample in a helium atmosphere. The oxygen uptake value was 0.29 mg O<sub>2</sub>/g taken after several reduction cycles. After reduction treatment with hydrogen, no weight difference was observed when carbon monoxide was exposed to the MnO sample. Since the BET surface area results indicate a small available surface, additional chemisorption experiments with a more finely divided MnO sample will be done in the future.

The scanning electron microscope is being utilized to study the physical structure of the catalysts and the oxide particle size and distribution. The SEM is equipped with an X-ray spectrometer which allows the identification of particular elements. Iron and manganese, being next to one another in the periodic table, have similar X-ray energies associated with their excited states; however, resolution is more than adequate to distinguish between the two elements with the present instrument. Examination of reduced catalyst #76 at the highest magnification and smallest scan, has been used to detect compositional differences in different surface locations of the catalyst. The existence of areas of high iron content can be detected. However, the oxide areas are more difficult to isolate. The SEM studies will be continued and more information is expected from this technique.

Another reduction run was performed on catalyst #76 in the microbalance. Glass wool was placed over the sample bucket to prevent catalyst loss during heating. The catalyst currently being examined "popped" upon heating, resulting in catalyst loss when done in a shallow, open container. Also precaution was taken to heat the catalyst slowly. This "popping" effect is probably due to the decomposition of the nitrate that may still be present in the catalyst from the preparation stage, though no specific tests of this hypothesis have been made. The reduced weight of the catalyst during this repeat run was about 43% that of the initial catalyst weight. The previous experimental value was 35%, where some catalyst evidently had been physically lost from the sample bucket. The weight loss profiles are given in Figure 2. The majority of the weight loss occurred between 160-200°C, with a smaller additional loss above 350°C. Previous results with this catalyst showed a greater loss in the 160-200°C region and a slightly greater loss occurring above

450°C. The overall shape of the weight loss curves are very similar in both cases.

#### Future Work

Work will be continued in each of the areas mentioned in this report, i.e., X-ray diffraction, SEM, BET surface area, and chemisorption studies. Examination of the catalyst with ESCA will be tried shortly. Additional information and experience is needed with these techniques before the Fe-MnO catalysts can be firmly characterized.

#### References

1. W.H. Wiser et al., DOE Contract No. E(49-18) - 2006, Quarterly Progress Report, Salt Lake City, Utah, Oct-Dec 1978.
2. P.K. Foster and D.J.E. Welch, Trans. Faraday Soc., 52, 1636 (1956).

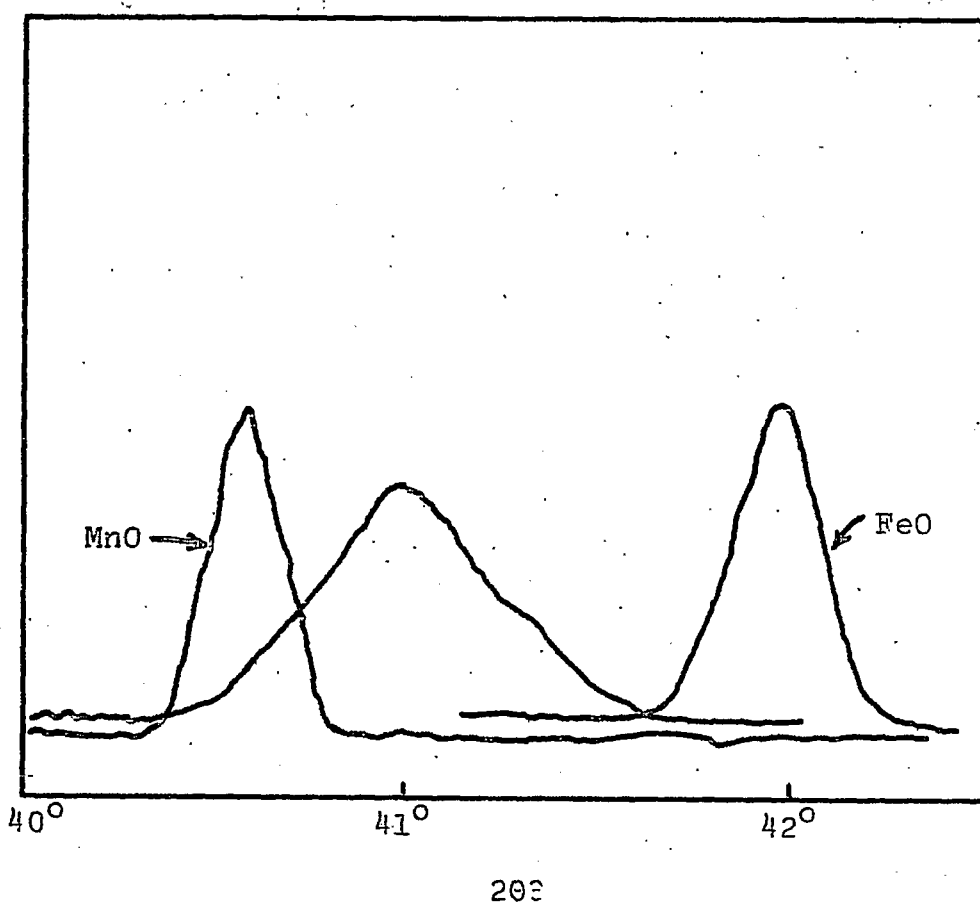


Figure 1. X-Ray Diffraction Pattern for Reduced Catalyst #76 Showing Principle Oxide Peak Compared to Bulk MnO + FeO.

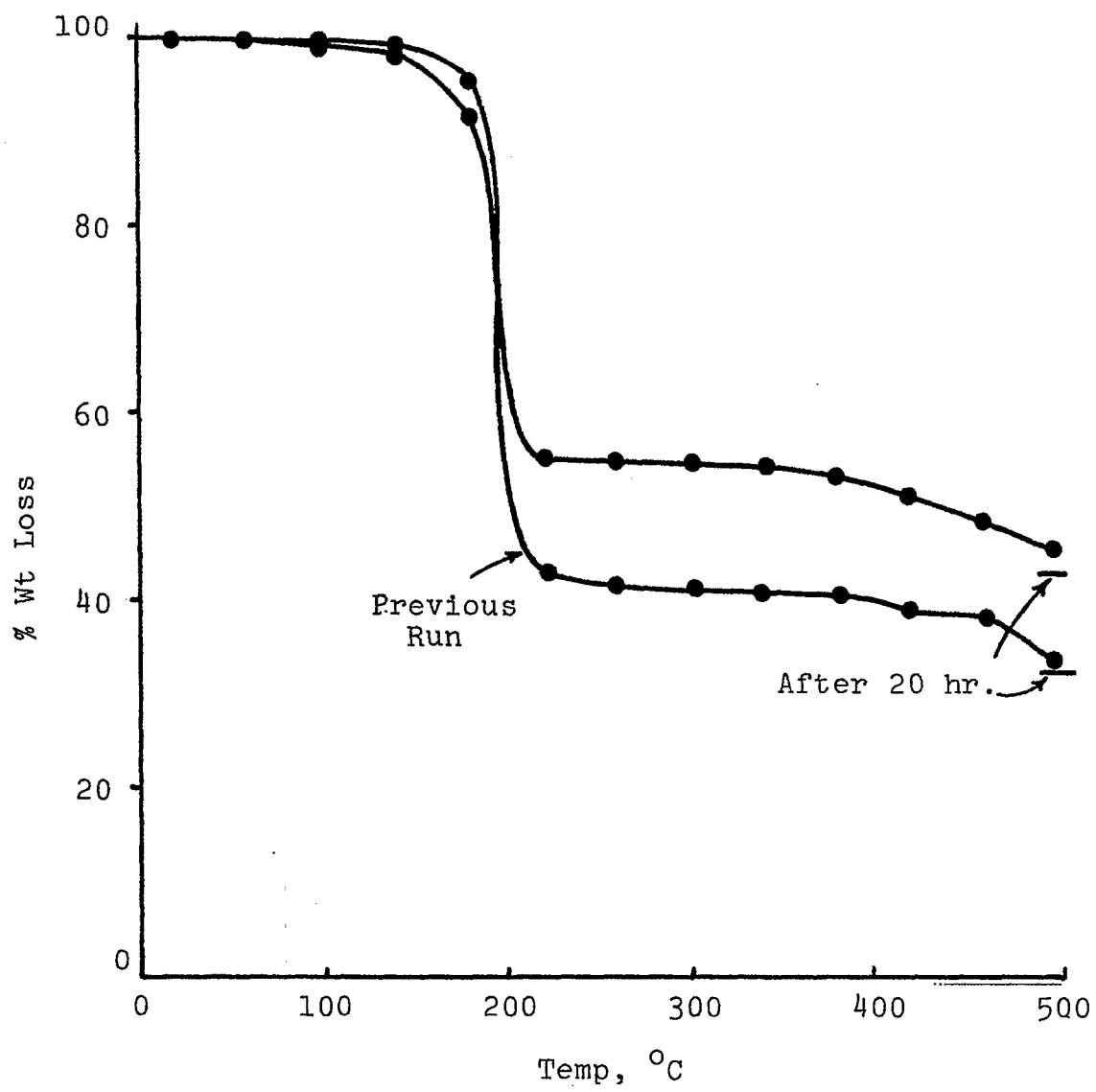


Figure 2. Reduction of Catalyst #76.

Mechanism of CO Hydrogenation

Faculty Advisor: S.W. Cowley  
Graduate Student: T.L. Cable

Introduction

The objective of this study is to supply detailed information about the surface mechanism of CO hydrogenation. The specific goal is to investigate the factors controlling catalyst product selectivities. Extensive technology exists for the production of methane, methanol and C<sub>5</sub><sup>+</sup> hydrocarbons from CO and hydrogen; however, no current technology exists for the production of light olefins. There is a need to identify the fundamental surface chemistry involved. An understanding of the surface reaction and kinetics can provide valuable information in the development of more selective and more effective catalysts, rather than relying on time consuming trial and error techniques. This knowledge would benefit the fuels industry as well as the chemical process industry.

Project Status

The equipment has been assembled and consists of a flow chemisorption apparatus, a volumetric chemisorption apparatus and a flow constant stirred tank reactor. The flow chemisorption apparatus is shown in Figure 1. The following procedure is used:

1. Reduce catalyst in H<sub>2</sub> at 500°C.
2. Flush with He at 500°C.
3. Cool catalyst in He to room temperature.
4. Introduce successive 50 ml pulses of substrate to be chemisorbed.
5. Monitor amount of substrate chemisorbed.
6. Temperature programmed desorption of substrate in He carrier.

The technique provides valuable information regarding the available metal surface area, the temperatures at which substrate desorption occurs (and thus the activation energy for chemisorption) and the nature of the desorbing species. For example, CO may chemisorb but at some particular temperature CO<sub>2</sub> and not CO may desorb. A quadrupole mass spectrometer and a thermal

conductivity detector will determine the nature and quantity of the desorbing species.

A volumetric chemisorption apparatus is available to check the validity of the flow chemisorption technique. A flow constant stirred tank reactor (Berty reactor) is required for detailed mechanistic studies and is shown in Figure 2. The Berty reactor was purchased from Autoclave Engineers and is capable of pressures of 500 psi and temperatures of 400°C. The product gases are monitored by gas chromatography. The reaction rate is obtained from direct experimental measurements. Information regarding the reaction mechanism is obtained from reaction kinetics and the product analysis. Valuable insight into the reaction mechanism is provided by introducing suspected labeled or unlabeled intermediates into the reactant stream. The amount of radioactivity in each of the products is monitored by a high temperature flow proportional detector. The detector signal is counted and recorded as shown in Figure 3.

### Future Work

The temperature programmed desorption CO from the CuCo/Al<sub>2</sub>O<sub>3</sub> catalysts and other selective hydrogenation catalysts will be investigated. The temperature at which CO dissociation occurs (CO<sub>2</sub> formation) will be determined for each catalyst. The difference in products above and below the CO dissociation temperature will be studied. Eventually radioactive intermediates will be introduced and, in conjunction with kinetic studies, the importance of competing CO hydrogenation mechanisms can be evaluated.

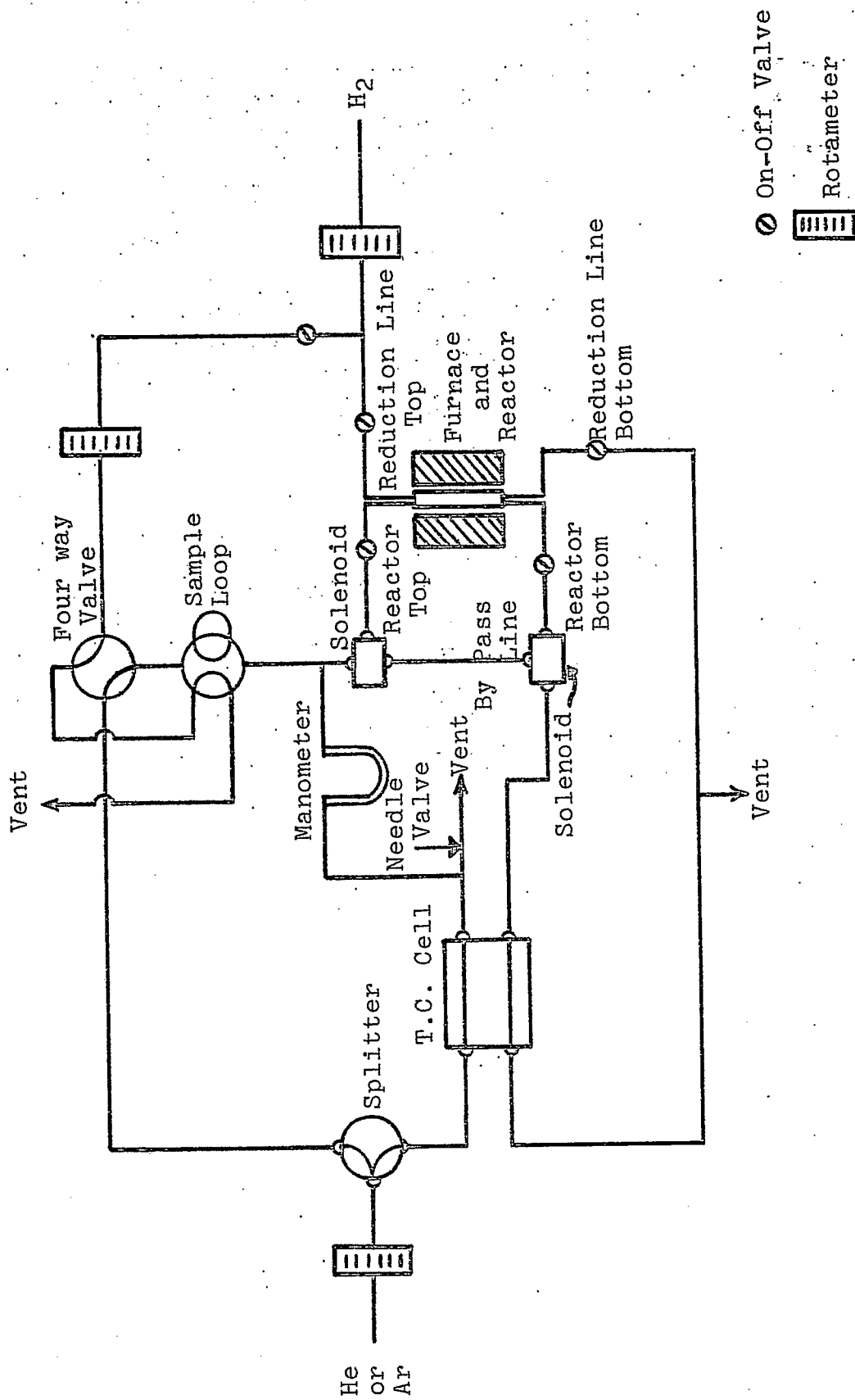


Figure 1. Temperature Programmed Desorption

- P = Pressure Gauge
- B = Back Pressure Regulator
- C = Flow Control Valve
- T = Flow Transducer
- S = Sampling Valve
- ⊗ = On-off valves
- = Injection Port

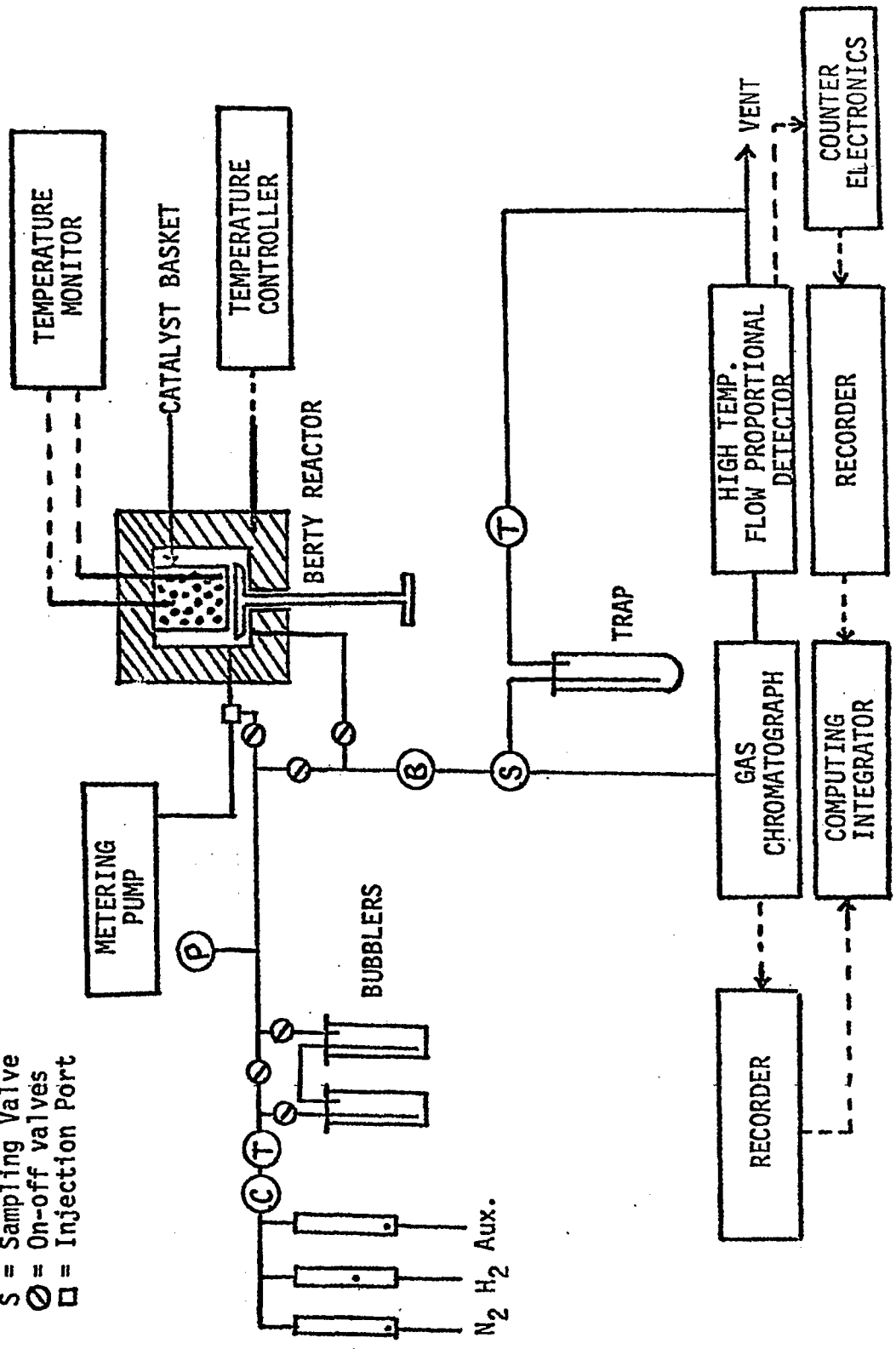


Figure 2. Stirred Flow Reactor System



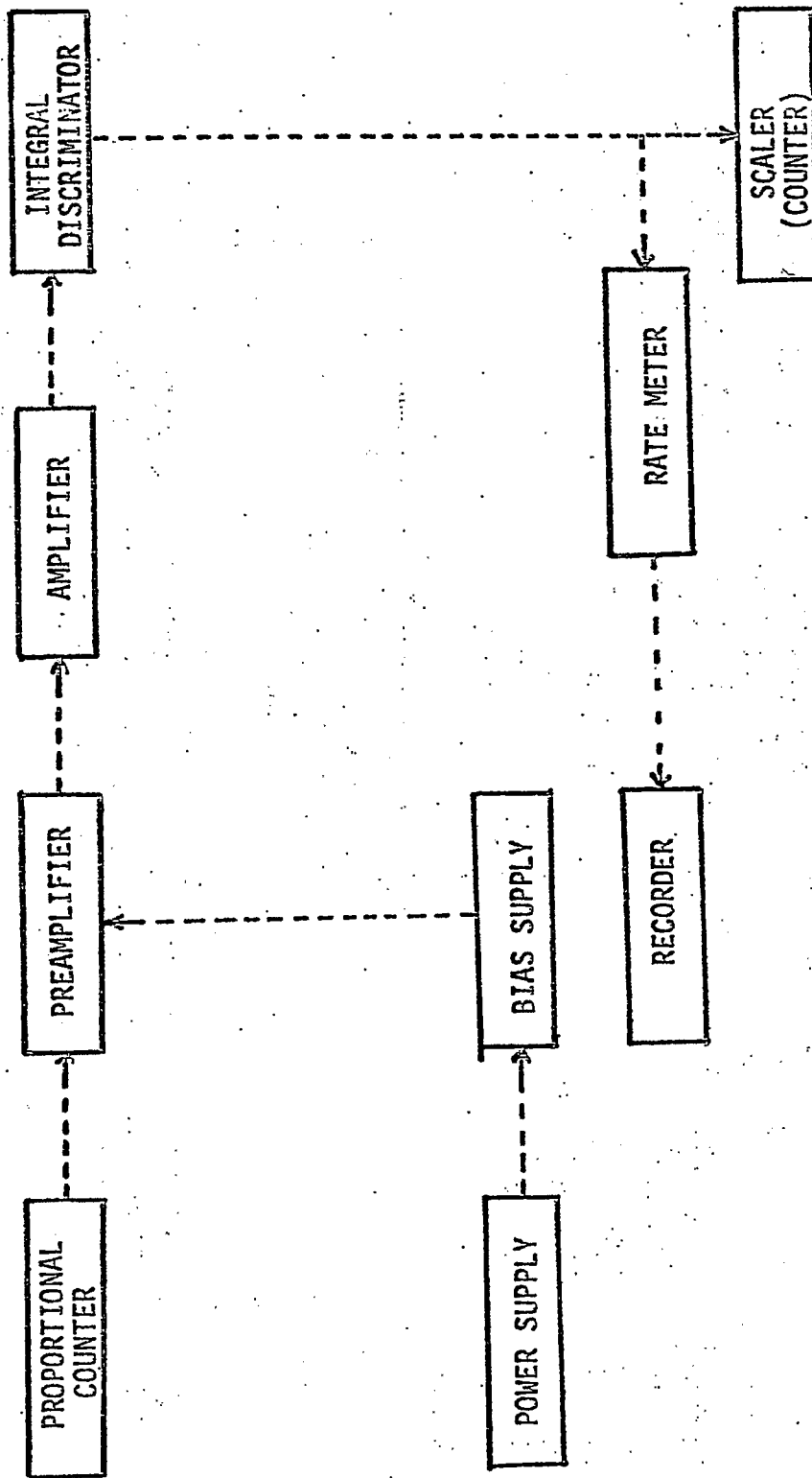


Figure 3. Electronics for Flow Proportional Counter

Development of Optimum Catalysts and Supports

Faculty Advisor: F.E. Massoth  
Graduate Student: A. Chantong

Introduction

This project involves assessing diffusional resistances within amorphous-type catalysts. Of primary concern is the question of whether the larger, multiringed aromatics found in coal-derived liquids will have adequate accessibility to the active sites of typical processing catalysts. When molecular dimensions approach pore size diameters, the effectiveness of a particular catalyst is reduced owing to significant mass transport resistance. An extreme case occurs when molecular and pore sizes are equivalent, and pores below this size are catalytically inactive.

The project objective can be achieved through a systematic study of the effect of molecular size on sorptive diffusion rates relative to pore geometry. Conceptually, the diffusion of model aromatic compounds is carried out using a stirred batch reactor. The preferential uptake of the aromatic from the aliphatic solvent is measured using a UV spectrometer. Adsorption isotherms are determined to supplement the diffusion studies.

Initial work entailed development of a suitable reactor, measurement techniques and methods of data analysis. These studies, employing chrysene and two different alumina supports, demonstrated that adsorption was diffusion-controlled. Effective diffusivities were larger than predicted for pore diffusion and a surface diffusion contribution was postulated. Subsequent studies were extended to other multiaromatic compounds and aluminas with similar results. The fractional surface diffusion contribution was appreciable and about the same in all cases. Because of this, restrictive diffusion effects could not be properly evaluated. However, for the largest size compound (20 Å) and smallest average pore size alumina (50 Å) tested, a markedly lower diffusivity was obtained, indicative of a restrictive diffusion effect.

Project Status

The phenomenon of surface diffusion occurring simultaneously with bulk diffusion has previously been reported. For a large aromatic ring compound like meso-tetraphenylporphine, this phenomenon is not considered likely to occur because of the high strength of adsorption of aromatic rings.

To better understand this system, equilibrium adsorption data were needed. Adsorption experiments with meso-tetraphenylporphine were carried out for extended periods of time (2-4 weeks) to assure that equilibrium had been achieved. Diffusion runs were also carried out to compare dynamic uptakes with the equilibrium values. The experiments were done with catalyst L (49. Å average pore diameter) which was calcinated at 116°C. Diffusion runs usually take 10-20 hours.

The adsorption data fit a Langmuir adsorption isotherm quite well, as shown in Figure 1. However, the uptake values at steady state in the diffusion runs were considerably less than the uptake from the equilibrium adsorption data at the same concentration, as shown in Figure 1. Therefore, at the steady state in the diffusion runs, the catalyst had not reached saturation adsorption, even though the concentration change was too small to detect. To confirm this, a diffusion run was performed with bigger catalyst extrudates. When the steady state was reached, several particles of the catalyst were removed, broken in half and examined under a microscope. A dark outer shell and a white inner core were observed, indicating that the solute had not completely penetrated the catalyst. Complete adsorption occurred after leaving the catalyst in the solution for 4 weeks, as attested by a uniform black color throughout the particle.

On the basis of these results, effective diffusivities were recalculated using the equilibrium adsorption data instead of the apparent steady state uptake values from the diffusion runs. The  $D_e$  values obtained were now lower and were less than the value of  $D_p \epsilon / x$  for simple pore diffusion. This indicates that there is a restrictive effect and no surface diffusion in the meso-tetraphenylporphine system.

#### Future Work

To confirm the above results, the isothermal adsorption and diffusion runs will be made with the catalyst at other calcination temperatures. If surface diffusion does not occur with meso-tetraphenylporphine, values of  $D_e$  should be independent of the calcination temperature of the catalyst. A similar study will be made with naphthalene, which should not exhibit restrictive diffusion, to check on the presence of surface diffusion in this system.

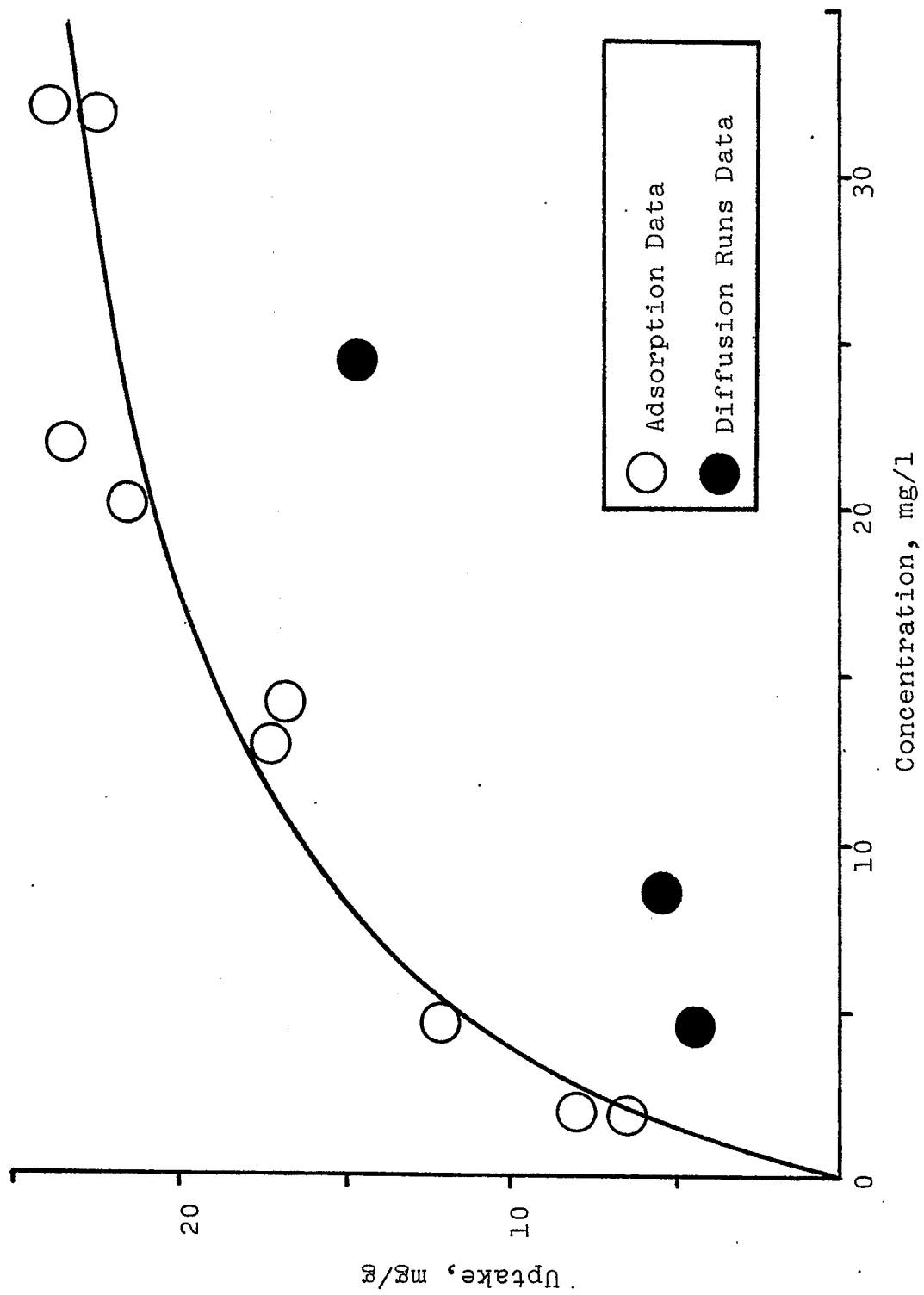


Figure 1. Adsorption isotherm for meso-tetraethylporphine/cyclohexane over alumina catalyst L.

## Project B-2 (alternate)

### The Effects of Poisoning on the Desulfurization Activity of Cobalt-Molybdate Catalysts

Faculty Advisor: F.E. Massoth  
Graduate Student: R. Ramachandran

#### Introduction

The importance of cobalt-molybdena catalysts for hydro-treating and hydrodesulfurization of petroleum feed stocks is well known. These catalysts are also being studied for hydrodesulfurization and liquefaction of coal slurries and coal-derived liquids. However, these complex feed stocks result in rapid deactivation of the catalysts. To gain an insight into the deactivation mechanism, detailed kinetics of the hydrodesulfurization of the model compound benzothiophene are compared before and after addition of various poisons and coke precursors. The studies are planned using a constant stirred microbalance reactor, which enables simultaneous measurement of catalyst weight change and activity.

Initial tests with the flow microbalance reactor showed that perfect gas mixing was not achieved when injecting a liquid feed (gaseous at reaction temperature) directly into the reactor. Modifications were incorporated into a new reactor design which have eliminated the problem and improved the mechanical stability of the system.

Preliminary tests of the benzothiophene hydrodesulfurization reaction showed the rate to be proportional to benzothiophene and hydrogen and inhibited by benzothiophene and  $H_2S$ . Pyridine and quinoline were poisons for the reaction. Advantage of this finding was taken to develop a technique for assaying active catalyst sites by successive poisoning-activity measurements.

Adsorption of  $H_2S$  on the sulfided catalyst was reversible and could be correlated with the Langmuir adsorption isotherm. Chemisorption of pyridine lowered  $H_2S$  adsorption, indicating a competition for adsorption sites. Temperature programmed desorption studies of thiophene also showed quinoline to compete with thiophene for adsorption sites.

#### Project Status

Temperature programmed desorption (TPD) studies were continued using thiophene as the adsorbate. The apparatus and procedure has been described earlier.<sup>1</sup> Catalysts were presulfided at  $400^\circ C$  for two hours and flushed with He at

temperature for several hours. Thiophene was absorbed at 100°C followed by He stripping until a base-line was achieved. The TPD of the remaining chemisorbed thiophene was carried out in a He flow of 50 cc/min at a heating rate of 16°C/min.

Figure 1 shows results of TPD of thiophene over a CoMo/Al<sub>2</sub>O<sub>3</sub> catalyst using a thermal conductivity detector in the desorption gas stream. The blank run (A) was performed before any thiophene was added. The start of a desorption peak above 350°C is probably due to a small amount of H<sub>2</sub>S desorption from the sulfided catalyst. The TPD of thiophene adsorbed at 100°C, Curve B, showed three peaks, a well-defined peak at 180°C, a shoulder at about 300°C and evidence of a high temperature peak (not resolvable because of the 370° limit on the GC heater unit). Products from this run were collected in a liquid N<sub>2</sub> trap and analyzed by mass spectrometry. Thiophene, C<sub>4</sub> hydrocarbons and some SO<sub>2</sub> were found. Since some air entered the sample bottle during transfer to the mass spectrometer, the SO<sub>2</sub> may have arisen from reaction with H<sub>2</sub>S. A subsequent blank run, Curve C, showed only the high temperature peak, which was somewhat larger than in the first blank run. Product analysis showed H<sub>2</sub>S and a small amount of SO<sub>2</sub>.

In contrast to these results, a repeat run with freshly sulfided catalyst was made with thiophene using an FID detector. Now, only the low temperature peak was observed, as shown in Curve A of Figure 2. The higher temperature peaks obtained with the TC detector are inorganic in nature, apparently arising from some thiophene decomposition during heat up. The first peak is probably due to desorption of thiophene.

After this run was completed, quinoline was adsorbed on the catalyst at 370°C by several injections followed by a 45 min purge in He. Then, the catalyst was cooled to 100°C, thiophene added as before and the TPD carried out. Curve B of Figure 2 shows the results obtained using FID response. The original peak at 180°C was greatly diminished and a higher temperature peak appeared around 230°C. The higher temperature indicates a stronger bonding of the desorbed specie. Although the nature of the species responsible for these peaks is unknown, the presence of quinoline on the catalyst surface greatly affects the adsorption characteristics of the unpoisoned sites on this catalyst.

Thiophene TPD over the Mo/Al<sub>2</sub>O<sub>3</sub> catalyst gave different results, as shown in Figure 3. On the freshly sulfided catalyst, two peaks were obtained, corresponding approximately to the two obtained on the poisoned CoMo/Al<sub>2</sub>O<sub>3</sub> catalyst. The quinoline-poisoned Mo/Al<sub>2</sub>O<sub>3</sub> catalyst gave a similar pattern as that for the fresh sulfided catalyst, but with reduced intensity. Apparently, for this catalyst, poisoning decreased the number of adsorption sites, but not their nature. This was expected. The results obtained with the CoMo/Al<sub>2</sub>O<sub>3</sub> catalyst discussed above were surprising and indicates that partial

site poisoning may affect catalytic activity over and above simple loss of some active sites.

Over the  $\text{Al}_2\text{O}_3$  support alone, thiophene adsorbed considerably less and TPD revealed only a single lower temperature peak, at about  $150^\circ\text{C}$ . The peak decreased in size after poisoning with quinoline. The absence of this peak in the runs with catalysts signifies that either  $\text{Al}_2\text{O}_3$ -like adsorption sites are not present on the sulfided catalyst or that they are altered by the presence of Mo.

Estimates of the activation energy of desorption were made by repeat runs at different heating rates. A summary of these is presented in Table 1. As expected, desorption activation energies increased with increasing peak temperature.

#### Future Work

Temperature programmed desorption experiments will be continued to establish the nature of the various peaks and with other poisons. After the microbalance has been repaired, benzothiophene kinetic studies will be started.

#### References

1. W.H. Wiser et al., DOE Contract No. E(49-18)-2006, Quarterly Progress Report, Salt Lake City, Utah, Jan-Mar 1978.

Table 1. Results of TPD of Thiophene.

Catalyst	Relative Amount Desorbed	Activation Energy of Desorption, kcal/mole, Approximate Peak Temp, $^\circ\text{C}$		
		<u>150<math>^\circ</math></u>	<u>170<math>^\circ</math></u>	<u>230<math>^\circ</math></u>
$\text{Al}_2\text{O}_3$	0.4	10	--	--
+ Quinoline	0.2	10	--	--
$\text{Mo}/\text{Al}_2\text{O}_3$	1.1	--	15	19
+ Quinoline	0.8	--	15	23
$\text{CoMo}/\text{Al}_2\text{O}_3$	1.0	--	15	--
+ Quinoline	0.8	--	--	18

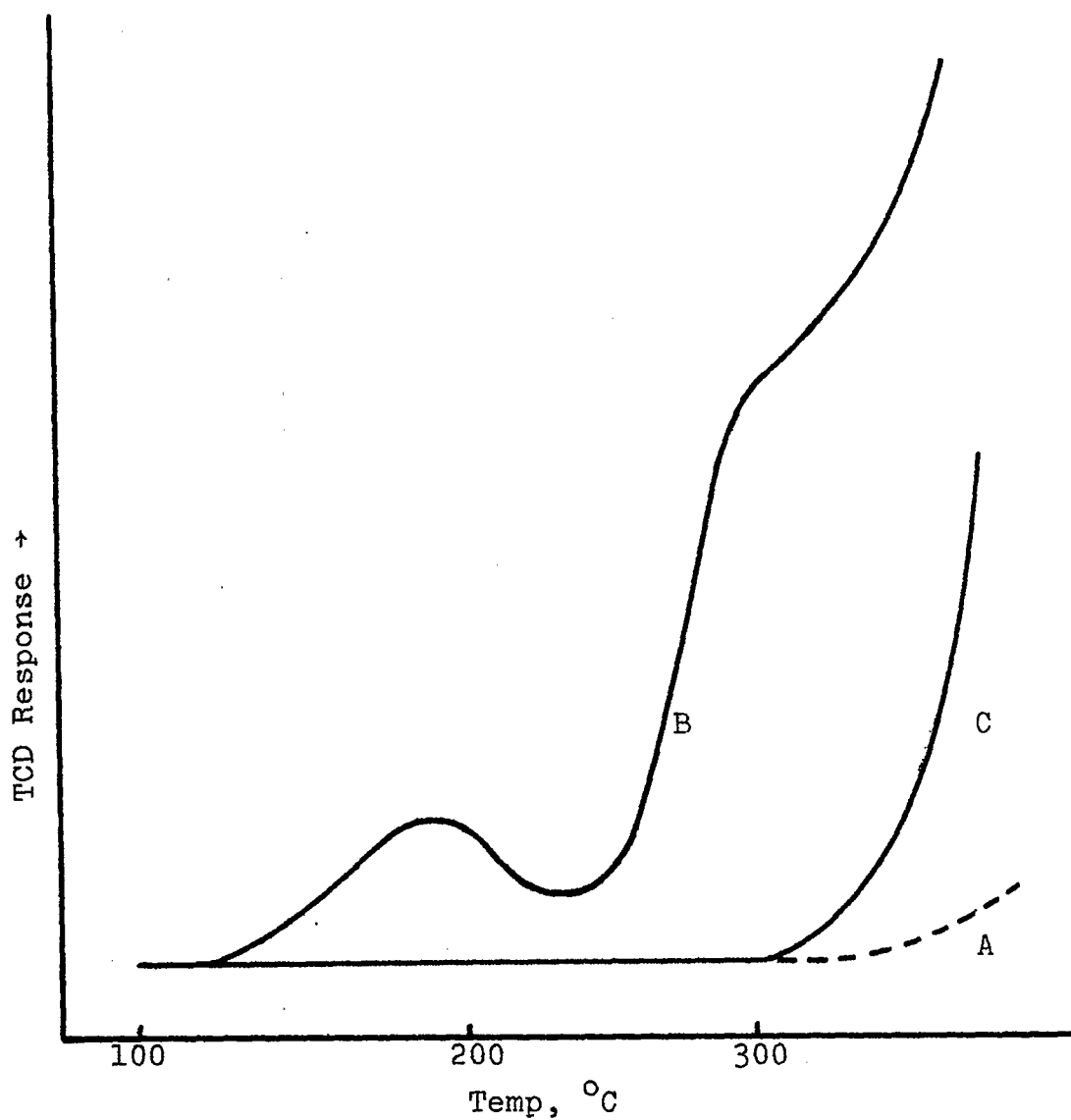


Figure 1. Thiophene TPD over CoMo/Al<sub>2</sub>O<sub>3</sub> catalyst.

A. Blank run. B. Thiophene run. C. Blank run after B.



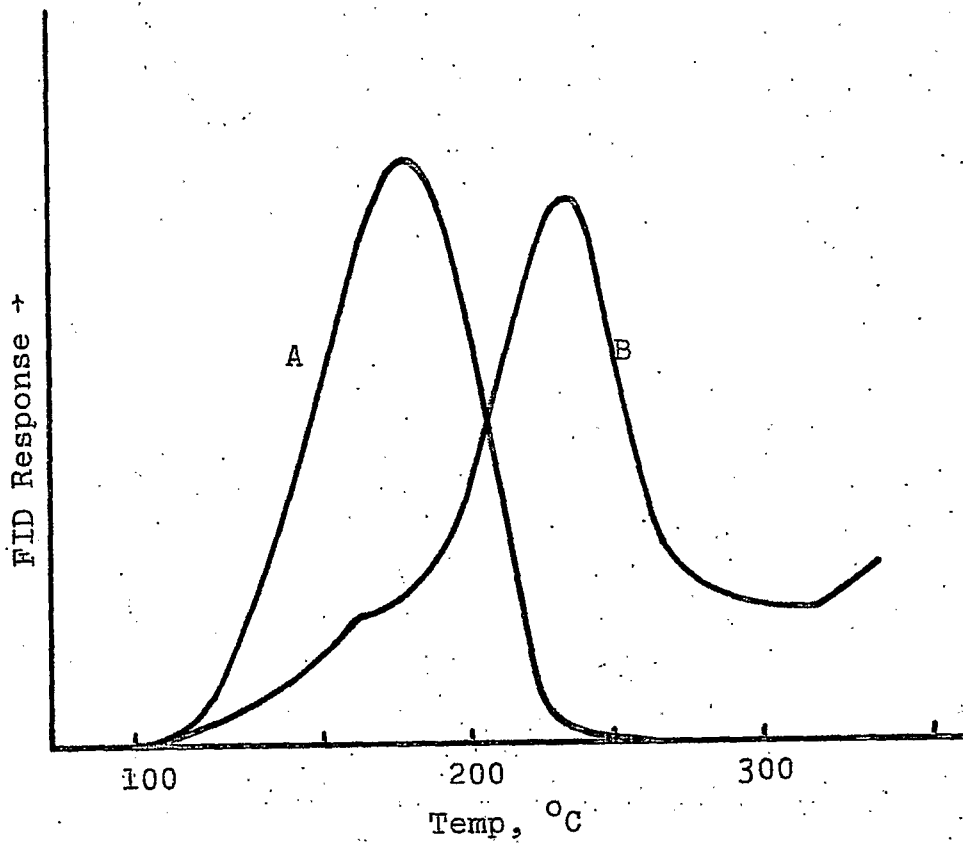


Figure 2. Thiophene TPD over  $\text{CoMo}/\text{Al}_2\text{O}_3$  catalyst.  
A. Thiophene run. B. Repeat after poisoning with quinoline.

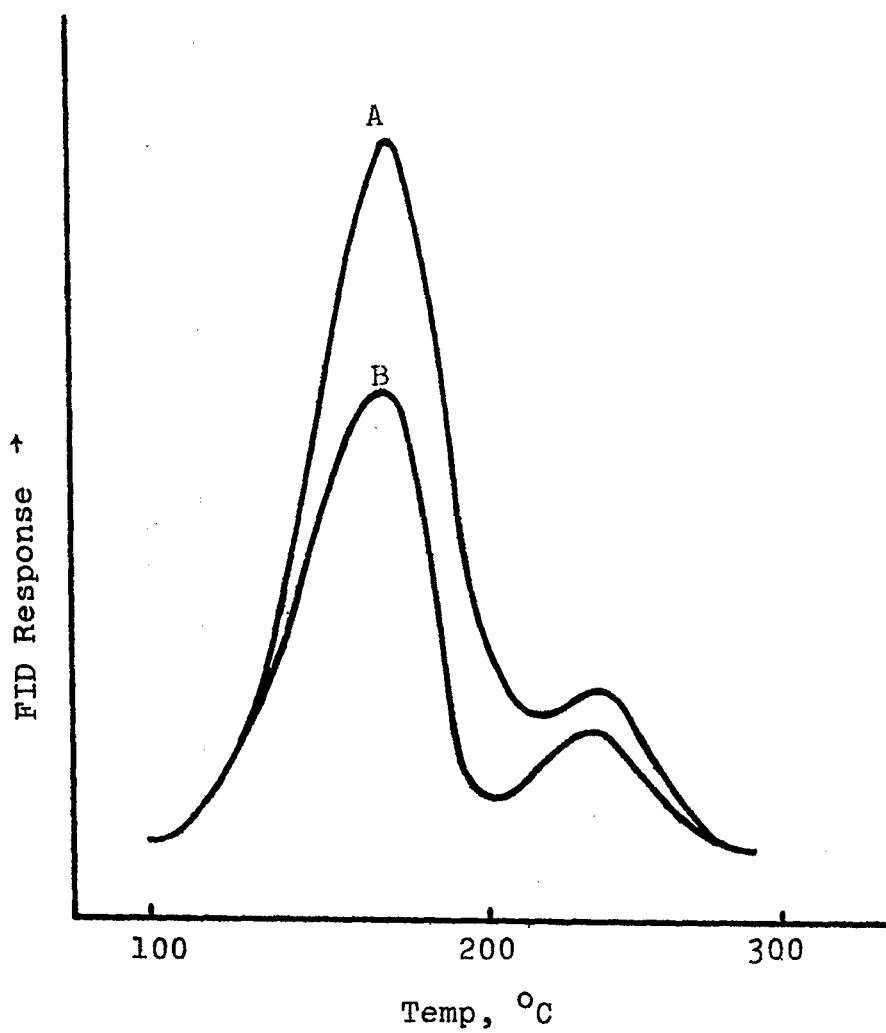


Figure 3. Thiophene TPD over Mo/Al<sub>2</sub>O<sub>3</sub> catalyst.  
A. Thiophene run. B. Repeat after poisoning with quinoline.

Mechanism of Catalytic Hydrogenation  
by Metal Halide Catalysts

The Initial Stage of Coal Hydrogenation in the Presence of  
Catalysts

Faculty Advisor: D.M. Bodily  
Postdoctoral Fellow: R. Yoshida

Introduction

Studies of the treatment of coal with hydrogen under mild reaction conditions indicate that the benzene-soluble products from the initial stages of the reaction are structurally different from the products obtained at longer reaction times. These products may originate from structurally different portions of the original coal. Kinetic studies of coal hydrogenation show that the reaction may be divided into two stages, an initial stage where the rate of reaction is rapid and a second stage where the reaction rate is comparatively slower.

The reaction rate of the initial stage is related to coal parameters such as volatile matter and fixed carbon content. These parameters are related to the thermal reactions which occur upon heating. The soluble products of the first stage are of relatively low molecular weight and could be attributed to the thermal reactions occurring in the initial stages of the reaction. The reaction rate of the second step is independent of coal rank. These results could also be interpreted in terms of a dual structural system in coal.

Hydrogasification of coal also occurs in two stages. The initial stage is very rapid while the second stage is much slower. Rate constants for the initial stage are proportional to the volatile matter of the feed coal, but at higher conversions the rate constants for all coals approach one another. Optimum conditions for the formation of organic liquid products during the initial stage have been determined.

Pyrolysis and dissolution of a high-volatile Utah coal have been discussed and compared with hydrogenation. These reactions involve an initial rapid process followed by a slower process. The original coal may contain considerable quantities of nonaromatic and low molecular weight aromatic constituents which can be liberated through purely thermal

rupture and internal stabilization of bonds during the initial stage. A recent study on flash heating of high volatile coal indicates that coal is composed of at least two very different structures, and the result of flash heating is the evolution of smaller molecules less tightly bound. The yield of these molecules is proportional to volatile matter content.

The postulate of a dual structure in coal is consistent with results of mass spectrometry and solvent extraction experiments on coal.

When coal hydrogenation is considered in terms of a dual structure model, the initial stage of the reaction is of great importance in the design of a hydrogenation process. The initial stages of coal hydrogenation will be studied using several catalyst systems.

### Project Status

Molecular weights (MW) measured by vapor pressure osmometry and the weight of the average structural unit (Mus) calculated numerically from structural parameters derived from the Brown-Ladner equation were compared for hydrogenation products. Molecular weights were determined by vapor pressure osmometry on Corona Wescan 117 Molecular Weight Apparatus in the concentration range of 0.4~2.5 g/kg of pyridine solution. In Table 1 MW, Mus and MW/Mus of liquid (oil + asphaltene-I) and asphaltene-II are listed where MW/Mus indicates the number of average structural units per molecule.

As shown in Figure 1, in liquid (oil + asphaltene-I) MW has a tendency to increase with conversion, however, Mus is almost constant (200). At about 20% conversion MW of liquid (oil + asphaltene-I) using a  $ZnCl_2$  catalyst is lower than those obtained with the other catalysts. This suggests that  $ZnCl_2$  catalyzes dealkylation as postulated previously on the basis of changes of  $\sigma$  and  $f_a$ . The asphaltene-II MW has a tendency to increase with conversion. The value is higher than that of liquid. Up to about 36% conversion, Mus for asphaltene-II decreases to almost the same value as for the liquid (oil + asphaltene-I). At about 75% conversion, Mus increases to almost the same value as MW. At about 20% conversion, Mus of asphaltene-II using a  $ZnCl_2$  catalyst is lower than the values obtained with the other catalysts. The MW/Mus indicates that the average molecules of liquid (oil + asphaltene-I) and asphaltene-II consist of 1 to 2 structural units.

The applicability of vapor pressure osmometry to the molecular weight measurements of coal-derived liquids has been examined. The molecular weight measured directly from

the whole liquid, MW measured, and the molecular weight calculated on the basis of the additive property using the molecular weights measured separately for oil and asphaltene-I, MW calculated, are compared in Table 2. The relative deviations of 7 of the 8 samples are less than + ca. 13%. For 4 samples the deviation is less + ca. 7%. This indicates that the additive property on the molecular weight of coal-derived liquids is valid with the relative deviation within + ca. 13%. The MW measured was obtained by extrapolating the plots to infinite dilution. Accordingly the association of molecules should be eliminated. The relative deviation of 3 to 26% in the additive property on molecular weight suggests the existence of factors (including experimental error) other than the association considered in measuring the molecular weights.

#### Future Work

Toluene-insolubles will be further extracted with pyridine. Structural analysis of pyridine-solubles will be performed.

Table 1. MW, Mus and MW/Mus of liquid (oil + asphaltene-I) and asphaltene-II.

<u>Sample</u>	<u>Liquid</u>			<u>Asphaltene-II</u>		
	Mus	MW	MW/Mus	Mus	MW	MW/Mus
ZnCl <sub>2</sub>						
400°C, 13 sec	200	290	1.5	350	430	1.2
450°C, 13 sec	240	310	1.3	310	490	1.6
500°C, 8 sec	-	-	-	280	530	1.9
, 21 sec	200	280	1.4	240	520	2.2
, 372 sec	200	340	1.7	510	430	0.8
Co-Mo						
500°C, 12 sec	190	280	1.5	290	380	1.3
Presulfided Red-Mud						
500°C, 12 sec	240	340	1.4	330	460	1.4
Red-Mud Plus Sulfur						
500°C, 12 sec	290	330	1.1	360	510	1.4
No						
500°C, 10 sec	190	370	1.9	310	450	1.5

Table 2. Comparison of molecular weights measured directly by VPO and calculated on the basis of additive property.

Sample	Oil		Asphaltene-I		Liquid (Oil + Asphaltene-I)		Relative Deviation (%)
	MW Measured		MW Measured		MW Calc.	MW Measured	
ZnCl <sub>2</sub>							
400°C, 13 sec	280 (0.68) <sup>a</sup>		270 (0.32) <sup>a</sup>		277	290	- 4.5
450°C, 13 sec	300 (0.47)		240 (0.53)		268	310	-13.5
500°C, 8 sec	320 (0.56)		340 (0.44)		329	-	-
, 21 sec	330 (0.41)		300 (0.59)		312	280	+11.4
, 372 sec	290 (0.90)		350 (0.10)		296	340	-12.9
Co-Mo							
500°C, 12 sec	270 (0.61)		330 (0.39)		293	280	+ 4.6
Presulfided Red-Mud							
500°C, 12 sec	290 (0.45)		360 (0.55)		329	340	- 3.2
Red-Mud Plus Sulfur							
500°C, 12 sec	280 (0.38)		400 (0.62)		359	330	+ 7.3
No Catalyst							
500°C, 10 sec	270 (0.52)		280 (0.48)		275	370	-25.7

<sup>a</sup>( ) = yield.

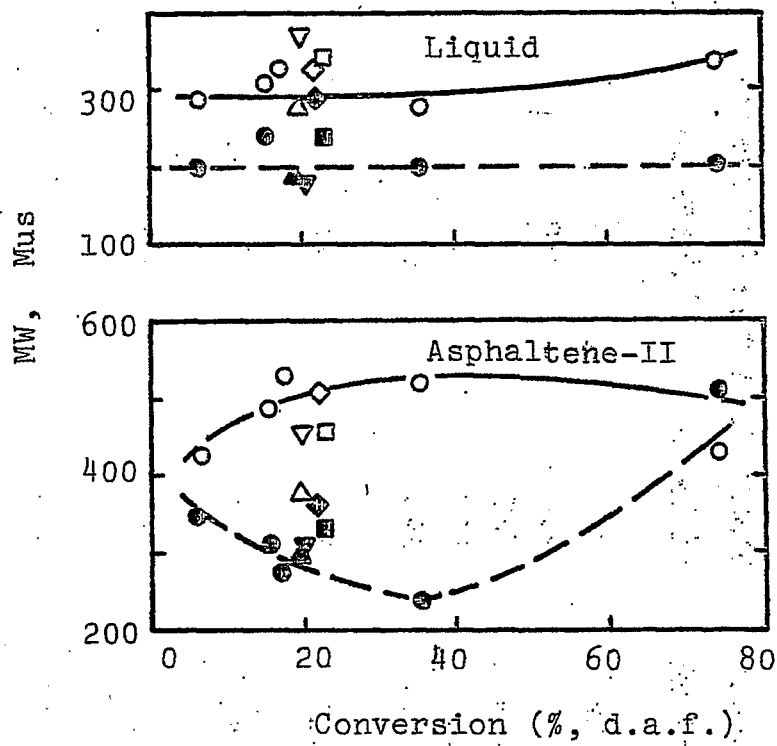


Figure 1. Change of MW and Mus of products with conversion.

ZnCl <sub>2</sub>	○	MW	○	Mus	●
Co-Mo	△		△		▲
Presulfided Red-Mud	□		□		■
Red-Mud Plus Sulfur	◇		◇		◆
No Catalyst	▽		▽		▼

Mechanism of Catalytic Hydrogenation by  
Metal Halide Catalysts

IR Studies of Coal Metal Salts Interactions

Faculty Advisor: R.E. Wood  
Graduate Student: Doug Stuart

Introduction

Coal catalyst interactions are being investigated using infrared spectroscopy. Various coal molecular bond structures have been associated with peaks in the IR spectrum. These peaks are being compared for different coals and chars to monitor change in the associated structure.

Compensations have been made for identified sample preparation parameters in the preparation procedure which was proposed last quarter.

Project Status

Problems experienced last quarter in pressing uniform, infrared transparent pellets have been overcome. By evenly tamping the powdered sample in the die with a flat faced cylinder of the same diameter, over 90% of the resulting pellets were uniform in appearance across the surface. Previously, when the pellets were pressed in a die heated to 110°C, they often split parallel to the face while being removed. Splitting did not occur when only the two inserts with mirrored surfaces were heated to 110°C. The heating of the inserts prevented sticking.

The adsorption law, commonly called Beer's Law, will be used in data interpretation. A series of pellets was prepared from one coal. The amount of coal used varied from 0.6 mg to 2.5 mg per pellet. The absorbancies of several major peaks in each spectrum were plotted against the amount of coal used. All plots except those of peaks affected by the KBr-H<sub>2</sub>O interactions were straight lines intersecting zero absorbance at zero concentration. Similar results were obtained for a char. Therefore, Beer's Law is valid in the above concentration range.

Infrared spectra have been obtained this quarter for twenty-four different coals and their chars. Two spectra were run for each sample. At concentrations up to 1 mg of sample per pellet, all peaks were on scale. Concentrations of 2 mg of sample per pellet showed more detail in the less intense



part of the spectrum. The two concentrations allowed a simple check on reproducibility.

#### Future Work

The coal and char spectra are now being compared to determine the most uniform method of analysis. When the spectral data is available, it will be correlated with other data previously obtained from the coals and chars.

## Project C-1

### The Mechanism of Pyrolysis of Bituminous Coal

Faculty Advisor: W.H. Wiser  
Graduate Student: John Shigley

#### Introduction

In the present state of knowledge concerning the fundamental chemistry of coal liquefaction, the liquefaction reactions are initiated by thermal rupture of bonds in the "bridges" joining configurations in the coal, yielding free radicals. The different approaches to liquefaction, except for Fischer-Tropsch variations, represent ways of stabilizing the free radicals to produce molecules. Hence, the stabilization involving abstraction of hydrogen from the hydroaromatic structures by the free radicals, believed to be the predominant means of yielding liquid size molecules in coal pyrolysis, is of major importance in all coal liquefaction, except Fischer-Tropsch variations. The objective of this research is to understand the chemistry of this pyrolytic operation.

#### Project Status

It has been consistently observed in kinetic studies of coal pyrolysis at the University of Utah that the overall kinetics are second order. Second order kinetics suggest a two body collision in the slow or rate determining step. This observation could also possibly be explained on the basis of a series of consecutive (but overlapping) first order reactions.

If the kinetics are really second order, the thermal bond rupture may be rapid followed by a slower abstraction of hydrogen from a hydroaromatic structure in a two body collision. A series of possible model compound structures have been considered and compared to bituminous coal using parameters normally used in describing coal structure (% carbon, % hydrogen, % hydroaromatic carbon, % aromatic carbon, % aliphatic carbon, H/C atomic ratio, etc.). The ability of the model compound to stay in the solid or liquid state at reaction conditions was another criterion used in the selection process. A chemical company has been contracted to synthesize two of these plausible compounds (Figure 1).

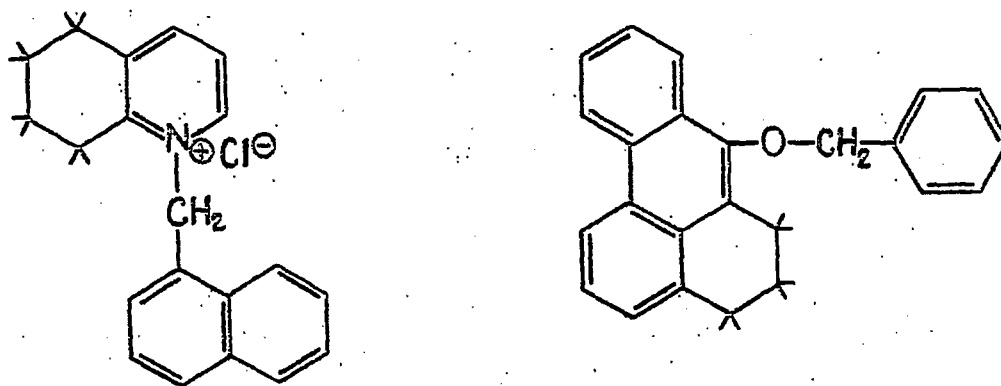
A thermogravimetric system has been assembled to follow the pyrolysis of these model compounds. The system will be connected to a gas chromatograph to permit analysis of pyrolysis products over a series of time intervals during pyrolysis. The compounds will be studied at several temperatures in the range of 325-450°.

The system has the capability of heating the samples to these temperatures in 2-3 minutes and can be followed as a function of time.

### Future Work

The mechanism and kinetics of the pyrolysis of these model compounds will be determined.

Figure 1. Model compounds to be used in the study of coal pyrolysis kinetics and mechanism.



## Project C-2

### Heat Transfer to Gas-Solid Suspensions in Vertical Cocurrent Downflow

Faculty Advisor: J.D. Seader  
Graduate Students: J.M. Kim  
B. Scott Brewster

#### Introduction

Experiments are being conducted to investigate the momentum and heat transfer mechanisms in flowing gas-solid suspensions in vertical downflow. Correlations for two-phase friction and heat transfer coefficient are being developed for use in the design of high velocity, continuous coal hydrogenation reactors.

#### Project Status

From a similarity analysis based on governing differential equations of gas-solids suspension flow, the two-phase friction factor,  $f_{tp,D}$  may be correlated in terms of the following dimensionless parameters:

$$f_{tp,D} = \phi \left[ \frac{D U_{sg} \rho_g}{\mu_g}, \frac{\rho_p}{\rho_g}, \frac{W_p}{W_g}, \frac{C_D E_p D}{(1-E_p) d_p} \right] \quad (1)$$

where  $f_{tp,D}$  is defined as

$$f_{tp,D} = \frac{\Delta P_f D}{2L \rho_g U_{sg}^2} \quad (2)$$

As the particle velocity and the holdup are both related to the density and loading ratio, it is assumed that the effect of density and loading ratios are incorporated in the term,  $C_D E_p D / (1-E) d_p$ .

Consequently, Eq (1) may be simplified to

$$f_{tp,D} = \phi \left[ \frac{D U_{sg} \rho_g}{\mu_g}, \frac{C_D E_p D}{(1-E_p) d_p} \right] \quad (3)$$

The dimensionless group,  $C_D E_p D / (1-E) d_p$ , represents the ratio of the gas-particle viscous drag force to the gas-phase inertial force and will be designated by  $\alpha_D$ .

In Figure 1 the two-phase friction factors calculated from the experimental pressure drop data are plotted as a function of  $N_{Re,sg}$  with a parameter of  $\alpha_D$ . The apparent transition from laminar flow to turbulent flow is delayed as the parameter  $\alpha_D$  is increased. Similar observations have been reported for curved tube flows, where the secondary flows caused by centrifugal forces stabilize the flow such that the transition occurs at higher Reynolds numbers. Also, adding more particles in a two-phase flow (i.e., increasing the holdup and thus the parameter  $\alpha_D$ ) might gradually stabilize the suspension flow, until finally no distinction between laminar and turbulent flow can be made above  $\alpha_D$  value of about 0.5.

The two-phase friction factors shown in Figure 1 for the glass-bead, air system were correlated empirically by the following equations.

Laminar flow regime:

$$f_{tp,D} = \frac{A_L}{N_{Re,sg}} \quad (4)$$

$$\text{where } A_L = 16 + 120 \alpha_D^{0.734}$$

Turbulent flow regime:

$$f_{tp,D} = A_t \cdot N_{Re,sg}^{(-0.25 - 0.195 \alpha_D^{0.137})} \quad (5)$$

$$\text{where } A_t = 0.0791 + 1.1 \alpha_D^{0.408}$$

Note that Eq (4) and (5) reduce to gas-alone friction factor equations if no particles are present.

Generalization of the relations between the two-phase friction factor and  $\alpha_D$  was attempted by extending the above similarity considerations to a packed-bed flow, an upper limiting case of the particle holdup or loading.

In a packed-bed flow, the system characteristic dimension is comparable to the particle diameter,  $d_p$ , due to the domination effect of the drag forces between the gas and particles. This dimensional consideration suggests a modification of Eq (3) as follows:

$$f_{tp,d_p} = \psi \left[ \frac{d_p U_{sg} \rho_g}{\mu_g}, \frac{C_D E_p}{(1-E_p)} \right] \quad (6)$$

$$\text{where } f_{tp,d_p} = \frac{\Delta P_f d_p}{2L \rho_g U_{sg}^2}$$

Again assuming that the effect of the term,  $d_p U_{sg} \rho_g / \mu_g$ , can be absorbed in the second term involving drag coefficient, Eq (6) may be simplified to

$$\begin{aligned}
 f_{tp,d_p} &= \psi \left[ \frac{C_D E_p}{1-E_p} \right] \\
 &= \psi [\alpha_{d_p}] \quad (7) \\
 \text{where } \alpha_{d_p} &= \frac{C_D E_p}{(1-E_p)}
 \end{aligned}$$

When the particle concentration exceeds about 2 percent by volume, the drag coefficient of a single particle can no longer apply to a suspension of particles. The correlation of the drag coefficient in a suspension in terms of the single particle drag coefficient and the particle concentration has been proposed by Wen and Yu<sup>1</sup> as

$$(C_D)_{U_{sg}} = (C_{D,S})_{U_{sg}} (1-E_p)^{-4.7} \quad (8)$$

The drag coefficients in Eq (8) were based on superficial velocities. Based on actual gas velocities, Eq (8) became

$$C_D = C_{D,S} (1-E_p)^{-2.7} \quad (9)$$

After substituting Eq (9) into Eq (7), it became

$$f_{tp,d_p} = \psi \left[ \frac{C_{D,S} E_p}{(1-E_p)^{3.7}} \right] \quad (10)$$

The validity of Eq (10) was tested by plotting  $f_{tp,d_p}$  versus  $\alpha_{d_p}$  as shown on the right upper corner in Figure 2, where a split coordinate is employed to show the friction factors for a dilute phase transport on the same graph. The friction factor,  $f_{tp,d_p}$ , can be correlated as a function of  $\alpha_{d_p}$  only, and therefore Eq (10) holds true for a packed-bed flow.

The friction factor curves for a dilute phase transport, as plotted on the lower left corner, show a complicated trend since, in this regime, both  $N_{Re,sg}$  and the parameter  $\alpha_D$  affect the frictional pressure drop.

The effect of the parameter  $\alpha_D$  or  $\alpha_{d_p}$  may be better understood by plotting the friction factors as a function of

gas Reynolds numbers with  $\alpha_D$  or  $\alpha_{Dp}$  as parameters, as shown in Figure 3.

An increase in  $\alpha_D$  changes the laminar turbulent flow transition characteristics, and upon reaching  $\alpha_D \approx 0.5$ , transition phenomena disappear for a dilute phase transport. At even higher  $\alpha_D$  in the packed-bed regime, the friction factors become independent of gas Reynolds numbers.

Experiments with the coal particle, air system were continued. The equipment and experimental design have been reported in earlier reports. During the last quarter, axial pressure drop data at several solids flow rates were obtained for three gas Reynolds numbers: 10000, 20000 and 30000. These data are shown in Figures 4 and 5. Figure 4 is a plot of the axial pressure drop profiles for gas Reynolds numbers of 10000 and 30000 and two solids flow rates. This graph agrees with the conclusions derived from the glass bead experiments, i.e., the addition of solids to the gas stream increases the hydraulic entry length, and the hydraulic entry length is independent of the Reynolds number for the range of investigation.

Figure 5 is a plot of the measured pressure drop as a function of coal flow rate for each of the three Reynolds numbers that were investigated. As in the glass bead experiments, this graph shows that the measured pressure drop first increases with solids loading and then decreases at the lower Reynolds number. This behavior is due to the interaction of two opposing terms in the total pressure drop equation: the hydrostatic head component and the frictional component. As described in a previous report, the frictional component of the pressure drop will be calculated and correlated.

A screening test revealed that attrition has reduced the average size of the coal particles from 360 microns to 300 microns. The major source of attrition was probably due to the impacting of particles against the vane of the two-way solids sampling valve located at the lower end of the test section and the 45° pipe elbow connecting the valve to the receiving hopper. Consequently, the connection between the test section and hopper was modified so that the suspension flows in a straight path downward into the hopper with as little disturbance as possible. A cyclone separator was also fabricated and installed to help clean up the outlet stream from the lower hopper and reduce the load on the filter bag.

Construction of the heat transfer test section was initiated. Flanges and phenolic insulating sections were added to the pressure drop test section at the location where the heat transfer section will be installed. After the modifications

were completed, the system performance was again checked by measuring the pressure drop for air alone. The resulting friction factors agreed with the equation of Nikuradse to within five percent.

### Future Work

Correlation of the heat transfer data for the glass bead, air system will be attempted. More pressure drop data will be obtained and processed for the coal particle, air system. Fabrication of the heated section will be completed, and heat transfer experiments will be conducted. All of the experiments will be completed by the end of March.

### Reference

1. C.Y. Wen and Y.H. Yu, Chem. Eng. Progr., Symp. Ser., 62, 100 (1966).

### Nomenclature

$C_D$	Drag coefficient in a suspension
$C_{D,S}$	Drag coefficient of a single particle
$D$	Tube diameter, ft
$d_p$	Particle diameter, ft
$E_p$	Particle holdup
$f_{tp,D}$	Two-phase friction factor based on the tube diameter
$f_{tp,d_p}$	Two-phase friction factor based on the particle diameter
$L$	Length, ft
$N_{Re,sg}$	Gas Reynolds numbers, $\frac{DU_{sg}\rho_g}{\mu_g}$
$\Delta P_f$	Frictional pressure drop, lbf/ft sec <sup>2</sup>
$U_{sg}$	Superficial gas velocity, ft/sec
$W_p, W_g$	Particle and gas flow rate, lbf/sec
$\alpha_D$	Dimensionless parameter, $\frac{C_D E_p D}{(1-E_p) d_p}$
$\alpha_{d_p}$	Dimensionless parameter, $\frac{C_D E_p}{(1-E_g)}$
$\rho_p, \rho_g$	Particle and gas density, lbf/ft <sup>3</sup>
$\mu_g$	Gas Viscosity, lbf/ft sec



Figure 1. Correlation of Friction Factor.

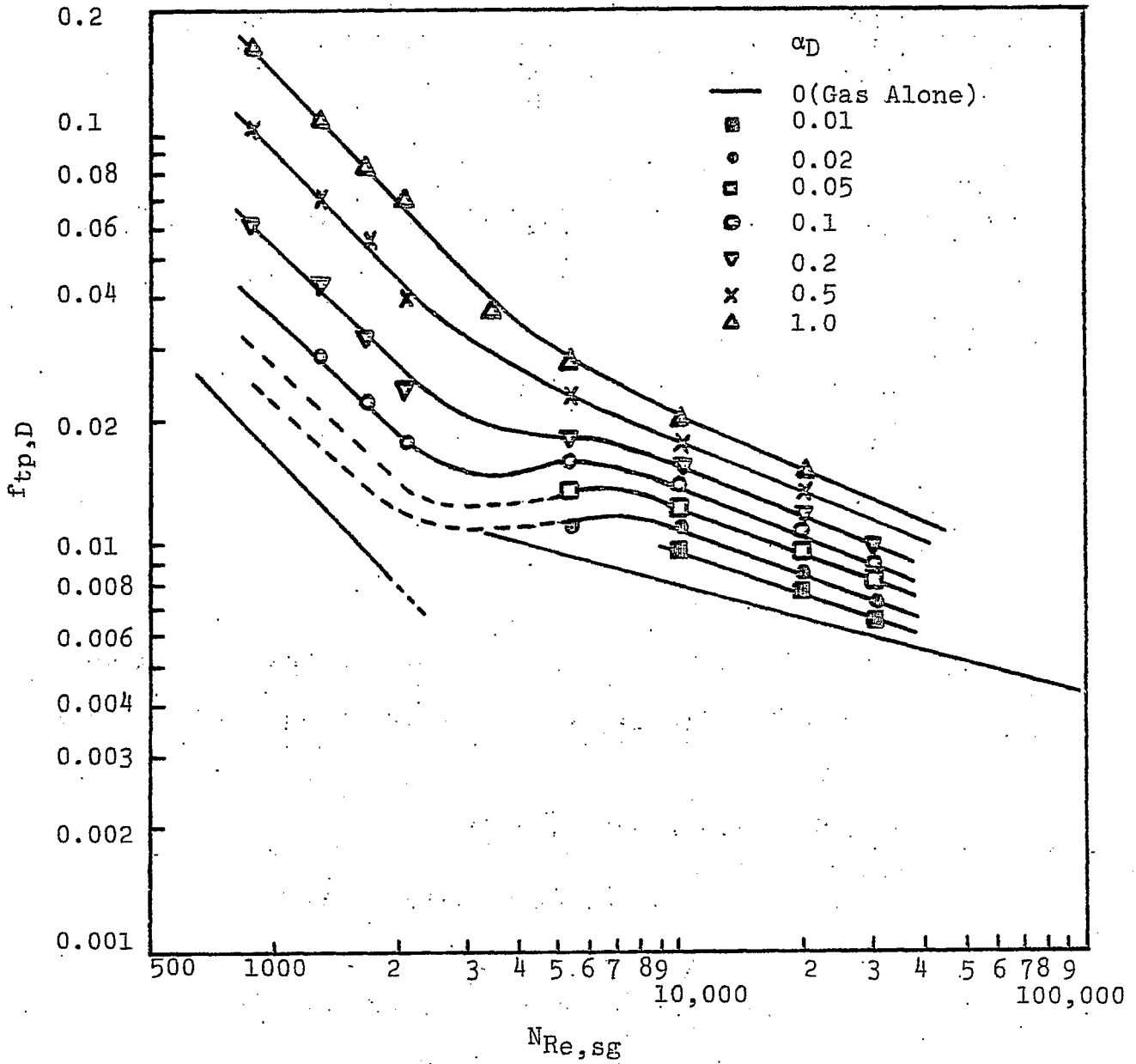


Figure 2. Effect of Gas Reynolds Number on Friction Factor.

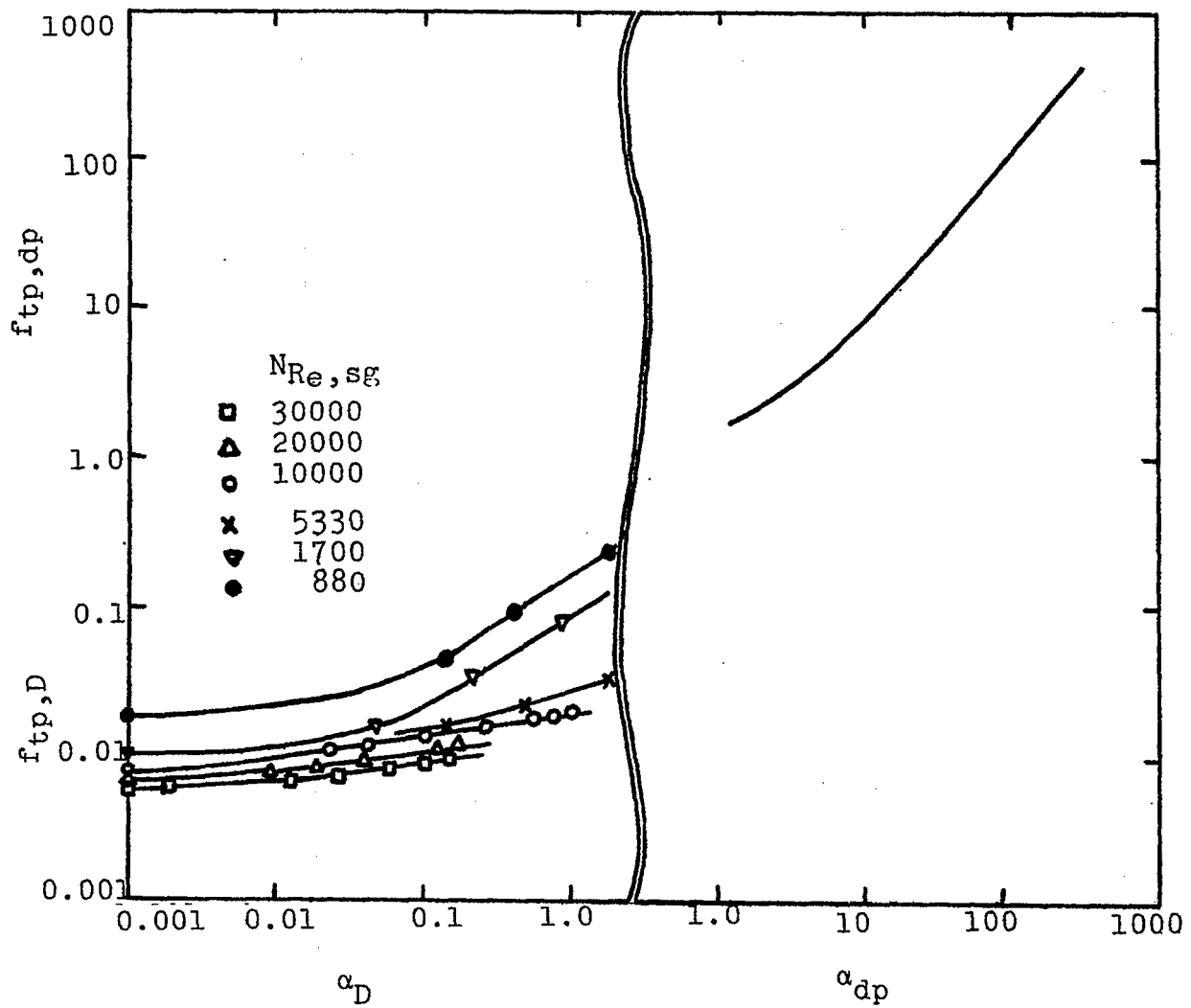
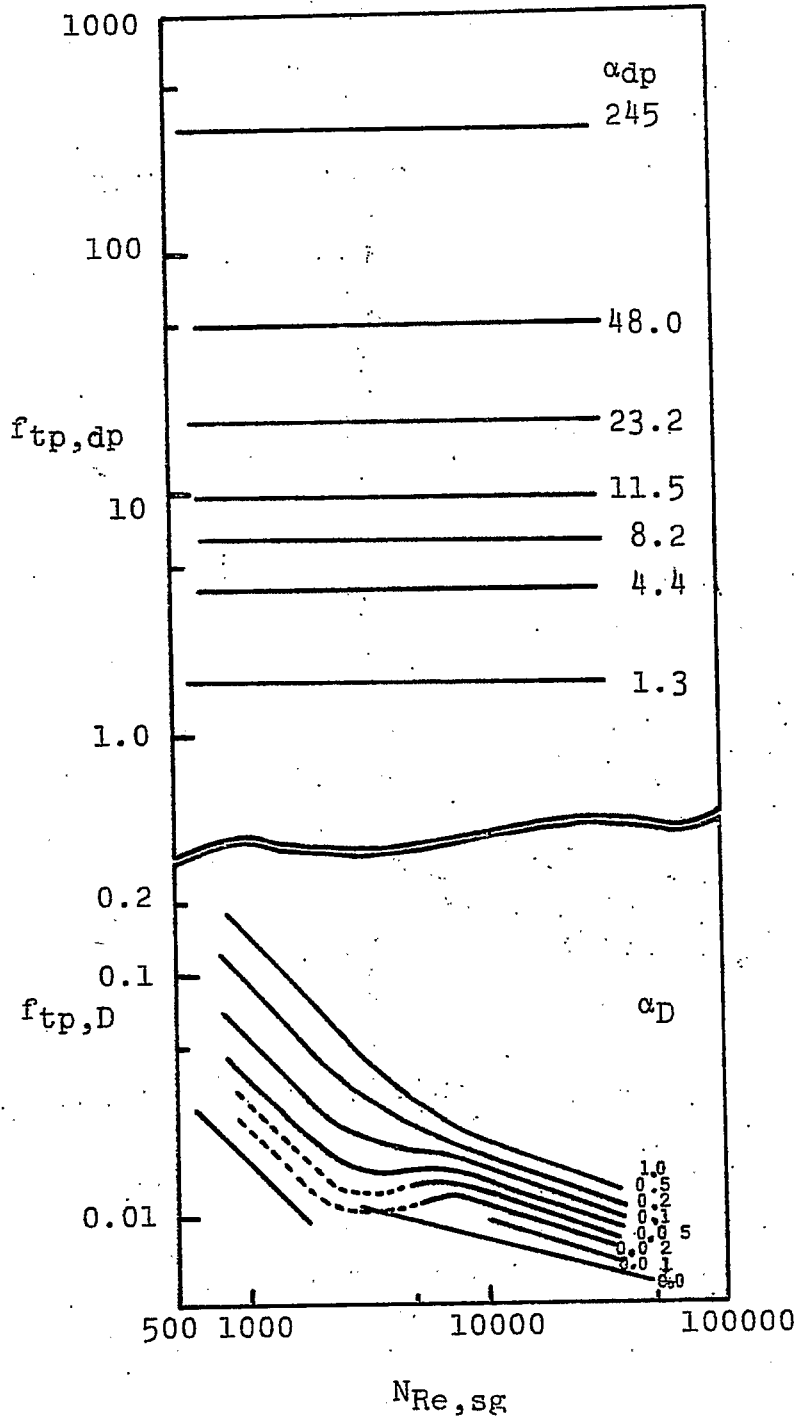


Figure 3. The Effect of the Parameter  $\alpha$  on the Friction Factor.



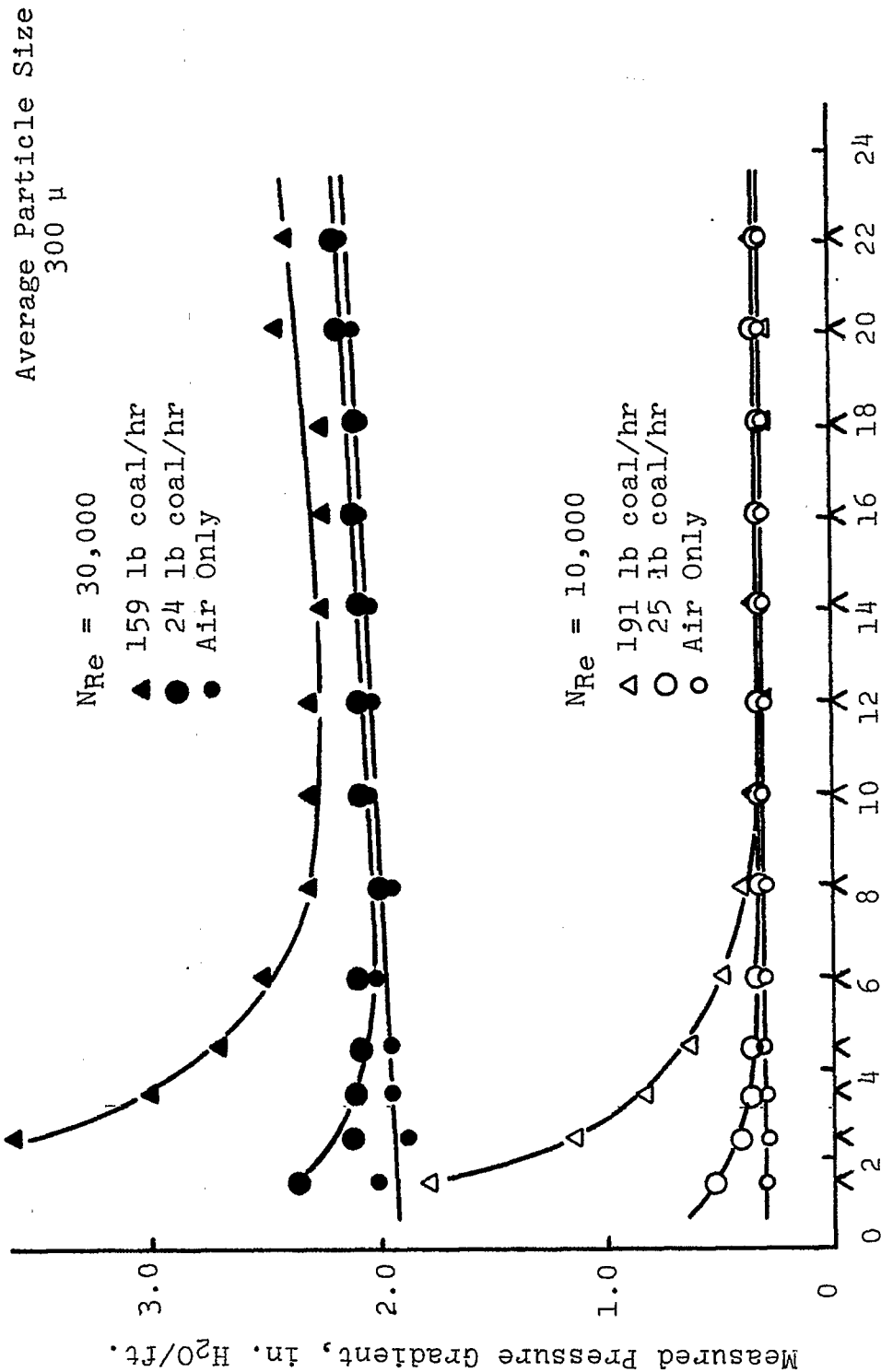
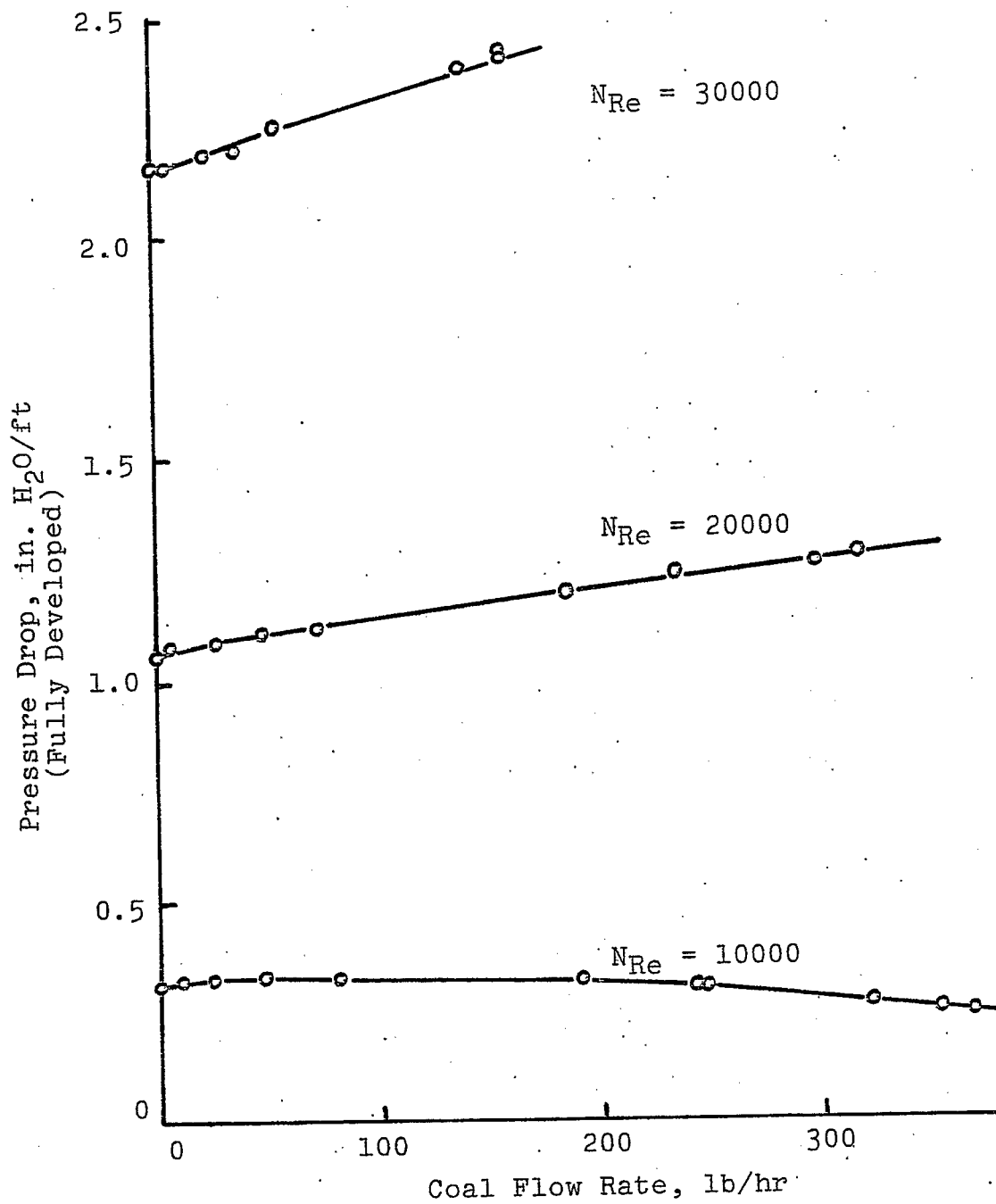


Figure 4. Effect of Solids on Hydraulic Entry Length.

Figure 5. Measured Pressure Drop as a Function of Solids Flow Rate.



Coal Particle and Catalyst Characteristics for  
Hydrogenation Evaluation and Testing

Faculty Advisor: R.E. Wood  
Graduate Student: J.M. Lytle

Introduction

This effort is related to the effects of coal particle size and temperature on the rate of coal hydrogenation in a coiled tube reactor and also a microreactor. The existing hydrogenation equipment was used with OCR (Office of Coal Research) Project, FE(49-18)-1200 and with ERDA-DOE Project, FE(49-18)-2006. The reaction vessel consists of a series of coiled tubes, each approximately 20 ft long and may be divided into two zones, preheater and reactor. The preheater consists of two coils each 20 ft long and 3/16 inch ID. The reactor consists of 1 to 4 coils, 20 ft long and 1/4 inch ID.

The residence time of coal and residual solids is measured in the reaction vessel of the coiled tube reactor using powdered iron as a tracer. The detection device consists of a coil of copper wire placed coaxially with the reactor tubing such that the ID of the copper coil is the same as that of the tubing. For residence time detection and measurement, one coil is placed at the beginning of the preheat section and a second at the end of the reactor.

The microreactor is a small batch reactor which may be heated rapidly to reaction temperature by a flame and cooled by water quench. Reactions normally may be considered nearly isothermal. The small size of the reactor also makes it convenient to weigh the whole system on a 5 place balance. This device will be used to study coal characteristics and coal-catalyst interactions.

Project Status

The data from Figures 1-6 of the last report have been applied to a heterogeneous reaction model for the hydrogenation liquefaction of coal. The model tested is termed the "unreacted-core-shrinking model." Use of this model is based on the solution of a second order differential equation relating to the material balance of the diffusing specie.<sup>1</sup>

$$\epsilon \frac{\partial C_A}{\partial t} = D_{eA} \left( \frac{\partial^2 C_A}{\partial r^2} + \frac{2}{r} \frac{\partial C_A}{\partial r} \right) \quad (1)$$

where  $C_A$  is the concentration of the diffusing specie,  $r$  is the radius of the spherical shaped solid reactant,  $\epsilon$  is the voidage of the particle and  $D_{eA}$  is the diffusivity of the diffusing specie in the inert layer. Wen<sup>1</sup> has described the boundary conditions for the spherical particle as

$$D_{eA} \left( \frac{\partial C_A}{\partial r} \right)_R = k_{mA} (C_{A0} - C_{As}) \quad (2)$$

at the surface of the particle,

$$D_{eA} \left( \frac{\partial C_A}{\partial r} \right)_{r_c} = a k_s C_{S0} C_{Ac} \quad (3)$$

and

$$-D_{eA} \left( \frac{\partial C_A}{\partial r} \right)_{r_c} = a C_{S0} \left( \frac{\partial r_c}{\partial t} \right) \quad (4)$$

at the interface or surface of the unreacted core of the particle. The mass transfer coefficient across the fluid boundary layer is  $k_{mA}$ ,  $C_{S0}$  is the solid reactant concentration;  $k_s$  is the rate constant of the chemical reaction at the unreacted core surface,  $R$  is the initial radius of the particle,  $r_c$  is the radius of the unreacted core,  $C_{As}$  and  $C_{Ac}$  are the concentrations of the diffusing specie at the outer surface of the particle and at the unreacted core, respectively, and  $a$  is the moles of A reacted per mole of the solid.

For an analytical solution to Eq (1), the pseudo steady state is assumed where  $\epsilon \partial C_A / \partial t$  equals 0. This assumption holds except for cases of extremely high pressure and very low solid concentration.<sup>1</sup> The reaction is first order with respect to the diffusing specie and zero order with respect to the solid reactant.

Wen has given a solution to Eq (1) based on the above assumptions.<sup>1</sup> For film resistance controlling

$$t = \frac{a R C_{S0}}{3 k_{mA} C_{A0}} X \quad (5)$$

where  $X$  is the fractional conversion of the solid. For ash or inert layer diffusion control,

$$t = \frac{aR^2C_{So}}{6D_{eA}CA_o} [1-3(1-X)^{2/3} + 2(1-X)] \quad (6)$$

and for chemical reaction control

$$t = \frac{R}{k_sCA_o} [1-(1-X)^{1/3}] \quad (7)$$

If  $D_{eA}$  is defined as a function of the surface area of the unreacted core, Eq (6) becomes

$$t = \frac{aC_{So}R^2}{2CA_oD'_{eA}} [1-(1-X)^{1/3}]^2 \quad (8)$$

This model may be tested by performing heterogeneous reactions to determine whether the reaction is diffusion controlled by using Eq (7) and (8). A plot of  $\ln t$  vs.  $\ln [1-(1-X)^{1/3}]$  will have a slope of one for chemical control and two for ash diffusion control.

The unreacted-core-shrinking model described above can be applied to the coal hydrogenation reaction in the coiled tube reactor. The solid reactant followed for this purpose is the fixed carbon. Fractional fixed carbon conversion ( $X_{FC}$ ) is used because it has been shown by Mazumdar et al.<sup>2-4</sup> that the change in fixed carbon is directly proportional to the amount of hydrogen added to the coal.

Figure 1 shows  $\ln t$  vs.  $\ln [1-(1-X_{FC})^{1/3}]$  for Clear Creek, Utah coal processed at various temperatures and particle sizes. The points on a given line from left to right represent  $X_{FC}$  values of 0.1, 0.2, 0.3, 0.4, 0.5 and 0.6, respectively. For conversion levels of 0.1 and 0.3, the slopes of the lines are approximately one indicating a reaction which is chemically controlled at the surface of the unreacted core. For temperatures of 471 and 482°C, the chemically controlled reaction continues to  $X_{FC}$  equal to 0.6. However, at higher temperatures the reaction reverts to a physically controlled reaction as shown by the slope of approximately two. This probably happens because at the higher temperature the chemical reaction rate is increased. Then, as the inert outer layer of the particle thickens, the flux of hydrogen to the unreacted core is inhibited. The slow step in the reaction in this manner is transferred from chemical to physical. The data for Figure 1 is shown in Table 1.

Figure 1 shows data at four different temperatures. This data may be used to evaluate the activation energy for hydrogen addition to coal. This is done by an extrapolation of the points at  $X_{FC}$  equal to 0.1 to the y axis with a slope of one.



Table 2 shows the results of this extrapolation. Figure 2 shows a plot of  $\ln k$  vs.  $1/T$  from which the activation energy is obtained. The data is shown in Table 2. The activation energy for the addition of hydrogen to coal is calculated to be 44.5 kcal per mole of hydrogen.

Activation energies of various coal reactions, i.e., pyrolysis, hydrogenation and dissolution, have been reported in the literature. The values have ranged between 25 and 50 kcal per mole.<sup>5-10</sup> The activation energy for diffusion of hydrogen in coal char has been reported as 8.5 kcal per mole.<sup>11</sup> The activation energy for coal hydrogenation as measured by extrapolation to the data of Figure 2 and Table 2 is in the range accepted for a chemically controlled reaction.

A diffusivity may be evaluated from the particle size data of Figure 1 and Table 1. However, the calculated diffusivity is not precise. Errors are introduced because of extrapolation of the data and because of lack of knowledge of the stoichiometry of the reaction. The numbers leading to the calculation of the diffusivity are shown in Table 3. The diffusivity may change as a function of time and conversion because of the changing nature of the inert layer of the reacting coal particle.

#### Future Work

Data will be further analyzed and experiments with the microreactor will continue.

#### References

1. C.Y. Wen, Ind. Eng. Chem., 60 (9), 34 (1968).
2. A.C. Bhattacharyya, B.K. Mazumdar and A. Lahiri, Fuel, 43, 181 (1964).
3. S. Ganguley and B.K. Mazumdar, Fuel, 43, 281 (1964).
4. B.K. Mazumdar and N.N. Chatterjie, Fuel, 52, 11 (1973).
5. W.H. Wiser, L.L. Anderson, S.A. Quader and G.R. Hill, J. Appl. Chem., Biotechnol., 21, 82 (1971).
6. W.H. Wiser, G.R. Hill and N.J. Kertamus, Ind. Eng. Chem., Process Des. Develop., 6, 133 (1967).
7. A.A. Elmowafi and W.H. Wiser, OCR Technical Report 32, U.S. Dept of the Interior, Washington, D.C., Sept 1969.
8. M.M. El-Mogazi, W.H. Wiser and G.R. Hill, OCR Technical Report 55, U.S. Dept of the Interior, Washington, D.C., Feb 1967.

9. H.A.G. Chermin and D.W. Van Krevelen, Fuel, 36, 85 (1957).
10. D. Fitzgerald, Trans. Faraday Soc., 52, 362 (1956).
11. P.L. Walker, Jr., L.G. Austin and S.P. Nandi, "Chemistry and Physics of Carbon," Vol. 2, P.L. Walker, Jr., Ed., Marcel Dekker, Inc., New York, N.Y., 1966, p 325.

Table 1. Times for various conversion levels of fixed carbon ( $X_{FC}$ ) at various particle sizes and reaction temperatures with their logs for Clear Creek, Utah coal processed in the coiled tube reactor at 122 atm and 6%  $ZnCl_2$ .

Particle Size in $10^{-6}$ meters	105	195	364	364	364	364
Reaction Temp in $^{\circ}C$	493	493	471	482	493	504
$X_{FC}$	Time in Seconds (t)					
0.1	4.1	5.4	27.0	21.5	21.3	9.0
0.2	9.0	12.3	54.0	44.0	27.6	19.9
0.3	15.3	21.7	81.0	68.3	47.0	33.4
0.4	24.0	35.4	108.1	95.0	72.7	50.9
0.5	37.2	56.9	135.3	125.2	108.8	75.5
0.6	61.6	95.7	162.7	161.6	163.9	115.8
$\ln(1-(1-X_{FC})^{1/3})$ for resp. $X_{FC}$	$\ln(t)$ for respective t					
-1.336	1.411	1.686	3.296	3.068	2.510	2.197
-1.580	2.197	2.510	3.989	3.784	3.318	2.991
-1.852	2.728	3.077	4.394	4.224	3.850	3.500
-2.189	3.178	3.567	4.683	4.554	4.286	3.930
-2.631	3.616	4.041	4.907	4.830	4.690	4.324
-3.352	4.121	4.561	5.092	5.085	5.099	4.752

Table 2. The chemical reaction rate constant at various temperatures where the units of rate are moles per (second, surface area) for Clear Creek, Utah coal process in the coiled tube reactor at 122 atm H<sub>2</sub> and with 6% ZnCl<sub>2</sub>. The Arrhenius activation energy is 44.5 kcal/mole H<sub>2</sub>. The diameter (D) of the coal particle at X<sub>FC</sub>=0.3 is 0.0950 cm.

T(°C)	1/T(°K)	$k\left(\frac{\text{cm}^4}{\text{mole sec}}\right)$	ln k	t <sup>a</sup> (sec)	(CH <sub>2</sub> ) <sub>o</sub> (mole/cm <sup>3</sup> )
471	0.001344	0.03236	-3.431	782.9	0.001875
482	0.001325	0.04124	-3.188	623.3	0.001848
493	0.001305	0.07313	-2.616	356.7	0.001821
504	0.001287	0.1014	-2.288	260.9	0.001795

<sup>a</sup>t=time for complete conversion (X<sub>FC</sub>=1).

$$k = \frac{D}{2t(\text{CH}_2)_o}$$

Table 3. Diffusivity evaluated by extrapolation of the diffusion controlled region for various particle sizes. (CH<sub>2</sub>)<sub>o</sub>=0.001821 mole/cm<sup>3</sup>, C<sub>S0</sub>=1=the initial solids concentration,  $\frac{DeA}{a} = \frac{C_{S_0} D^2}{24(\text{CH}_2)_o t}$

t=time for complete reaction (X<sub>FC</sub>=1) if the reaction is diffusion controlled throughout. The a is the moles of H<sub>2</sub>/mole of carbon in the reaction.

D <sub>o</sub> (cm)	D (cm)	t (sec)	$\frac{DeA}{a}$
0.0105	0.041	863	4.46x10 <sup>-5</sup>
0.0195	0.077	1339	10.13x10 <sup>-5</sup>
0.0364	0.095	2298	8.99x10 <sup>-5</sup>

average  $\frac{DeA}{a} = 7.86 \times 10^{-5}$

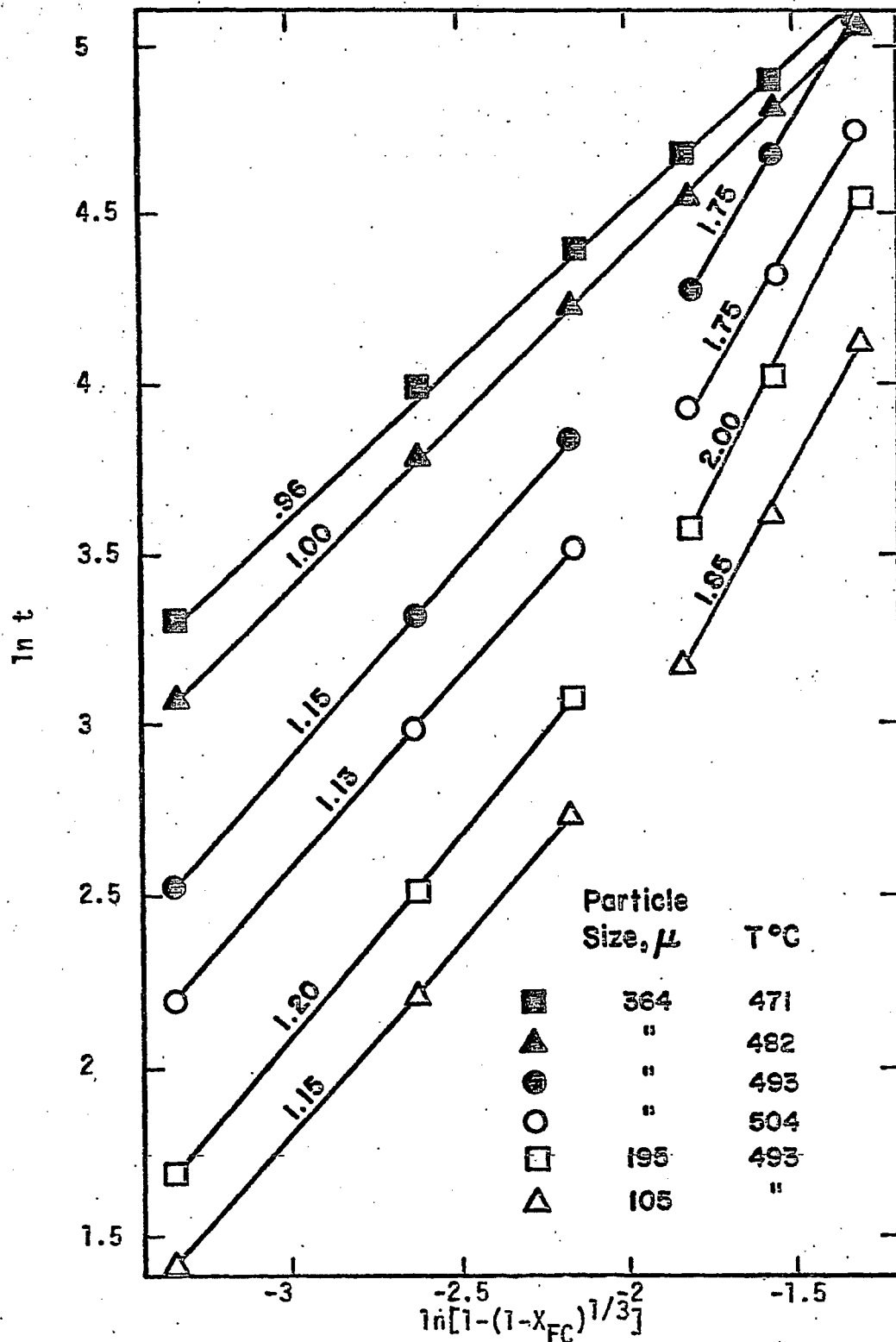


Figure 1. Graph showing chemical and diffusion controlled regimes for the hydrogenation of Clear Creek, Utah coal in the "coiled tube reactor" set at 12.4 MPa H<sub>2</sub> and with 6.25% ZnCl<sub>2</sub> added to the coal. (Slopes listed on lines) Data is listed in Tables 12 & 15.

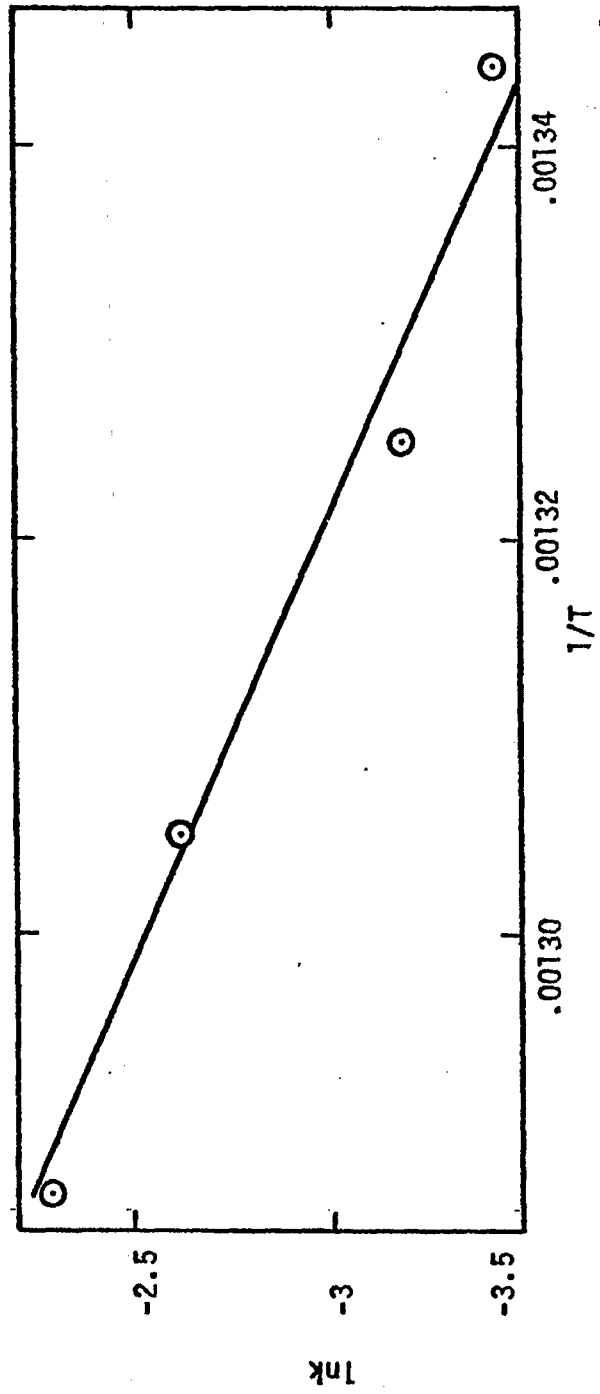


Figure 2. Activation energy plot for the hydrogenation of Clear Creek, Utah coal processed in the coiled tube reactor set at 12.4 MPa H<sub>2</sub> and with 6.25% ZnCl<sub>2</sub> added to the coal. E = 44,452 cal/mole H<sub>2</sub> = energy of activation and the frequency factor, A = 3.53 x 10<sup>11</sup>.

## Project D-1

### Coal Particle and Catalyst Characteristics for Hydrogenation Evaluation and Testing

Faculty Advisor: R.E. Wood  
Graduate Student: R. Jensen

#### Introduction

The mechanism of coal hydrogenation will be studied using  $ZnCl_2$  as a catalyst and a small pressurized reactor, called a microreactor. This work will be a continuation of previous studies cited in a paper by D.P. Mobley et al.<sup>1</sup> The same model compounds will be studied using the optimum conditions of the University of Utah's coal hydrogenation system. These compounds represent various connecting groups found in coal and will be subjected to different temperatures, catalyst concentration and reaction times. The reaction products will be analyzed by gas chromatography and compared to proposed products from dealkylation of the model compounds, yielding reaction mechanism information.

Previous work includes 1) the acquisition of model compounds, 2) the manufacture of reactors and 3) a preliminary study of model compound fragmentation using catalyzed hydrogenation.

#### Project Status

Additional model compounds have been acquired that will supplement previously obtained compounds and give a clearer picture of the mechanism pathways. A Porasil C column has been chosen and the gas chromatograph has been calibrated for the expected products of the hydrogenation reaction.

#### Future Work

Model compounds will be catalytically hydrogenated using  $ZnCl_2$  as the catalyst. Reaction variables will be temperature, catalyst concentration and reaction time. After the products are identified by GC, a reaction mechanism will be proposed.

#### Reference

1. D.P. Mobley, S. Salim, K.I. Tanner, N.D. Taylor and A.T. Bell, Preprints, Div. of Fuel Chemistry, American Chemical Society, Miami, Florida, Sept 1978, Vol 25 No. 4.

A Pyrolysis-Gas Chromatography Study of Coals and  
Related Model Compounds

Faculty Advisor: R.R. Beishline

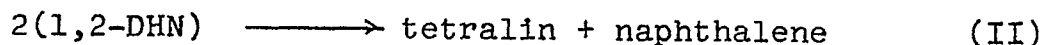
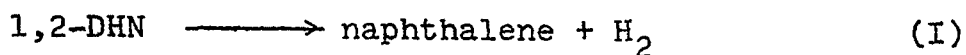
Introduction

This project deals with the pyrolysis and hydrogenation of coal and coal-related model compounds both in the presence and absence of catalysts.

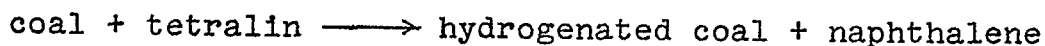
Since coal hydrogenations are normally carried out at thermolytic temperatures, reactions other than hydrogenation likely occur concurrently, e.g., pyrolysis and reactions that can be catalytically initiated at subthermolytic temperatures and that would proceed at accelerated rates at thermolytic temperatures. A knowledge of these latter reactions is a necessary background to the understanding of the hydrogenation chemistry. To elucidate some of this background, the subthermolytic (165°C) zinc chloride-catalyzed decomposition of the model compound 1,2-dihydronaphthalene (1,2-DHN) has been studied.

The decomposition occurs by a mechanism in which hydrated zinc chloride donates a proton to the double bond of 1,2-DHN to form a carbonium ion. This carbonium ion adds to 1,2-DHN to give two dimers and abstracts hydride from 1,2-DHN to produce tetralin and naphthalene.

A study of the pyrolysis of 1,2-DHN has been initiated, and preliminary kinetic results suggest that the following scheme of simultaneous first and second order reactions is operative.



The 1,2-DHN is an intermediate in the hydroligue fraction of coal when tetralin is used as the hydrogen donor solvent.<sup>1</sup> Reactions (I) and (II) are thus part of the overall hydrogen transfer scheme



and are of considerable interest.



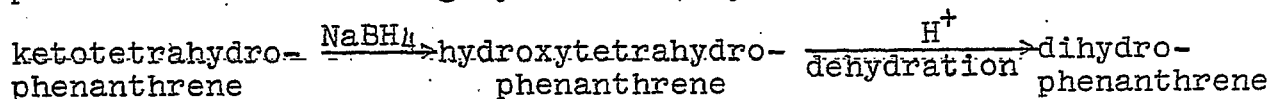
## Project Status

Collection of the kinetic data for Reactions (I) and (II) has been completed, and the data are now being analyzed. The results of this study will be presented in the next quarterly report.

Past Work has shown that at higher temperatures (400°C), 1,2-DHN can dehydrogenate a dihydroaromatic ring to an aromatic ring, the 1,2-DHN being hydrogenated to tetralin. The question arises, "Can 1,2-DHN dehydrogenate a tetrahydroaromatic ring to a dihydroaromatic ring?" If this reaction were studied in the tetralin system some tracer of labeling technique would be required, since the products are identical to the reactants. Therefore, this reaction will be studied by using 1,2-DHN and tetrahydrophenanthrene (THP) as the reactants. However, the pyrolytic behavior of THP must be known so that the decomposition of THP can be distinguished from the reaction of DHN with THP. The pyrolysis of THP through the temperature range 300°-500°C has been studied, and preliminary results were given in the last quarterly report.

If DHN dehydrogenates THP, dihydrophenanthrene (DHP) would be formed, and if DHP behaves like DHN (this has not yet been experimentally verified), the DHP would disproportionate into THP and phenanthrene, i.e., if DHN dehydrogenates THP, DHP and/or phenanthrene should appear as the THP disappeared. This experiment has been done by pyrolyzing an approximately equimolar mixture of DHN and THP at 400 and 450°C. Analysis of the reaction products showed no DHP and indicated the amount of phenanthrene formed was approximately equivalent to that formed when THP is pyrolyzed in the absence of DHN. Therefore up to 450°C, DHN does not dehydrogenate THP into DHP. If DHP behaves like DHN, the above conclusion will be valid. If not, the conclusion must be re-evaluated.

The pyrolysis of 1,2- and 3,4-DHP will be investigated as soon as these compounds have been synthesized. The dihydrophenanthrenes are being synthesized by the following reactions:



The starting ketones (1- and 4-keto-1,2,3,4-tetrahydro-phenanthrene) have been prepared, and the 1-keto compound has been converted into the 1-hydroxy compound.

## Future Work

The results of the kinetic study of Reactions (I) and (II) will be reported. The synthesis of 1,2 and 3,4-DHP will be completed, and the study of the pyrolysis of these compounds will be initiated.

Reference

1. L.L. Anderson, D. Kang and W.H. Wiser, DOE Contract No. (49-18) - 2006, Quarterly Progress Report, Salt Lake City, Utah, July-Sept 1977.

# Hydrodesulfurization of Heavy Hydrocarbon Liquids in a Fluidized Bed Reactor with Hydrogen as the Continuous Phase

Faculty Advisor: A.G. Oblad  
Graduate Student: Hsiang-Yun Kung

## Introduction

Commercial hydrodesulfurization processes are operated mostly in fixed bed reactors. For these, fine catalyst particles cannot be used because of the excessive bed pressure drop; neither can fresh catalyst be added without reactor shut down. However, with a fluid bed reactor, it is possible to 1) operate at near isothermal conditions because of the radial and axial agitation induced by the bubbles, 2) maintain constant activity of the catalyst by continuous circulation of the spent or coked catalyst between the reactor and regenerator, 3) have an essentially constant yield and quality of the products from operating at a constant temperature and catalyst activity, 4) change the feed or product quality on a given feed by controlling the catalyst withdrawal rate which adjusts the equilibrium activity and 5) employ very small catalyst sizes for catalytic effectiveness.

Therefore, the objective of this study is to determine the feasibility of the vapor-phase fluidized bed hydrodesulfurization of feedstocks such as coal liquids, synthetic crudes produced from oil shale, tar sand, bitumens and petroleum gas oils and resids. The parameters are

Temperature: 400-450°C

Pressure: 1000-1500 psig

The catalysts being studied, along with their physical properties have been given in the previous report. The catalyst (average particle size: 49 microns) was prepared by grinding a commercial cobalt-molybdate oxide supported on alumina and subsequently sulfiding the selected size fraction with H<sub>2</sub>S for 2 to 4 hours at 300°C, 20 psig.

## Project Status

The minimum fluidization velocity at 1500 psig and 425°C was determined according to the method recommended by Kunii and Levenspiel and shown in Table 1 and Figures 1, 2 and 3.

Figures 1 and 2 depict curves for typical pressure drop vs. gas flow rate. In Figure 3 the ratio of the experimental

pressure drop across the bed to the pressure drop equivalent to the bed weight ( $\Delta p/\Delta p_{eq}$ ) is plotted against the superficial gas velocity (at bed conditions). The bed fluidized at a pressure drop which was close to the theoretical value equivalent to the bed weight. For a one inch diameter column and at a 4.9 initial fixed bed height/column diameter ratio, the  $\Delta p/\Delta p_{eq}$  ratio was greater than 1 at gas velocities higher than  $U_{mf}$ . This indicates an absence of channelling and slugging in the bed.

### Future Work

More fluidization tests will be done for various conditions, afterwhich, the experiments of HDS will begin.

### Reference

1. D. Kuni and O. Levenspiel, "Fluidization Engineering," John Wiley and Sons, Inc., New York, N.Y., 1969, p 74.

Table 1

### Bed Conditions

Temperature: 425°C  
 Pressure: 1500 psig  
 Particle: Sulfided Co-Mo-Al (Harshaw 0603)  
 Particle Size: 49 microns  
 Bed Weight: 64.79 grams  
 Pressure drop equivalent to bed weight,  $\Delta p_{eq}$ : 5.05 inches of water  
 Fixed Bed Depth/Column Diameter: 4.91

Rm Temp	H <sub>2</sub> Flow Rate cc/sec	std cc/sec	H <sub>2</sub> Velocity cm/sec at Rx Conditions	$\Delta p$ Across Bed, in. water	$\Delta p/\Delta p_{eq}$
15.20		13.93	0.068	1.75	0.3465
25.45		23.32	0.114	2.60	0.5149
31.65		29.00	0.142	3.10	0.6139
40.00		36.64	0.180	4.20	0.8317
43.10		39.48	0.194	5.40	1.0693
48.08		44.05	0.216	6.40	1.2673
51.20		46.90	0.230	6.05	1.1980
59.00		54.05	0.265	5.80	1.1485
70.00		64.13	0.314	5.85	1.1584
80.00		73.29	0.359	6.20	1.2277
95.00		87.03	0.427	6.0	1.1881
100.10		91.70	0.449	6.0	1.1881
108.00		98.94	0.485	5.4	1.0693

Figure 1. Pressure Drop Vs. Gas Flow Rate.

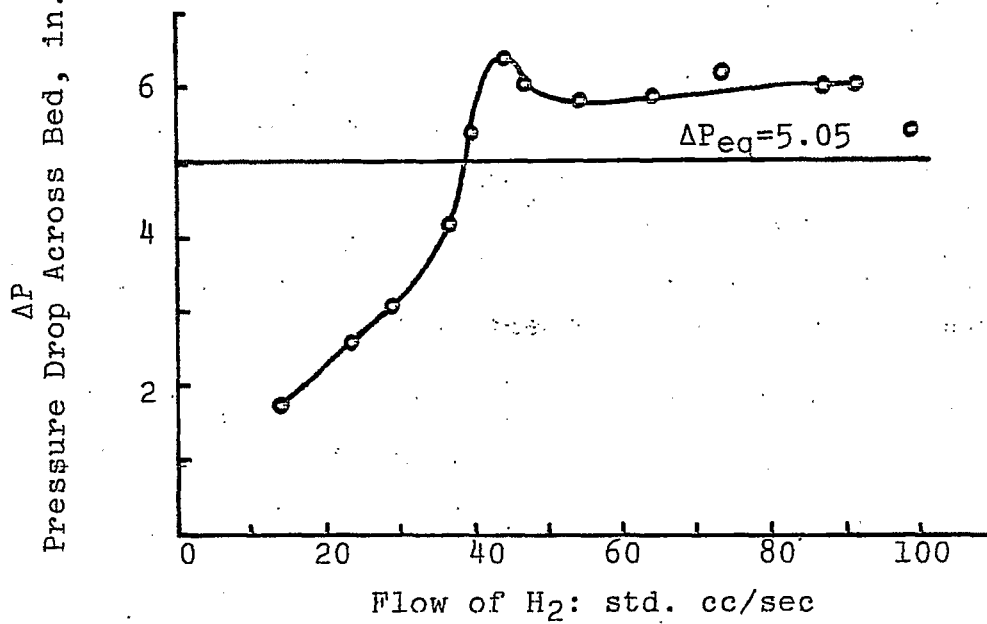
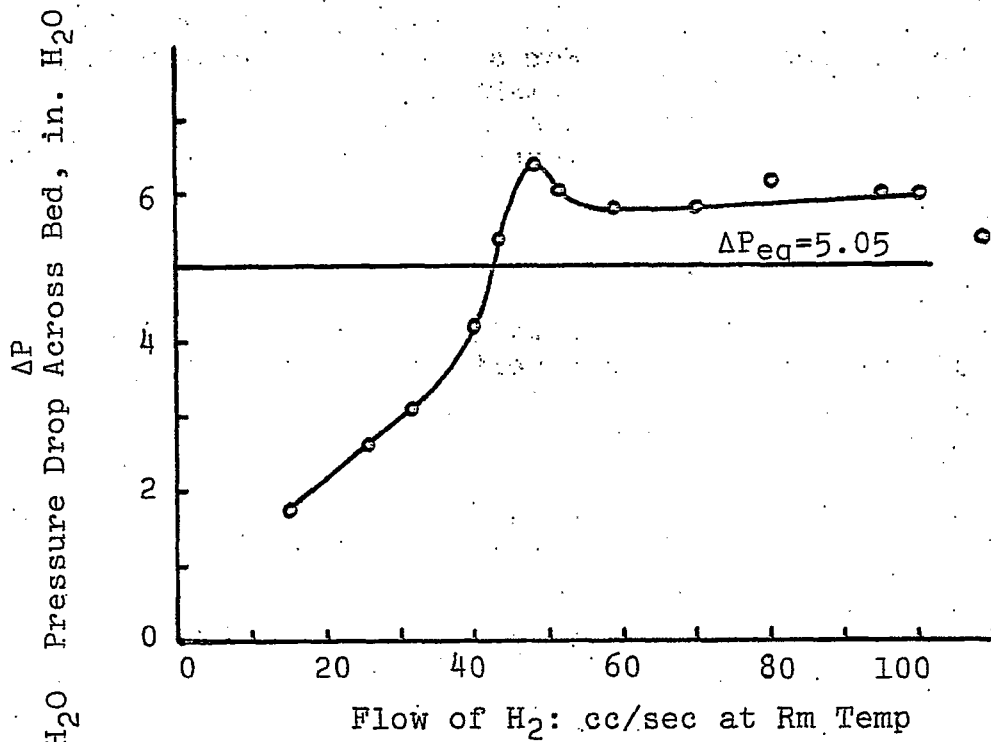
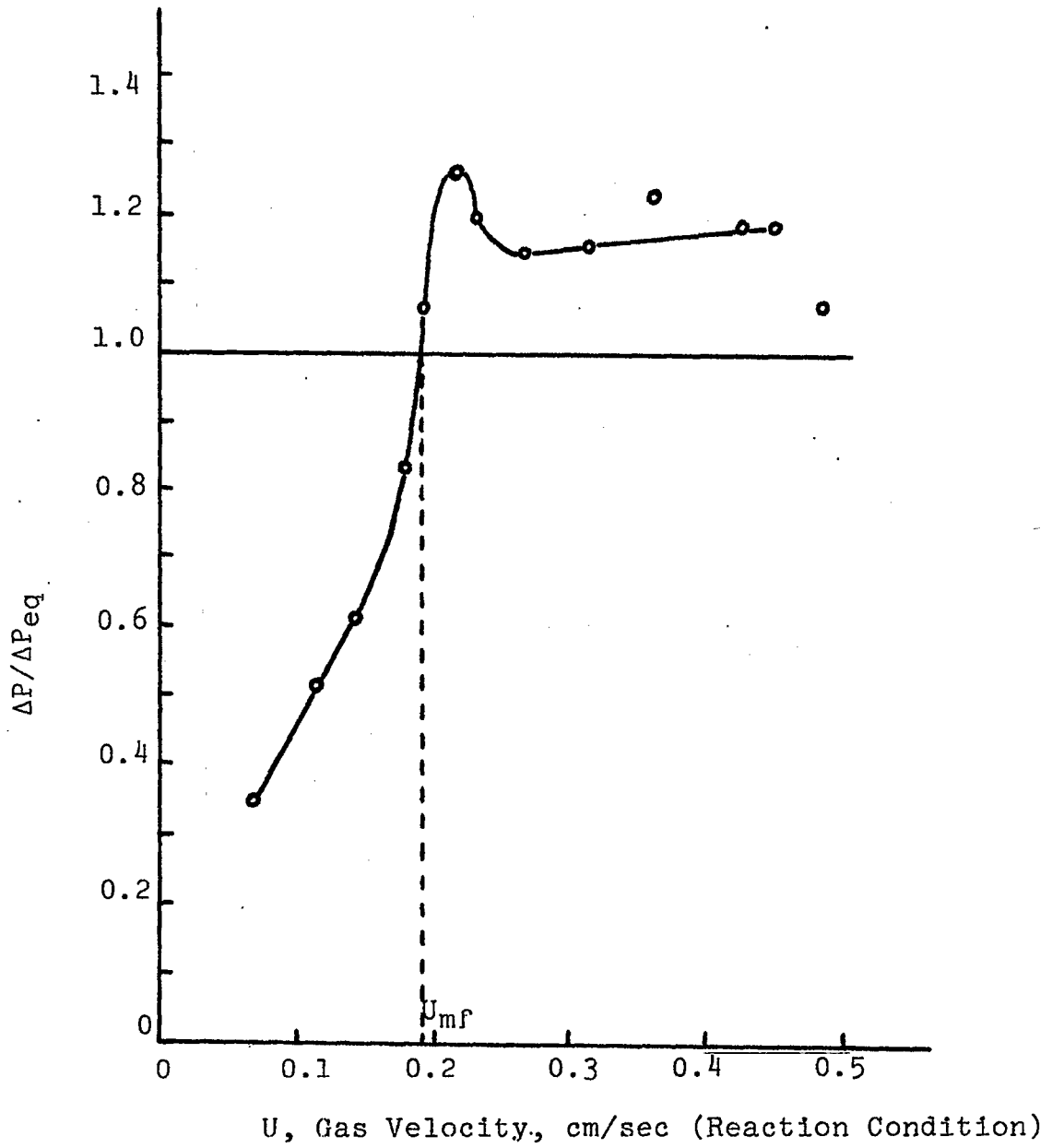


Figure 2. Pressure Drop Vs. Gas Flow Rate.

Figure 3. Ratio of Experimental Bed Pressure Drop to that Equivalent to the Bed Weight Vs. Hydrogen Velocity.



## **SATISFACTION GUARANTEED**

**NTIS strives to provide quality products, reliable service, and fast delivery. Please contact us for a replacement within 30 days if the item you receive is defective or if we have made an error in filling your order.**

▲ **E-mail: [info@ntis.gov](mailto:info@ntis.gov)**  
▲ **Phone: 1-888-584-8332 or (703)605-6050**

# **Reproduced by NTIS**

National Technical Information Service  
Springfield, VA 22161

***This report was printed specifically for your order from nearly 3 million titles available in our collection.***

For economy and efficiency, NTIS does not maintain stock of its vast collection of technical reports. Rather, most documents are custom reproduced for each order. Documents that are not in electronic format are reproduced from master archival copies and are the best possible reproductions available.

Occasionally, older master materials may reproduce portions of documents that are not fully legible. If you have questions concerning this document or any order you have placed with NTIS, please call our Customer Service Department at (703) 605-6050.

## **About NTIS**

NTIS collects scientific, technical, engineering, and related business information – then organizes, maintains, and disseminates that information in a variety of formats – including electronic download, online access, CD-ROM, magnetic tape, diskette, multimedia, microfiche and paper.

The NTIS collection of nearly 3 million titles includes reports describing research conducted or sponsored by federal agencies and their contractors; statistical and business information; U.S. military publications; multimedia training products; computer software and electronic databases developed by federal agencies; and technical reports prepared by research organizations worldwide.

For more information about NTIS, visit our Web site at <http://www.ntis.gov>.

# **NTIS**

**Ensuring Permanent, Easy Access to  
U.S. Government Information Assets**



U.S. DEPARTMENT OF COMMERCE  
Technology Administration  
National Technical Information Service  
Springfield, VA 22161 (703) 605-6000

---